β-Catenin sustains and is required for YES-associated protein oncogenic activity in cholangiocarcinoma

Yi Zhang, Hongwei Xu, Guofei Cui, Binyong Liang, Xiangzheng Chen, Sungjin Ko, Silvia Affo, Xinhua Song, Liao Yi, Jianguo Feng, Pan Wang, Haichuan Wang, Meng Xu, Jingxiao Wang, Giovanni M. Pes, Silvia Ribback, Yong Zeng, Aatur Singhi, Robert F. Schwabe, Satdarshan P Monga, Matthias Evert, Liling Tang, Diego F Calvisi, Xin Chen

Supplementary Data

Table of Contents

1. Supplementary Figures and Figure Legends

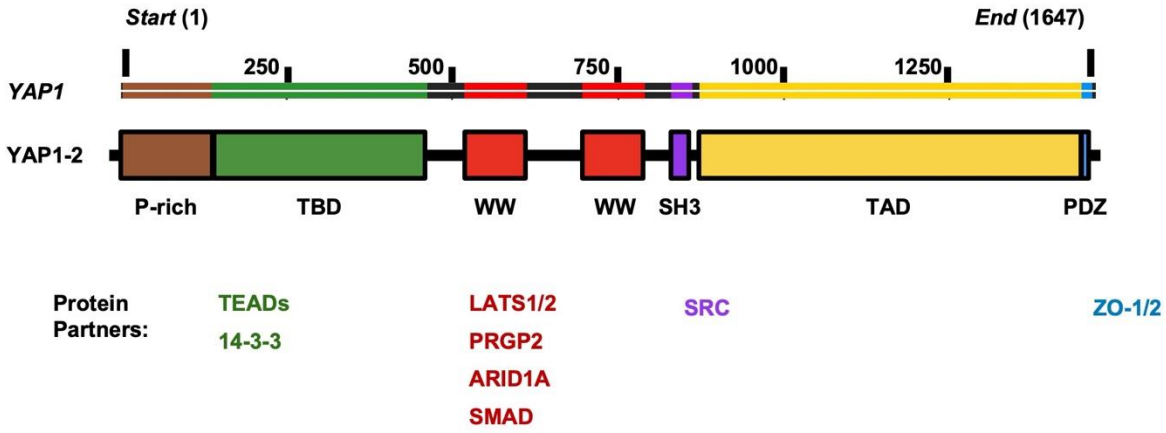

Supplementary Figure 1. Modular structure of *YAP1* gene and YAP1-2 isoform.

Illustration of the *YAP1* gene. Colors indicate the different functional domains. Prominent domains of YAP1-2 isoform include an N-terminal proline-rich domain, the TEAD binding domain (TBD), the WW domains, the SH3-binding domain, the transcriptional activation domain (TAD), and a C-terminal PDZ-binding domain. YAP protein partners [1-3] are colored by structural domains.

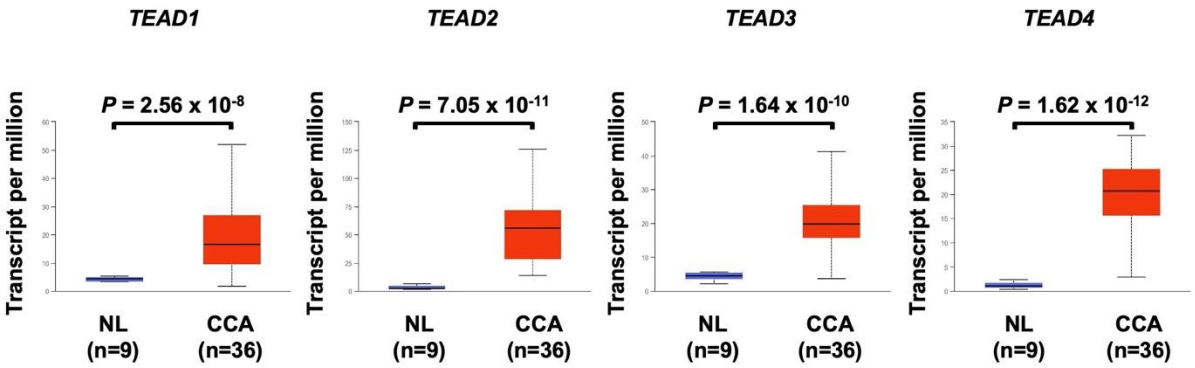
TEAD1
P = 2.56 x 10-8
Transcript per million
NL (n=9)
CCA (n=36)
TEAD2
P = 7.05 x 10-11
Transcript per million
NL (n=9)
CCA (n=36)
TEAD3
P = 1.64 x 10-10
Transcript per million
NL (n=9)
CCA (n=36)
TEAD4
P = 1.62 x 10-12
Transcript per million
NL (n=9)
CCA (n=36)

Supplementary Figure 2. *TEAD1-4* genes are highly expressed in human CCA.

Gene mRNA expression in human CCA tumors and corresponding non-tumorous surrounding livers based on the TCGA CHOL dataset. The pictures were downloaded from the UALCAN website (http://ualcan.path.uab.edu/index.html). Abbreviations: NL, Non-tumorous surrounding liver; CCA: Cholangiocarcinoma.

RBE

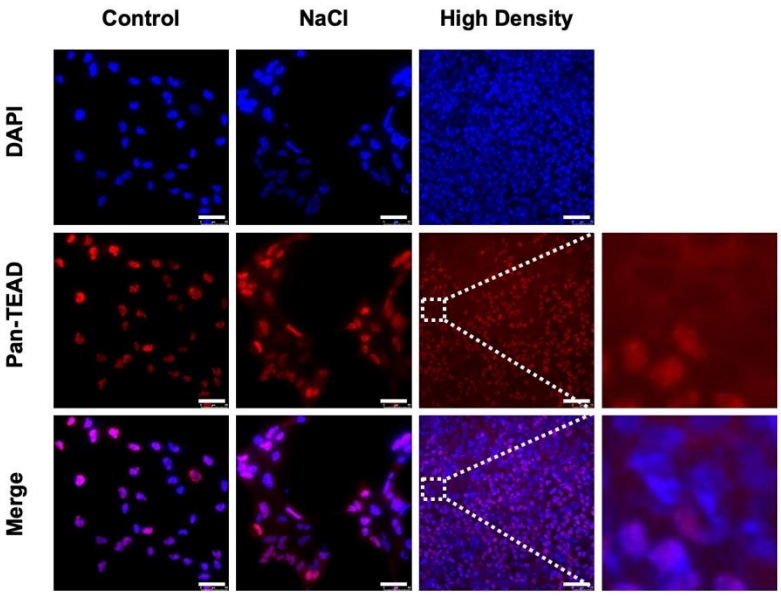

Supplementary Figure 3. TEAD factors stably accumulate in the nucleus of RBE cells.

Immunofluorescence staining of pan-TEAD proteins in RBE cells in normal condition or stimulated with environmental stresses. Immunofluorescence detected pan-TEADs subcellular localization following NaCl (200 mM; 8 h) or high cell density (72 h post-confluent) treatment. Scale bar: 50 μm.

HUCCT-1

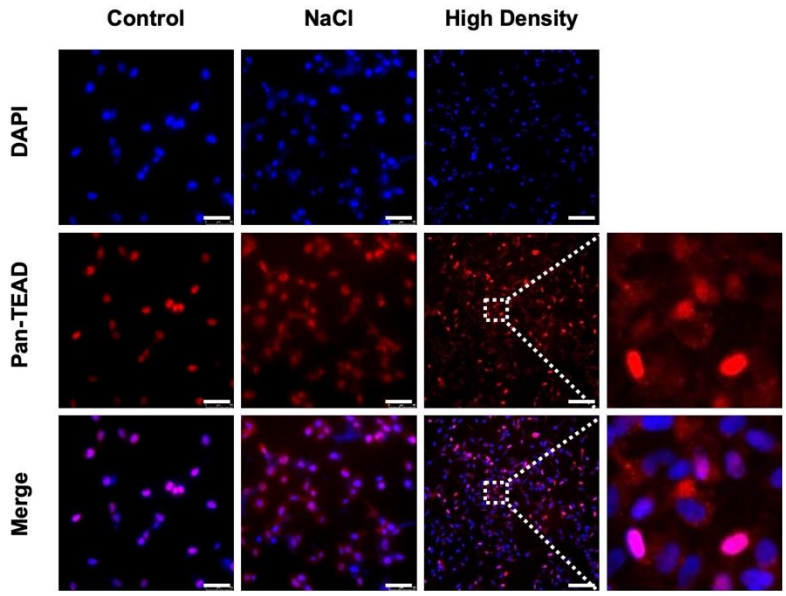

Supplementary Figure 4. TEAD factors stably accumulate in the nucleus of HUCCT-1 cells. Immunofluorescence staining of pan-TEAD proteins in HUCCT-1 cells in normal conditions or stimulated with environmental stresses. Immunofluorescence detected pan-TEADs subcellular localization following NaCl (200 mM; 8 h) or high cell density (72 h post-confluent) treatment. Scale bar: 50 μm.

KKU156

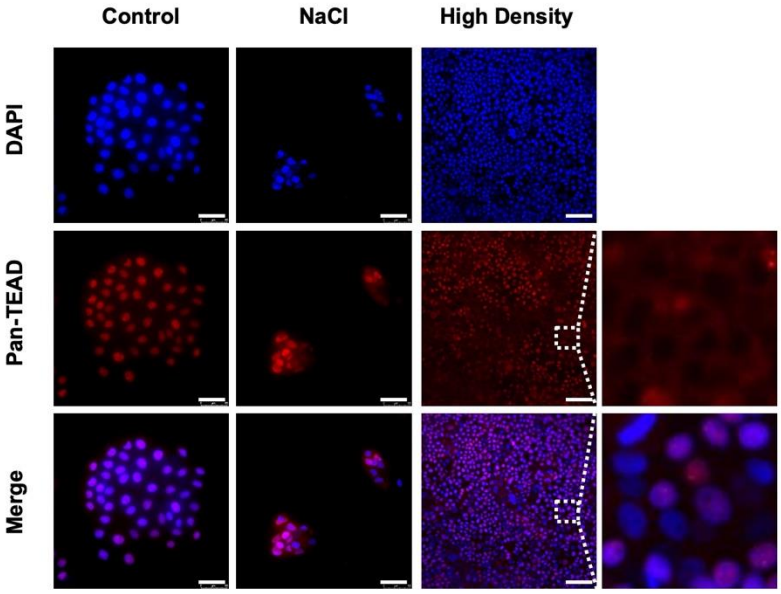

Supplementary Figure 5. TEAD factors stably accumulate in the nucleus of KKU156 cells. Immunofluorescence staining of pan-TEAD proteins in KKU156 cells in normal condition or stimulated with environmental stresses. Immunofluorescence detected pan-TEADs subcellular localization following NaCl (200 mM; 8 h) or high cell density (72 h post-confluent) treatment. Scale bar: 50 μm.

Akt/YapS94A

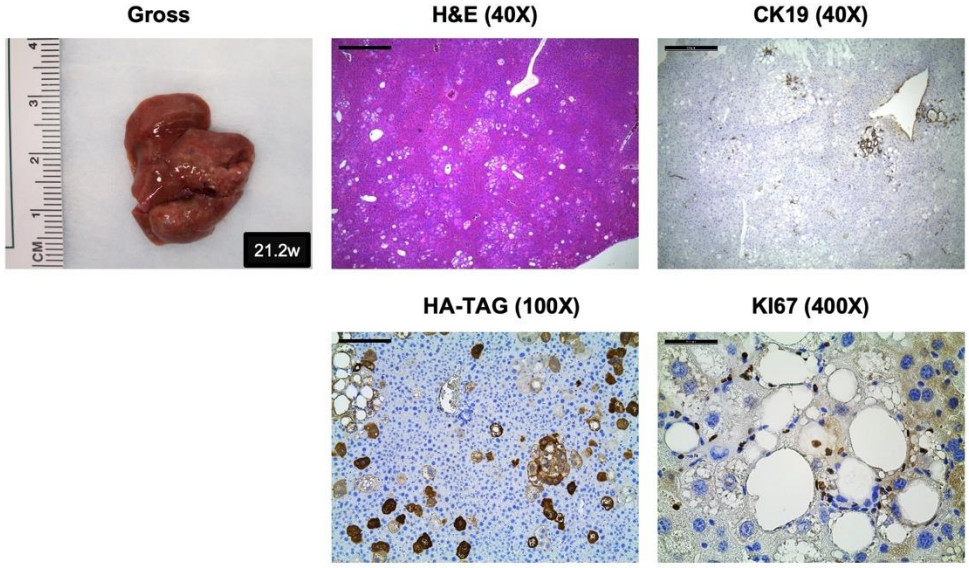

Supplementary Figure 6. Blockade of Yap/TEADs prevents iCCA formation in mice.

AKT-induced hepatic steatosis but not tumor development could be observed in the liver tissue from *Akt/YapS94A* (F21.2w.p.i) mice. Representative gross images, H&E, and immunohistochemistry for CK19, HA-TAG, and KI67 of liver tissue. Scale bar: 500 μm (40x), 100 μm (100x), and 50 μm (400x). Abbreviations: H&E, hematoxylin and eosin staining; w.p.i, weeks post-injection.

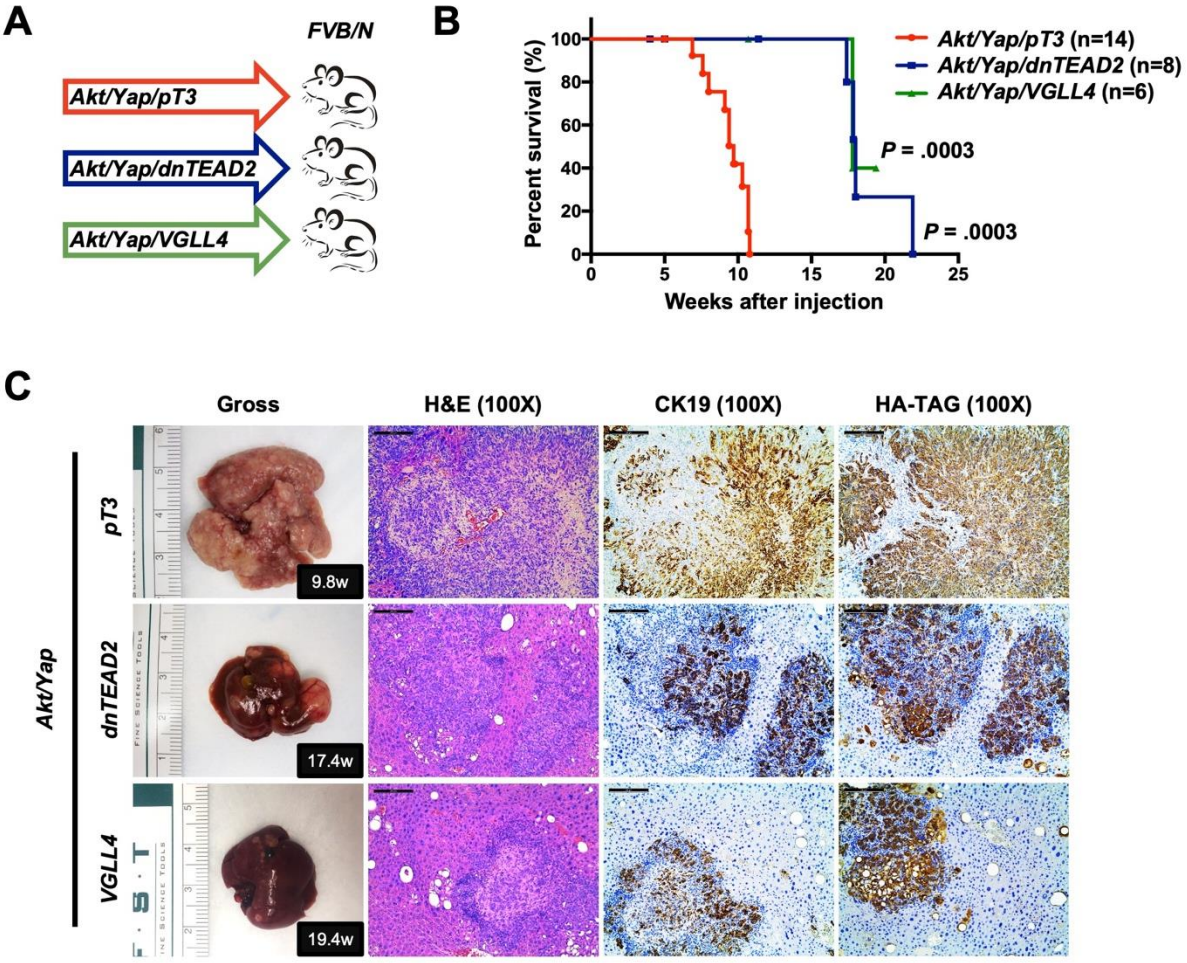
A
FVB/N
Akt/Yap/pT3
Akt/Yap/dnTEAD2
Akt/Yap/VGLL4
B
Percent survival (%)
100
80
60
40
20
0
0
5
10
15
20
25
Weeks after injection
Akt/Yap/pT3 (n=14)
Akt/Yap/dnTEAD2 (n=8)
Akt/Yap/VGLL4 (n=6)
P = .0003
P = .0003
C
Gross
H&E (100X)
CK19 (100X)
HA-TAG (100X)
Akt/Yap
pT3
dnTEAD2
VGLL4
9.8w
17.4w
19.4w

Supplementary Figure 7. Inhibition of Yap/TEADs robustly suppresses iCCA development in mice.

(A) Study design. *FVB/N* mice were subjected to HTVi of either *Akt/Yap/pT3* (n=14), *Akt/*Yap*/dnTEAD2* (n=8) or *Akt/Yap/VGLL4* (n=6) plasmids. (B) Mouse survival curves. (C) Representative gross images, H&E, and immunohistochemistry for CK19 and HA-TAG of liver sections from *Akt/Yap/pT3* (9.8w.p.i), *Akt/*Yap*/dnTEAD2* (M17.4w.p.i), and *Akt/Yap/VGLL4* (M19.4w.p.i) mice. Scale bar: 100 μm (100x). Abbreviations: H&E, hematoxylin and eosin staining; M, male; F, female; w.p.i, weeks post-injection.

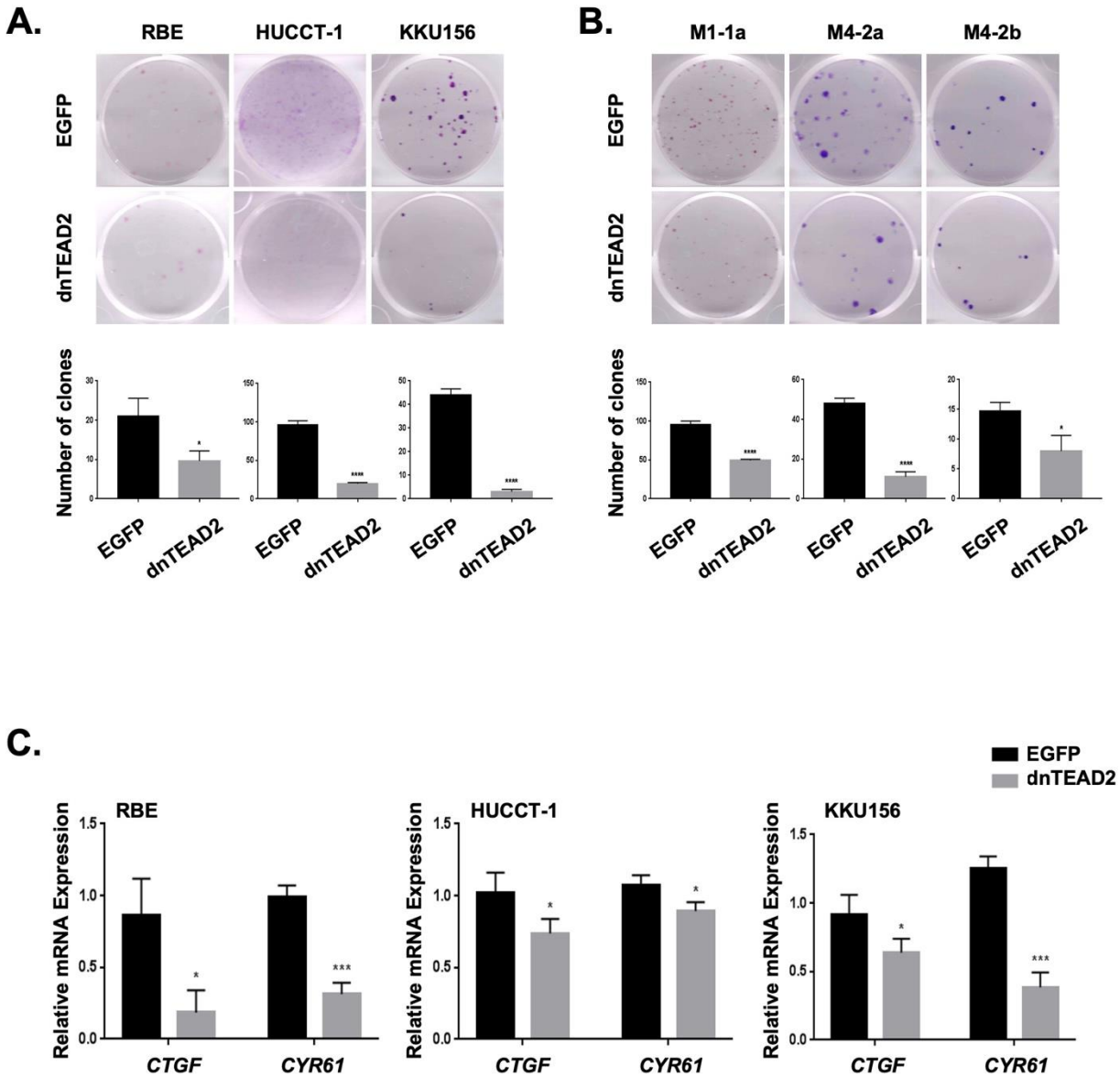
A.
RBE
HUCCT-1
KKU156
EGFP
dnTEAD2
Number of clones
EGFP
dnTEAD2
B.
M1-1a
M4-2a
M4-2b
EGFP
dnTEAD2
Number of clones
EGFP
dnTEAD2
C.
EGFP
dnTEAD2
RBE
HUCCT-1
KKU156
Relative mRNA Expression
CTGF
CYR61

Supplementary Figure 8. Overexpression of dnTEAD2 suppresses iCCA growth and Yap target expression in intrahepatic cholangiocarcinoma (iCCA) cell lines.

(A, B) (A) Human CCA and (B) mouse iCCA cells were transfected with plenti-EGFP or plenti-dnTEAD2 plasmids. The colony formation assay was performed to detect the ability of a single cell to grow into a colony. Quantification of colonies in each group. (C) mRNA expression of *CTGF* and *CYR61*. Data were analyzed by the Mann-Whitney test. Statistical significance: **P* < .05, ***P* < .01, *****P* < .0001.

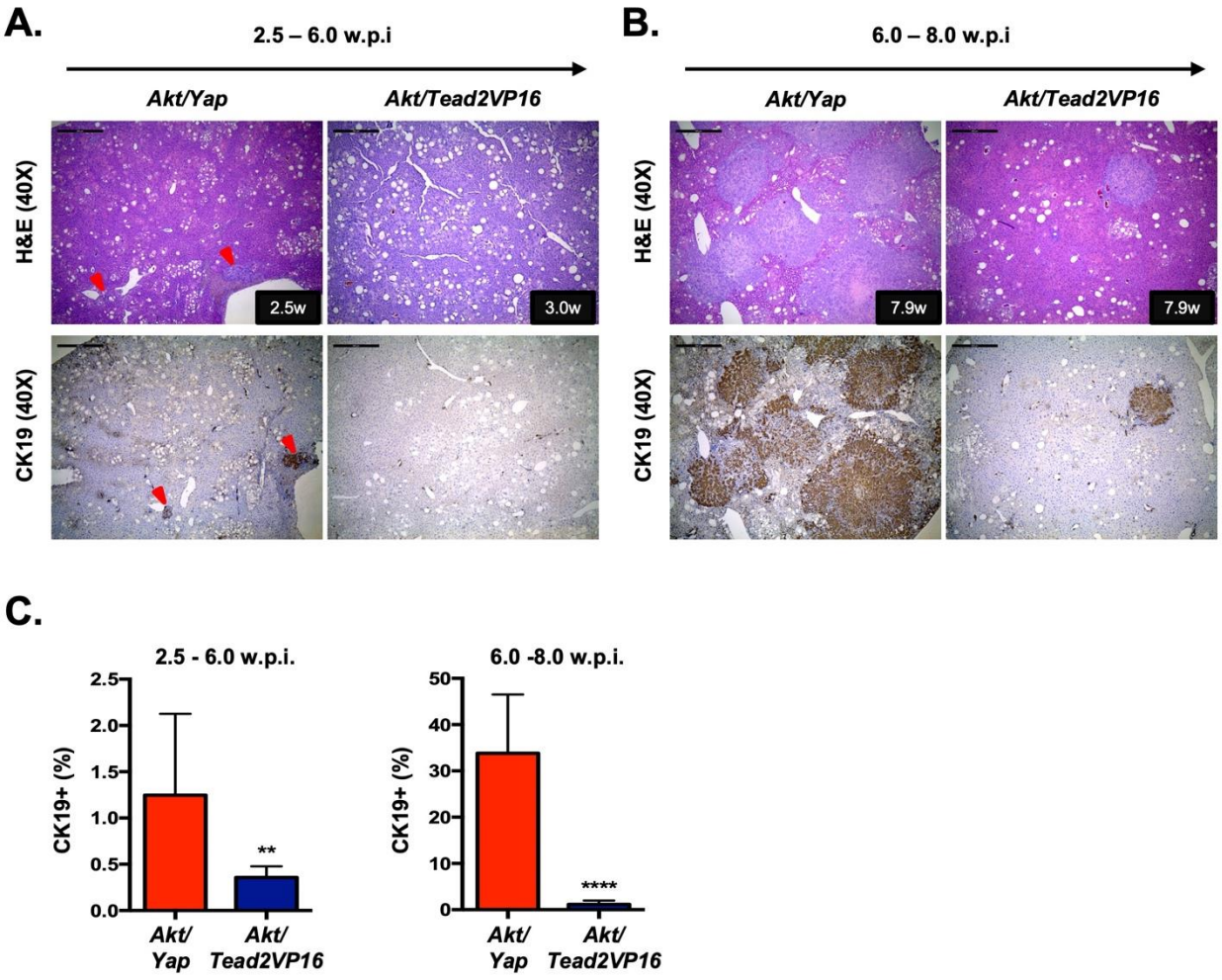
A.
2.5 – 6.0 w.p.i
Akt/Yap
Akt/Tead2VP16
H&E (40X)
CK19 (40X)
2.5w
3.0w
B.
6.0 – 8.0 w.p.i
Akt/Yap
Akt/Tead2VP16
H&E (40X)
CK19 (40X)
7.9w
7.9w
C.
2.5 - 6.0 w.p.i.
CK19+ (%)
2.5
2.0
1.5
1.0
0.5
0.0
**
Akt/ Yap
Akt/ Tead2VP16
6.0 -8.0 w.p.i.
CK19+ (%)
50
40
30
20
10
0
****
Akt/ Yap
Akt/ Tead2VP16

Supplementary Figure 9. *Akt/Tead2VP16* mice exhibit a significant delay of tumor initiation compared with *Akt/Yap* mice.

(A, B) H&E and immunohistochemical staining of CK19 in liver tissues from *Akt/Yap* and *Akt/Tead2VP16* mice at (A) 2.5 to 6.0 w.p.i. or (B) 6.0 to 8.0 w.p.i. (C) Quantification of the CK19 positive area in liver sections from the depicted mice. Statistical significance: ***P* < .01, *****P* < .0001. Abbreviations: H&E, hematoxylin and eosin staining; w.p.i, weeks post-injection.

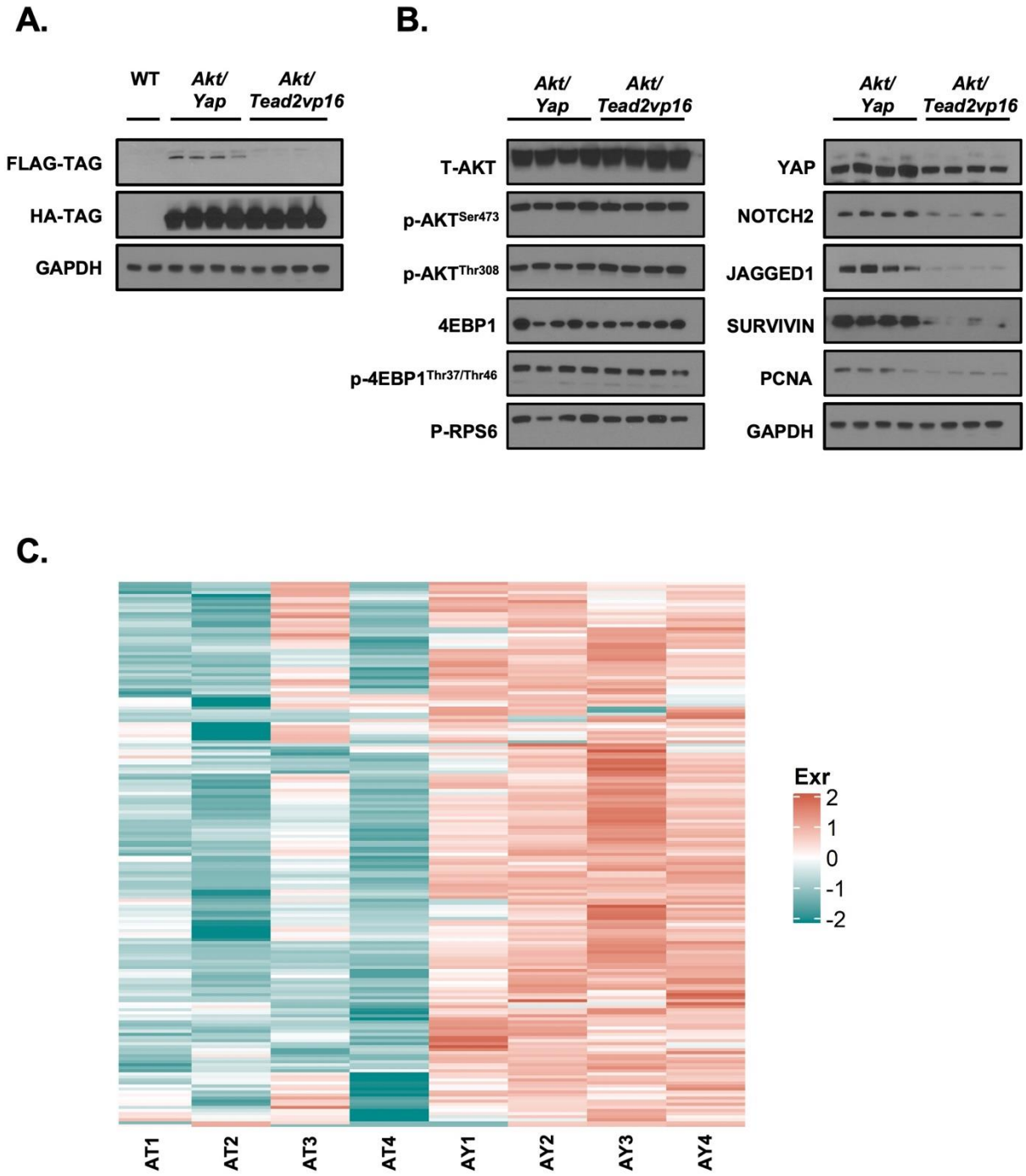
A.
WT
Akt/ Yap
Akt/ Tead2vp16
FLAG-TAG
HA-TAG
GAPDH
B.
Akt/ Yap
Akt/ Tead2vp16
T-AKT
p-AKTSer473
p-AKTThr308
4EBP1
p-4EBP1Thr37/Thr46
P-RPS6
Akt/ Yap
Akt/ Tead2vp16
YAP
NOTCH2
JAGGED1
SURVIVIN
PCNA
GAPDH
C.
Exr
2
1
0
-1
-2
AT1
AT2
AT3
AT4
AY1
AY2
AY3
AY4

Supplementary Figure 10. Molecular differences between *Akt/Yap* iCCA and *Akt/Tead2VP16* iCCA lesions.

(A) Western blot analysis revealing the overexpression of exogenous tagged oncogenes in *Akt/Yap* and *Akt/Tead2VP16* iCCA. (B) Western blot analysis of AKT and NOTCH signaling levels, YAP, β-Catenin, and cell proliferation-related proteins of tumor tissues from *Akt/Yap* and *Akt/Tead2VP16* mice. GAPDH was used as a loading control. (C) Heatmap of the expression of Yap target genes in *Akt/Yap* and *Akt/Tead2VP16* iCCA lesions. Red, up-regulated; green, down-regulated. Abbreviations: AT, *Akt/Tead2VP16* iCCA; AY, *Akt/Yap* iCCA.

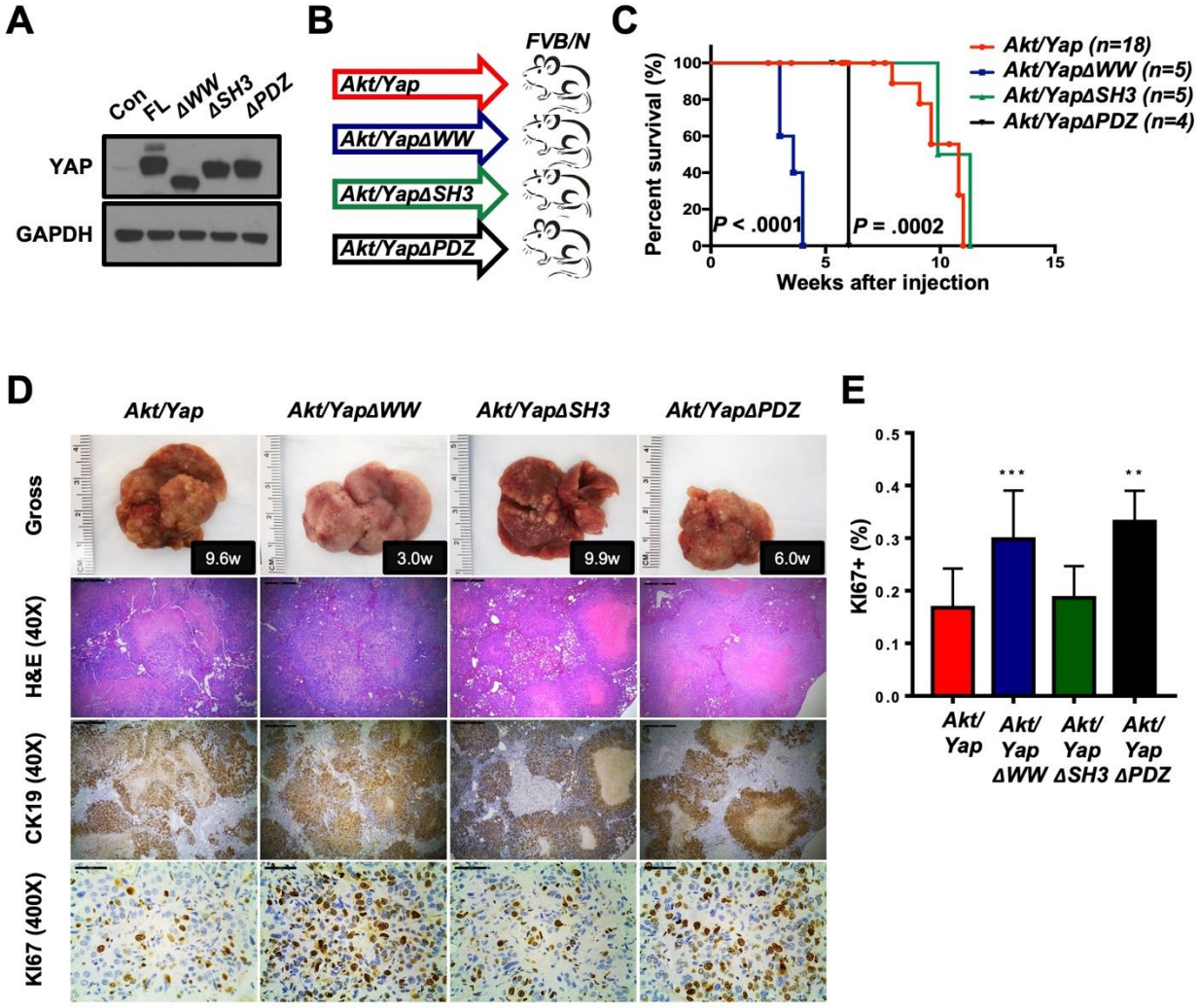
A
Con
FL
ΔWW
ΔSH3
ΔPDZ
YAP
GAPDH
B
FVB/N
Akt/Yap
Akt/YapΔWW
Akt/YapΔSH3
Akt/YapΔPDZ
C
Akt/Yap (n=18)
Akt/YapΔWW (n=5)
Akt/YapΔSH3 (n=5)
Akt/YapΔPDZ (n=4)
Percent survival (%)
100
80
60
40
20
0
P < .0001
P = .0002
0
5
10
15
Weeks after injection
D
Akt/Yap
Akt/YapΔWW
Akt/YapΔSH3
Akt/YapΔPDZ
Gross
9.6w
3.0w
9.9w
6.0w
H&E (40X)
CK19 (40X)
KI67 (400X)
E
KI67+ (%)
0.5
0.4
0.3
0.2
0.1
0.0
***
**
Akt/ Yap
Akt/ Yap ΔWW
Akt/ Yap ΔSH3
Akt/ Yap ΔPDZ

Supplementary Figure 11. YAP WW, SH3, and PDZ domains play inhibitory functions in *Akt/Yap* tumorigenesis.

(A) Western blot showing the expression of YAP and truncated YAP mutants. 293FT cells were transfected with full-length *YAP* (FL) or truncated *YAP,* progressively deleting WW, SH3, or PDZ domain. Untreated 239FT cells were used as a control (Con). (B) Study design. *FVB/N* mice were subjected to HTVi of either *Akt/Yap* (control, n=18), *Akt/*Yap∆*WW* (n=5), *Akt/Yap*∆*SH3* (n=5), or *Akt/Yap*∆*PDZ* (n=4) plasmids. The indicated mice, *Akt/YapS94A* (Fig.1B), and *Akt/Tead2VP16* (Fig.2B) mice were generated in parallel. (C) Mouse survival curves. (D) Representative gross images, H&E, and immunohistochemistry for CK19 and KI67 of liver sections from *Akt/Yap* (F9.6w.p.i), *Akt/*Yap∆*WW* (M3.0w.p.i), *Akt/Yap*∆*SH3* (M9.9w.p.i), or *Akt/Yap*∆*PDZ* (F6.0w.p.i) mice. (E) Quantification of KI67 positive nuclei in the indicated mouse livers. Statistical significance: ***P* < .01, *** *P* < .001. Scale bar: 500 μm (40x) and 50 μm (400x). Abbreviations: H&E, hematoxylin and eosin staining; w.p.i, weeks post-injection.

A

Group	N Genes	Direction	FC	P Value
AT vs AY	890	Down	>2.0	*P* < .05
AT vs AY	464	Up	>2.0	*P* < .05

B

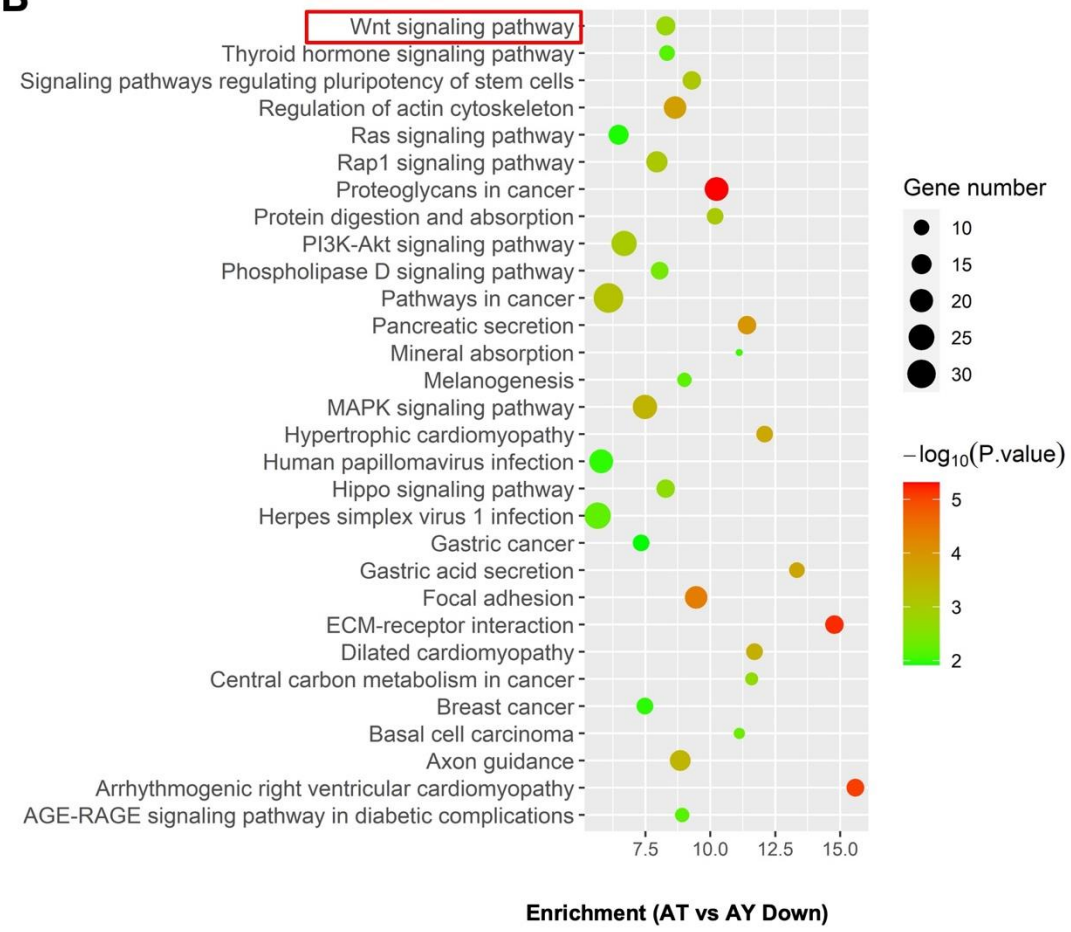

Supplementary Figure 12. RNA sequencing of *Akt/Tead2VP16* and *Akt/Yap* iCCA lesions.

(A) Significant downregulated and upregulated genes in *Akt/Tead2VP16* iCCA lesions when compared with *Akt/Yap* iCCA lesions are shown in the Table. (B) KEGG analysis of downregulated genes in *Akt/Tead2VP16* iCCA lesions. Genes were ranked by *P*-value. Abbreviations: AT, *Akt/Tead2VP16* iCCA; AY, *Akt/Yap* iCCA; FC, fold change.

A

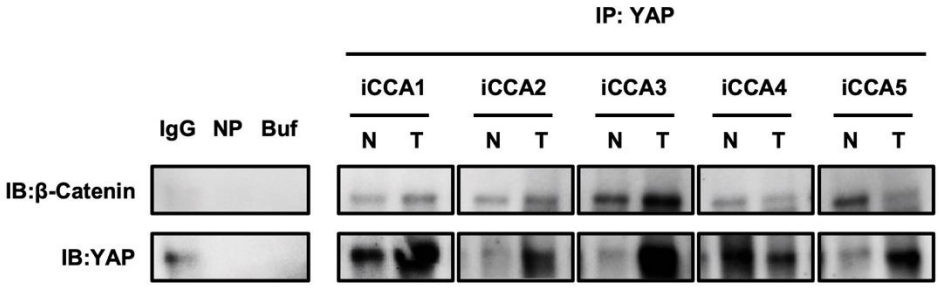
IP: YAP
iCCA1
iCCA2
iCCA3
iCCA4
iCCA5
IgG NP Buf
N T N T N T N T N T
IB:β-Catenin
IB:YAP

B

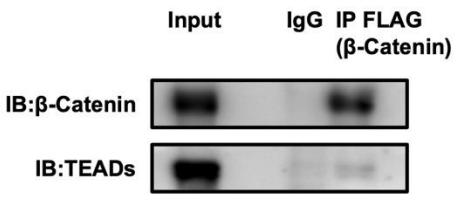
Input
IgG
IP FLAG
(β-Catenin)
IB:β-Catenin
IB:TEADs

Supplementary Figure 13. β-Catenin interacts with YAP and TEAD factors in human intrahepatic cholangiocarcinomas (iCCAs).

(A) Human liver tissues were homogenized in RIPA buffer. Lysates were precleared with Protein A/G PLUS-Agarose and incubated with anti-YAP antibody or IgG. Western blotting of endogenous β-Catenin protein coimmunoprecipitating with endogenous YAP protein (IP) from human liver tissues extracts. IgG co-precipitating protein (IgG), protein A/G PLUS-Agarose conjugated with antibody (NP), and RIPA buffer (Buf) were loaded as the negative control. (B) Co-immunoprecipitation assays to detect β-Catenin and TEADs interaction. Lysates from RBE cells overexpressed with FLAG-β-Catenin-WT were subjected to immunoprecipitation with an anti-FLAG antibody. Western blotting of β-Catenin protein coimmunoprecipitating with endogenous Pan-TEADs protein (IP) from cell extracts. Abbreviations: N, surrounding non-tumorous liver; T: intrahepatic cholangiocarcinoma.

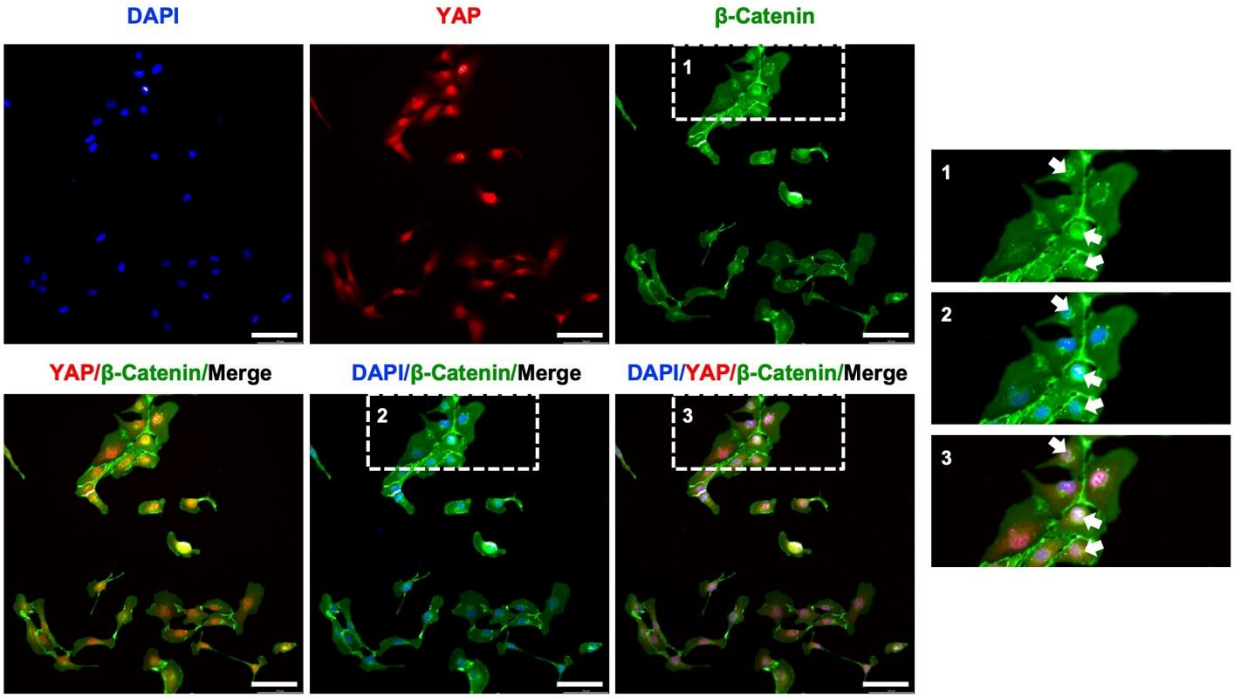
DAPI
YAP
β-Catenin
1
YAP/β-Catenin/Merge
DAPI/β-Catenin/Merge
DAPI/YAP/β-Catenin/Merge
2
3
1
2
3

Supplementary Figure 14. YAP and β-Catenin nuclear co-localization occurs in a small subset of RBE cells.

Immunofluorescence staining of DAPI (Blue), YAP (Red), and β-Catenin (Green) in RBE cells. White arrows in panel 1 and panel 2 indicate positive β-Catenin nuclear staining. White arrows in panel 3 indicate YAP and β-Catenin nuclear co-localization. Scale bar: 100 μm.

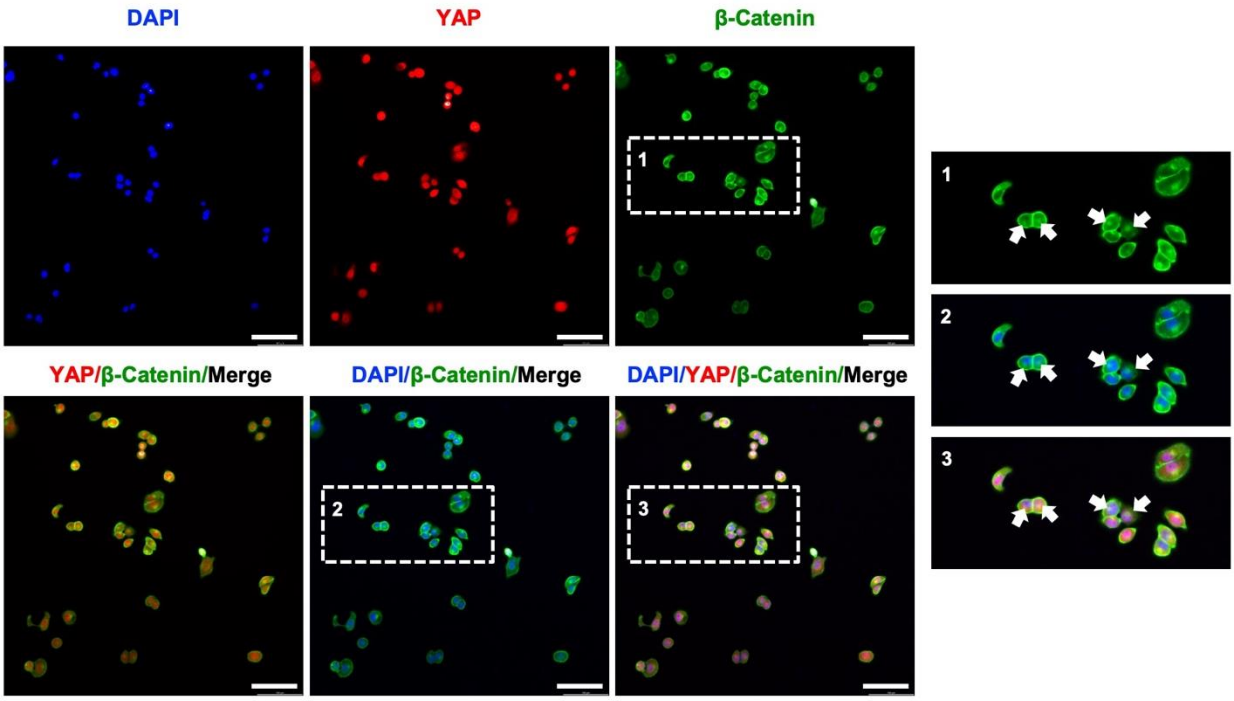
DAPI
YAP
β-Catenin
1
YAP/β-Catenin/Merge
DAPI/β-Catenin/Merge
DAPI/YAP/β-Catenin/Merge
2
3
1
2
3

Supplementary Figure 15. YAP and β-Catenin nuclear co-localization occurs in a small subset of KKU156 cells.

Immunofluorescence staining of DAPI (Blue), YAP (Red), and β-Catenin (Green) in KKU156 cells. White arrows in panel 1 and panel 2 indicate positive β-Catenin nuclear staining. White arrows in panel 3 indicate YAP and β-Catenin nuclear co-localization. Scale bar: 100 μm.

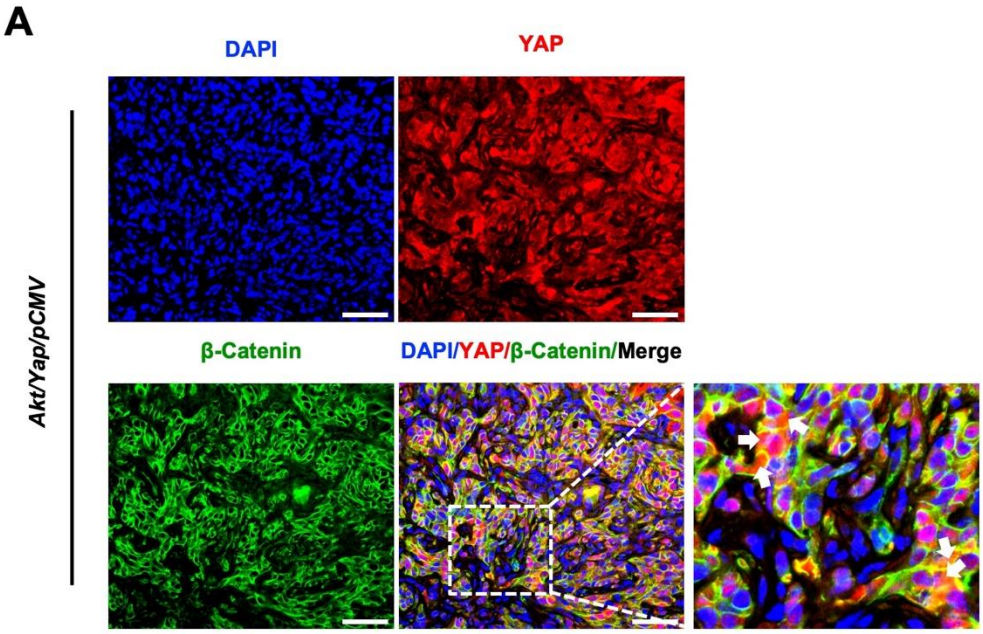
A
DAPI
YAP
Akt/Yap/pCMV
β-Catenin
DAPI/YAP/β-Catenin/Merge

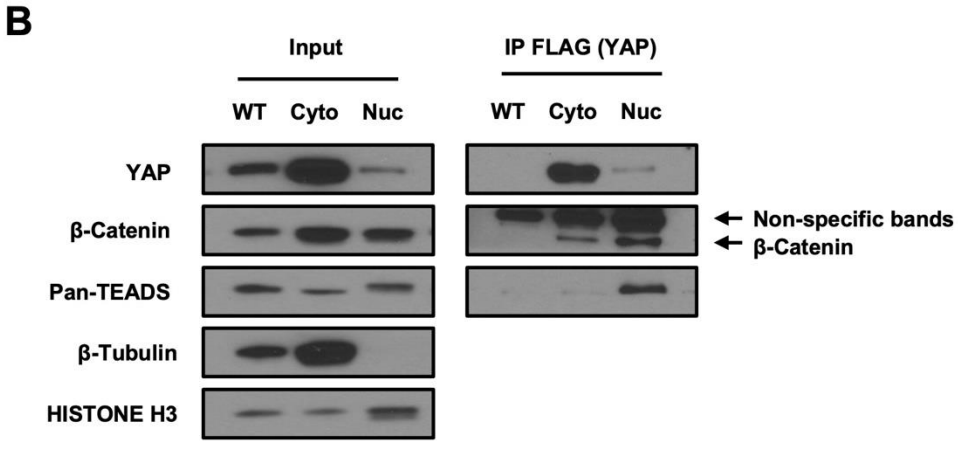
B
Input
IP FLAG (YAP)
WT
Cyto
Nuc
WT
Cyto
Nuc
YAP
β-Catenin
Pan-TEADS
β-Tubulin
HISTONE H3
Non-specific bands
β-Catenin

Supplementary Figure 16. Direct interaction of YAP and β-Catenin in the cytoplasm and nucleus of *Akt/Yap* iCCAs.

(A) Immunofluorescence staining of DAPI (Blue), YAP (Red), and β-Catenin (Green) in *Akt/Yap* iCCA sections. White arrows indicate YAP and β-Catenin nuclear co-localization. (B) The cytoplasmic and nuclear extracts from *Akt/Yap* iCCAs were isolated and subjected to immunoprecipitation with anti-FLAG beads. Lysates from *FVB/N* wildtype mouse livers were used as a control. Co-precipitating proteins were visualized by Western blotting. Scale bar: 100 μm. Abbreviations: WT, wildtype; Cyto, cytoplasm; Nuc, nucleus.

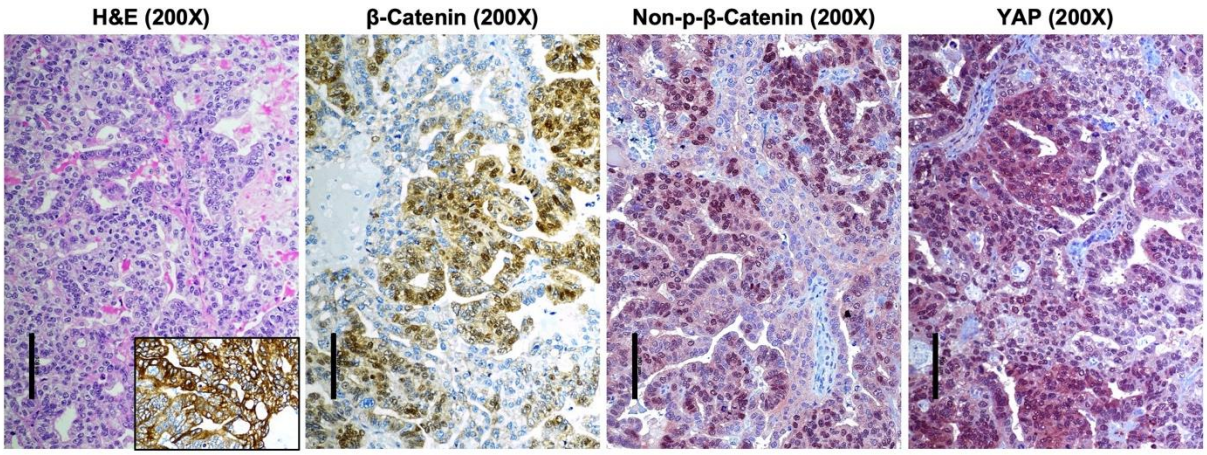
H&E (200X)
β-Catenin (200X)
Non-p-β-Catenin (200X)
YAP (200X)

Supplementary Figure 17. Concomitant nuclear and cytoplasmic immunoreactivity for β-catenin and YAP in human intrahepatic cholangiocarcinoma (iCCA).

H&E and immunohistochemical staining of total β-catenin, activated/non-phosphorylated β-Catenin (non-p-β-Catenin), and YAP in human iCCA sections. CK19 was used as a biliary marker (inset). Scale bar: 100μm (200X). Abbreviation: H&E, hematoxylin and eosin staining.

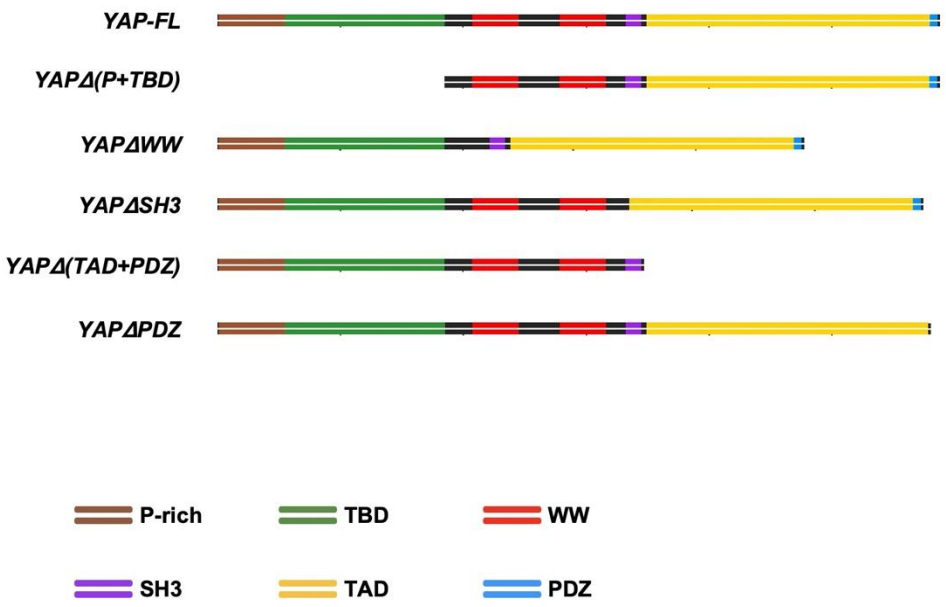
YAP-FL
YAPΔ(P+TBD)
YAPΔWW
YAPΔSH3
YAPΔ(TAD+PDZ)
YAPΔPDZ
P-rich
TBD
WW
SH3
TAD
PDZ

Supplementary Figure 18. Schematic representation of *YAP* deletion mutants.

Panels showing the full-length *YAP* (*YAP-FL*) and *YAP* deletion mutants, progressively deleting the P-rich and TEADs binding (TBD) domains (*YAP*Δ*(P+TBD)*), two WW domains (*YAP*Δ*WW*), SH3-binding domain (*YAP*Δ*SH3*), the transcriptional activation (TAD) and PDZ-binding domains (*YAP*Δ*(TAD+PDZ)*), and a C-terminal PDZ-binding domain *(YAP*Δ*PDZ*).

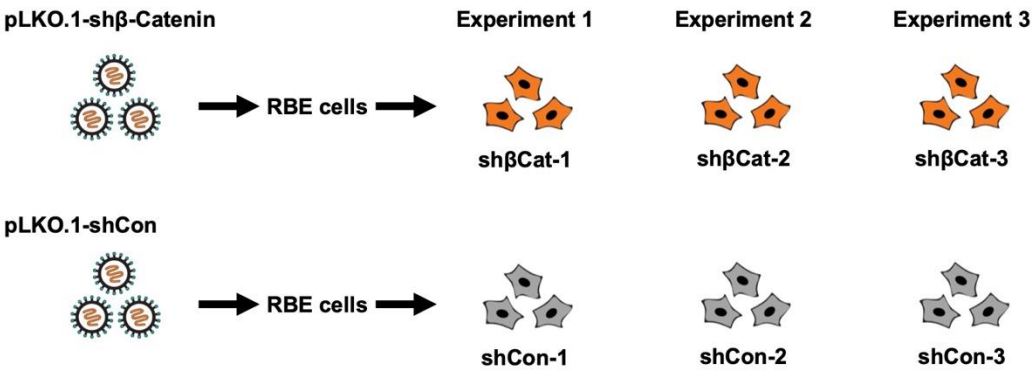
pLKO.1-shβ-Catenin
Experiment 1
Experiment 2
Experiment 3
RBE cells
shβCat-1
shβCat-2
shβCat-3
pLKO.1-shCon
RBE cells
shCon-1
shCon-2
shCon-3

Supplementary Figure 19. Study design of RNA sequencing in β-Catenin knockdown iCCA cell lines.

Human RBE cells transfected with pLKO.1-shCon (shCon, n=3) or pLKO.1-shβ-Catenin (shβCat, n=3) through lentivirus transduction were prepared for RNA sequencing.

A

Group	N Genes	Direction	FC	P Value
shβCat vs shCon	3338	Down	>1.3	*P* < .05
shβCat vs shCon	3259	Up	>1.3	*P* < .05

B

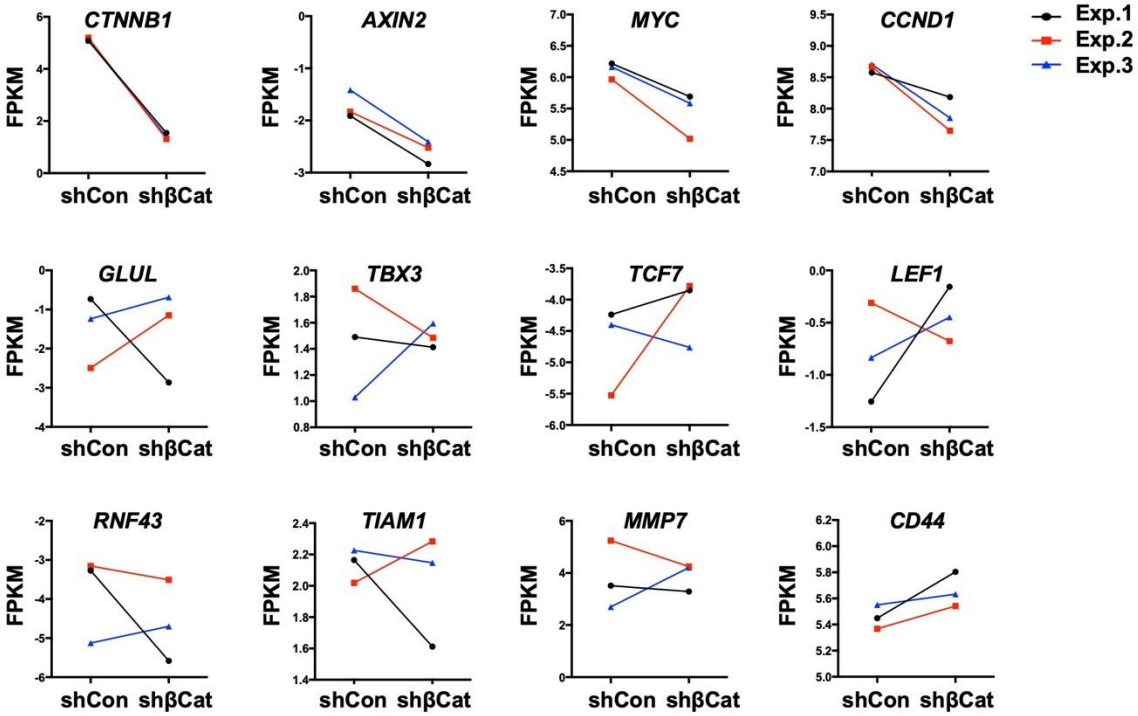

C

GO:ID	Term	N genes downregulated by shβCat	P value
GO: 0060070	Canonical Wnt signaling pathway (358 genes)	77	ns

Supplementary Figure 20. Silencing of β-Catenin in iCCA does not affect the expression of canonical Wnt targets.

(A) Significant downregulated and upregulated genes in β-Catenin knockdown RBE cells were shown in Table. (B) Fragments per kilobase of transcript per million mapped reads (FPKM) results of *CTNNB1*, *AXIN2*, *MYC*, *CCND1*, and liver-specific Wnt canonical target genes expression. (C) RNA sequencing analysis showing that Wnt canonical pathway-related genes were not enriched in those genes downregulated by β-Catenin knockdown. Abbreviations: FC, fold change; ns, not significant.

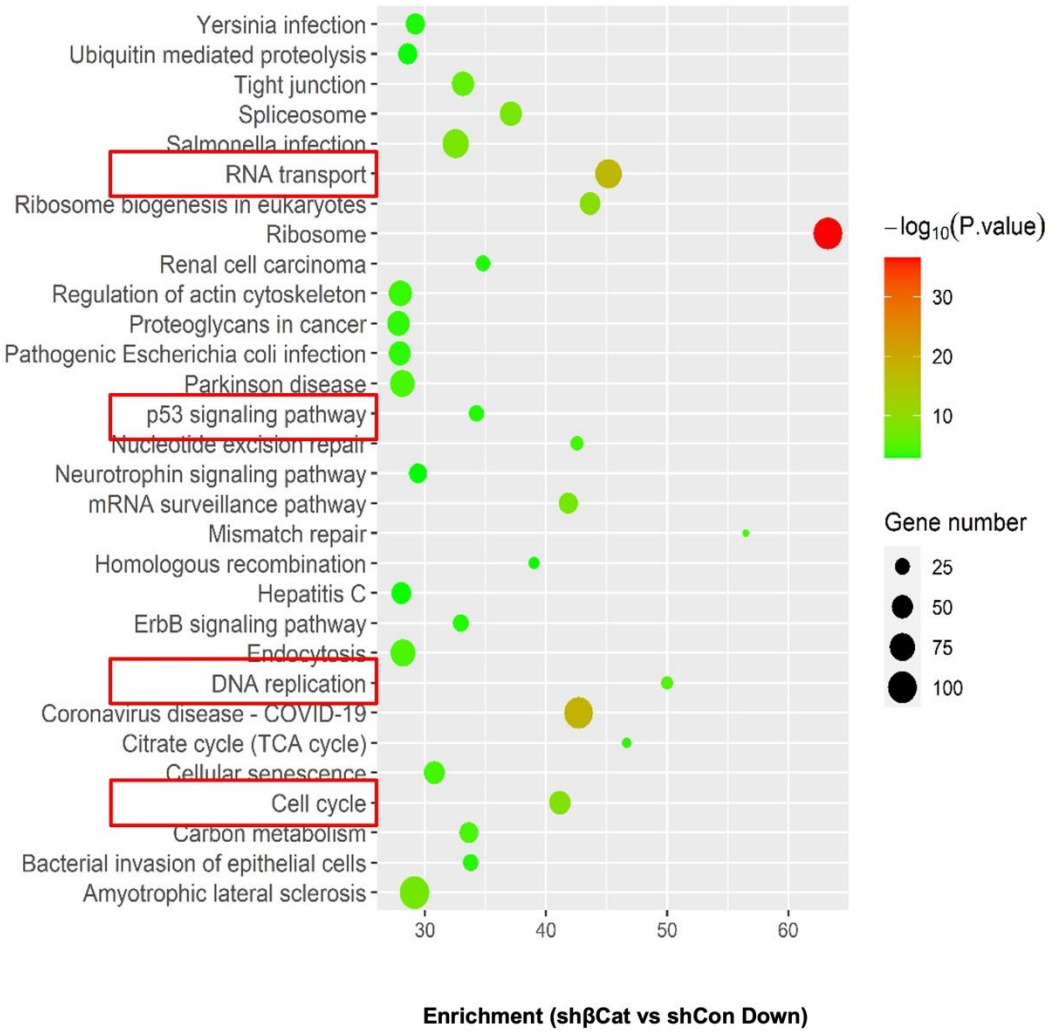
Yersinia infection
Ubiquitin mediated proteolysis
Tight junction
Spliceosome
Salmonella infection
RNA transport
Ribosome biogenesis in eukaryotes
Ribosome
Renal cell carcinoma
Regulation of actin cytoskeleton
Proteoglycans in cancer
Pathogenic Escherichia coli infection
Parkinson disease
p53 signaling pathway
Nucleotide excision repair
Neurotrophin signaling pathway
mRNA surveillance pathway
Mismatch repair
Homologous recombination
Hepatitis C
ErbB signaling pathway
Endocytosis
DNA replication
Coronavirus disease - COVID-19
Citrate cycle (TCA cycle)
Cellular senescence
Cell cycle
Carbon metabolism
Bacterial invasion of epithelial cells
Amyotrophic lateral sclerosis
30
40
50
60
Enrichment (shβCat vs shCon Down)
−log10(P.value)
30
20
10
Gene number
25
50
75
100

Supplementary Figure 21. KEGG analysis of downregulated genes in β-Catenin silenced RBE cells.

β-Catenin silencing leads to the downregulation of genes enriched in RNA transport, p53 signaling pathway, DNA replication, and cell cycle pathway (Red inserts). Genes were ranked by *P*-value.

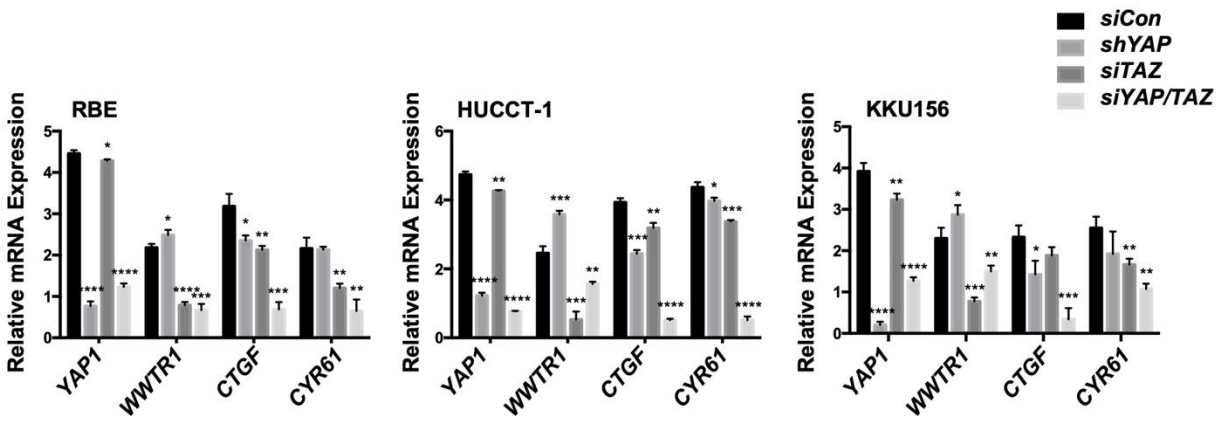
siCon
shYAP
siTAZ
siYAP/TAZ
RBE
HUCCT-1
KKU156
Relative mRNA Expression
YAP1
WWTR1
CTGF
CYR61

Supplementary Figure 22. YAP and TAZ have redundant roles in regulating iCCA.

RBE, HUCCT-1, and KKU156 cells were transfected with *siCon*, *siYAP*, *siTAZ*, or *siYAP/siTAZ* and cultured for 48 hours. qRT-PCR detected the mRNA expression of *YAP1*, *TAZ(WWTR1)*, *CTGF*, and *CYR61*. Data were analyzed by the Mann-Whitney test. Statistical significance: **P* < .05, ***P* < .01, ****P* < .001, *****P* < .0001. Abbreviations: *siCon*, scrambled small interfering RNA; *siYAP*, small interfering RNA targeting *YAP*; *siTAZ*, small interfering RNA targeting *TAZ*.

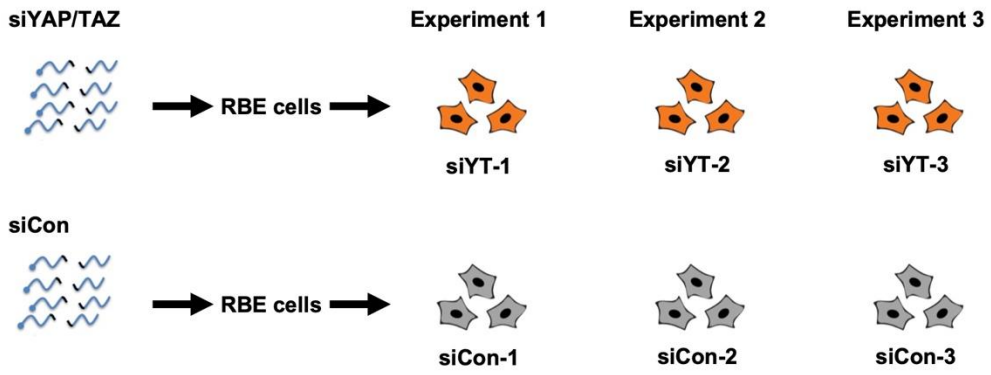
siYAP/TAZ
Experiment 1
Experiment 2
Experiment 3
RBE cells
siYT-1
siYT-2
siYT-3
siCon
RBE cells
siCon-1
siCon-2
siCon-3

Supplementary Figure 23. Study design of RNA sequencing analysis in YAP/TAZ silenced iCCA cells.

Human RBE cells transfected with scrambled *siRNA* (siCon, n=3) or *siRNA* targeting *YAP/TAZ* (siYT, n=3) were prepared for RNA sequencing. Abbreviation: *siCon*, scrambled small interfering RNA.

A

Group	N Genes	Direction	FC	P Value
siYT vs siCon	2519	Down	>1.3	*P* < .05
siYT vs siCon	1994	Up	>1.3	*P* < .05

B

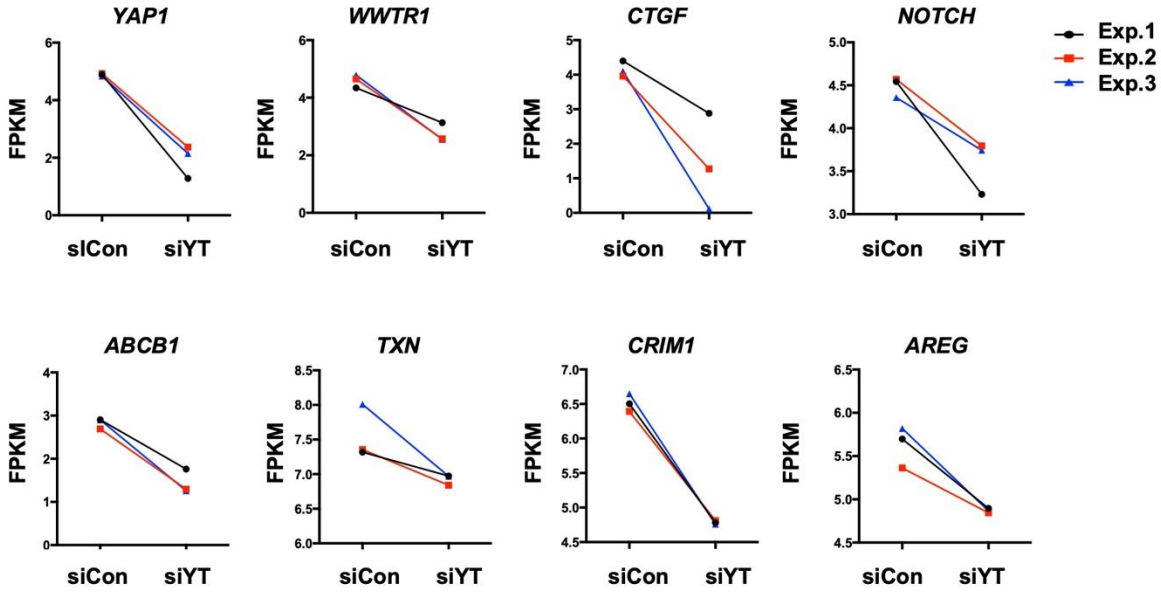

Supplementary Figure 24. YAP/TAZ silencing leads to consistent downregulation of a set of genes identified in β-Catenin silenced iCCA cells.

(A) Significant downregulated and upregulated genes in YAP/TAZ silenced RBE cells were shown in Table. (B) Fragments per kilobase of transcript per million mapped reads (FPKM) results of *YAP1*, *WWTR1*, *CTGF*, *CYR61*, *NOTCH2*, *ABCB1*, *TXN*, *CRIM1,* and *AREG* expression. Abbreviation: FC, fold change.

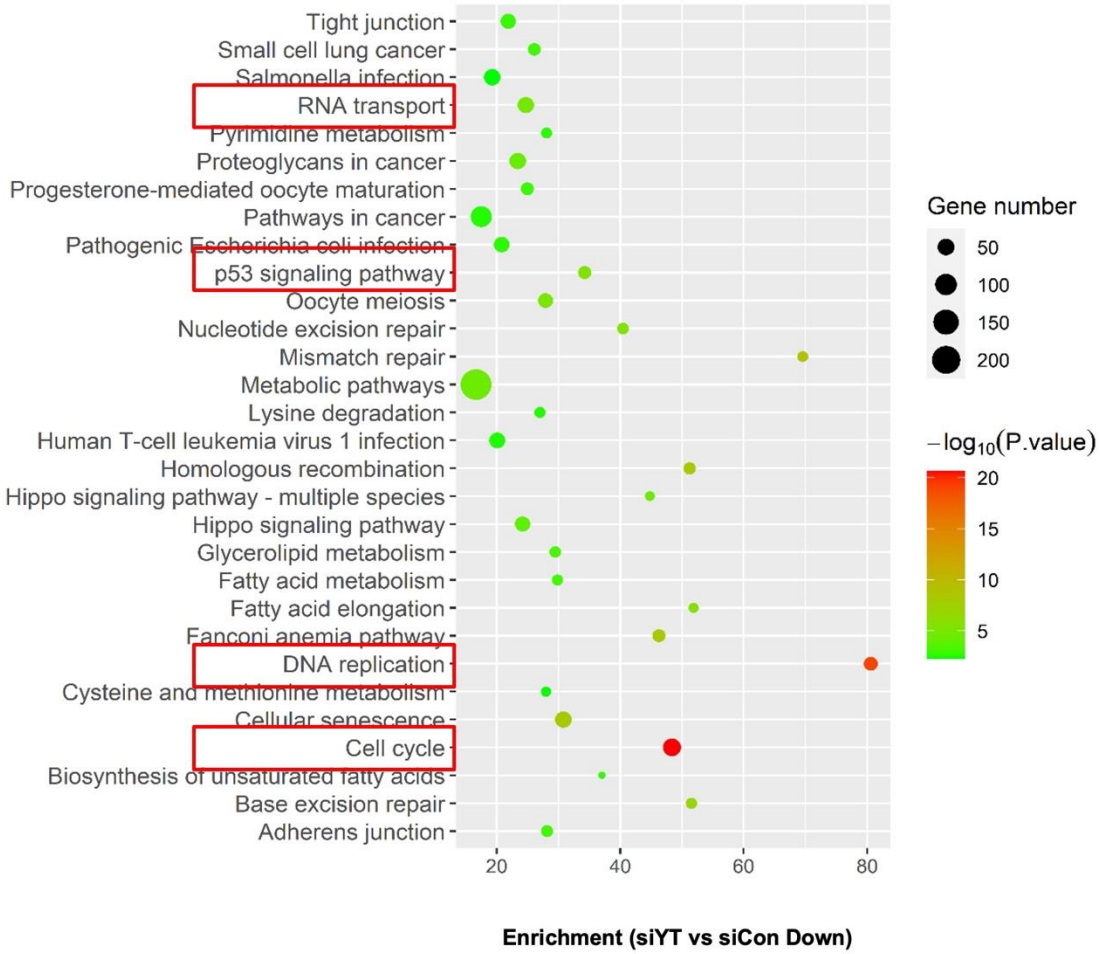
Tight junction
Small cell lung cancer
Salmonella infection
RNA transport
Pyrimidine metabolism
Proteoglycans in cancer
Progesterone-mediated oocyte maturation
Pathways in cancer
Pathogenic Escherichia coli infection
p53 signaling pathway
Oocyte meiosis
Nucleotide excision repair
Mismatch repair
Metabolic pathways
Lysine degradation
Human T-cell leukemia virus 1 infection
Homologous recombination
Hippo signaling pathway - multiple species
Hippo signaling pathway
Glycerolipid metabolism
Fatty acid metabolism
Fatty acid elongation
Fanconi anemia pathway
DNA replication
Cysteine and methionine metabolism
Cellular senescence
Cell cycle
Biosynthesis of unsaturated fatty acids
Base excision repair
Adherens junction
20
40
60
80
Enrichment (siYT vs siCon Down)
Gene number
50
100
150
200
−log10(P.value)
20
15
10
5

Supplementary Figure 25. KEGG analysis of downregulated genes in YAP/TAZ silenced RBE cells.

YAP/TAZ knockdown leads to downregulation of genes enriched in RNA transport, p53 signaling pathway, DNA replication, and cell cycle pathway (Red inserts). Genes were ranked by *P*-value.

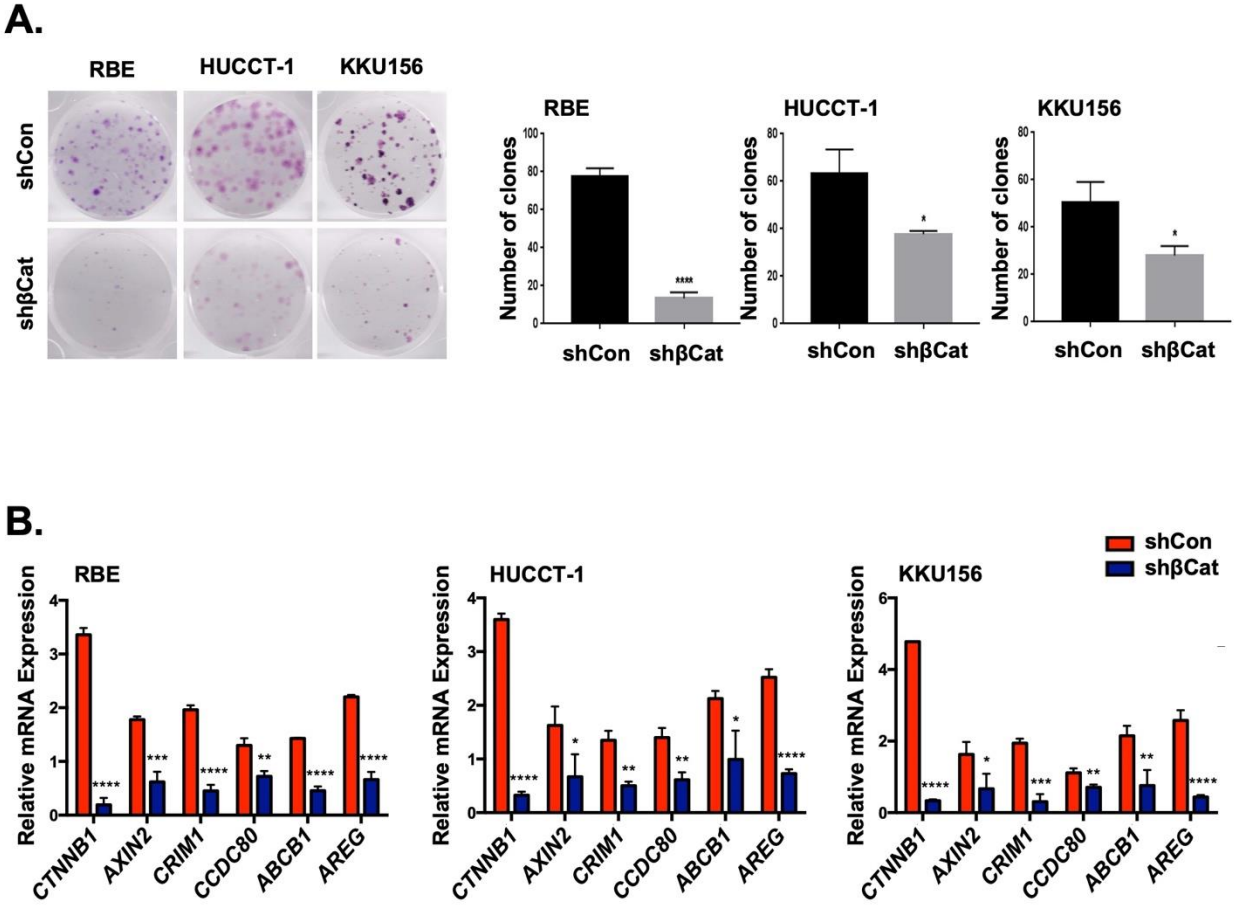
A.
RBE
HUCCT-1
KKU156
shCon
shβCat
Number of clones
shCon
shβCat
B.
Relative mRNA Expression
CTNNB1
AXIN2
CRIM1
CCDC80
ABCB1
AREG

Supplementary Figure 26. Silencing of β-Catenin in iCCA inhibits cell growth and YAP targets transcription in human intrahepatic cholangiocarcinoma (iCCA) cell lines.

Human iCCA cells were stably transfected with pLKO.1-shCon or pLKO.1-shβ-Catenin through lentivirus transduction, respectively. (A) Representative images of colony formation assays in transfected RBE, HUCCT-1, and KKU156 cells. Quantification of colonies in each group. (B) mRNA expressions of *CTNNB1*, *AXIN2*, and YAP target genes. Data were analyzed using the Mann-Whitney test. Statistical significance: **P* < .05, ***P* < .01, ****P* < .001, *****P* < .0001.

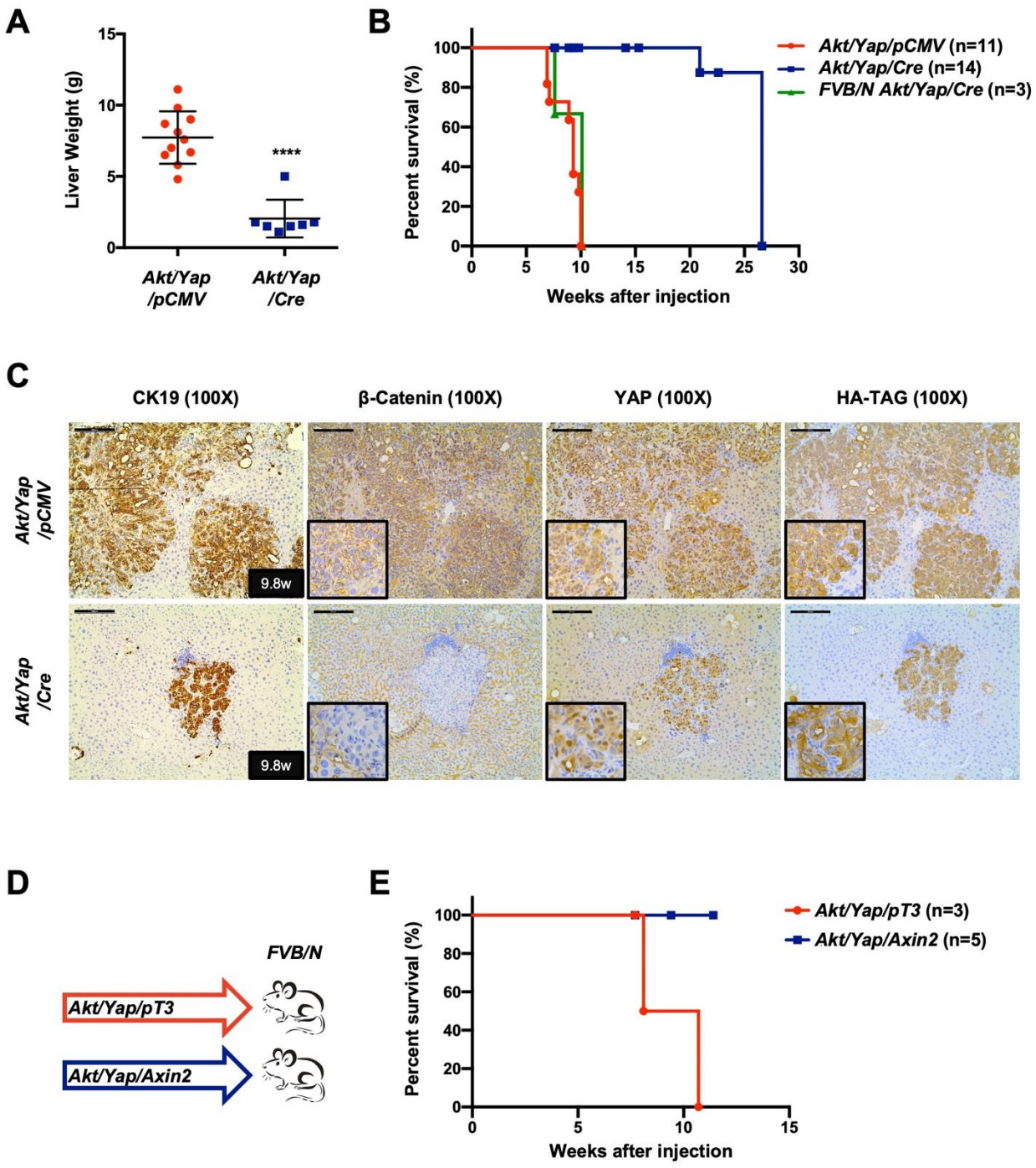
A
Liver Weight (g)
15
10
5
0
****
Akt/Yap /pCMV
Akt/Yap /Cre
B
Percent survival (%)
100
80
60
40
20
0
0
5
10
15
20
25
30
Weeks after injection
Akt/Yap/pCMV (n=11)
Akt/Yap/Cre (n=14)
FVB/N Akt/Yap/Cre (n=3)
C
CK19 (100X)
β-Catenin (100X)
YAP (100X)
HA-TAG (100X)
Akt/Yap /pCMV
Akt/Yap /Cre
9.8w
9.8w
D
FVB/N
Akt/Yap/pT3
Akt/Yap/Axin2
E
Percent survival (%)
100
80
60
40
20
0
0
5
10
15
Weeks after injection
Akt/Yap/pT3 (n=3)
Akt/Yap/Axin2 (n=5)

Supplementary Figure 27. Deletion or suppression of β-catenin inhibits liver tumor development.

(A) Liver weight of *Ctnnb1*$^{flox/flox}$ *Akt/Yap/pCMV* and *Akt/Yap/Cre* mice. Statistical significance: ****$P < .0001$. (B) *FVB/N* mice were co-injected with *Akt/Yap/Cre* (n=3) plasmids. Mouse survival curves. (C) Immunohistochemical staining of CK19, β-Catenin, YAP, and HA-TAG in *Ctnnb1*$^{flox/flox}$ *Akt/Yap/pCMV* (M9.8w.p.i) and *Akt/Yap/Cre* (M9.8w.p.i) iCCA lesions. (D) Study design. *FVB/N* mice were subjected to HTVi of either *Akt/Yap/pT3* (n=3) or *Akt/Yap/Axin2* (n=5) plasmids. (E) Survival curves of *Akt/Yap/pT3* and *Akt/Yap/Axin2* mice. Scale bar: 100 μm (100x). Abbreviations: M, male; F, female; w.p.i, weeks post-injection.

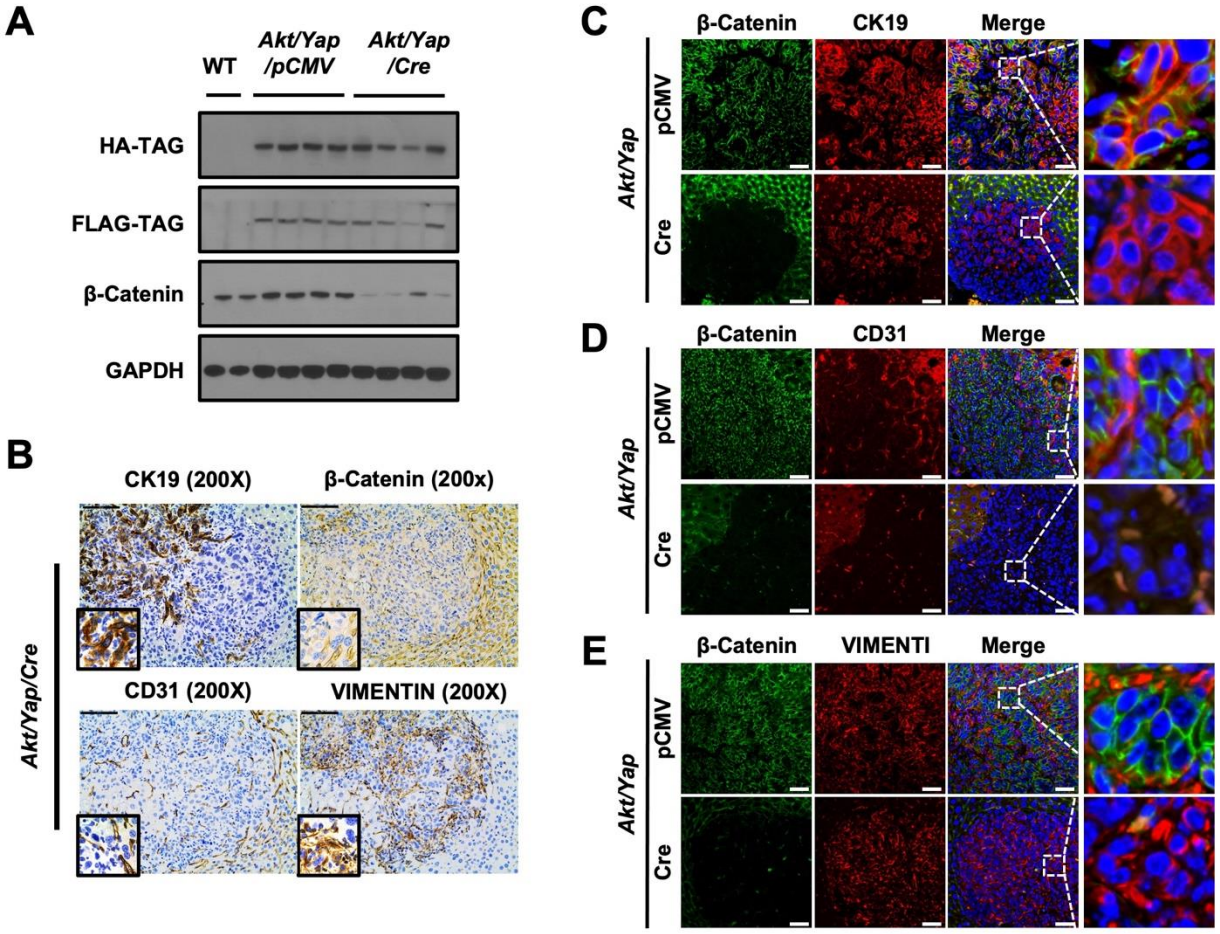
A
WT
Akt/Yap /pCMV
Akt/Yap /Cre
HA-TAG
FLAG-TAG
β-Catenin
GAPDH
B
CK19 (200X)
β-Catenin (200x)
CD31 (200X)
VIMENTIN (200X)
Akt/Yap/Cre
C
β-Catenin
CK19
Merge
Akt/Yap
pCMV
Cre
D
β-Catenin
CD31
Merge
Akt/Yap
pCMV
Cre
E
β-Catenin
VIMENTI
Merge
Akt/Yap
pCMV
Cre

Supplementary Figure 28. Sporadic β-Catenin positive cells within the *Akt/Yap/Cre* lesions are confirmed as fibroblasts or endothelial cells.

(A) Western blotting analysis of tagged oncogenes and β-Catenin in *Ctnnb1*$^{flox/flox}$ *Akt/Yap/pCMV* and *Ctnnb1*$^{flox/flox}$ *Akt/Yap/Cre* lesions. (B) Immunohistochemical staining of CK19, β-Catenin, CD31, and VIMENTIN in iCCA lesions from *Ctnnb1*$^{flox/flox}$ *Akt/Yap/Cre* mice. (C-E) Double immunofluorescence staining for β-Catenin (Green), (C) CK19 (Red), (D) CD31 (Red), or (E) VIMENTIN (Red) with DAPI (Blue), and merged images in *Ctnnb1*$^{flox/flox}$ *Akt/Yap/Cre* iCCA lesions. Scale bar: 100 μm (200X).

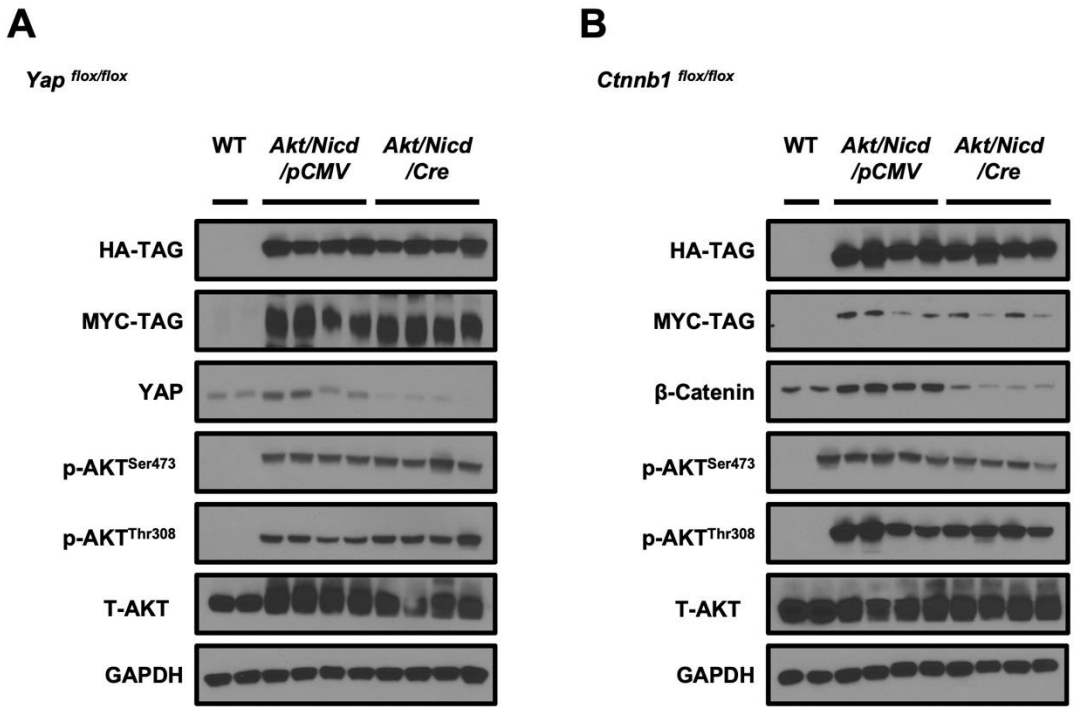
A
Yap flox/flox
WT
Akt/Nicd /pCMV
Akt/Nicd /Cre
HA-TAG
MYC-TAG
YAP
p-AKTSer473
p-AKTThr308
T-AKT
GAPDH
B
Ctnnb1 flox/flox
WT
Akt/Nicd /pCMV
Akt/Nicd /Cre
HA-TAG
MYC-TAG
β-Catenin
p-AKTSer473
p-AKTThr308
T-AKT
GAPDH

Supplementary Figure 29. Western blot analysis confirms the deletion of YAP or β-Catenin in *Yap*$^{flox/flox}$ *or Ctnnb1*$^{flox/flox}$ iCCA lesions.

(A) Western blotting analysis of YAP, fusion tags, total and phosphorylated AKT expression in *Yap*$^{flox/flox}$ *Akt/Nicd/pCMV* and *Yap*$^{flox/flox}$ *Akt/Nicd/Cre* iCCA lesions. GAPDH was used as a loading control. (B) Western blot analysis of β-Catenin, fusion tags, total and phosphorylated AKT expression in *Ctnnb1*$^{flox/flox}$ *Akt/Nicd/pCMV* and *Ctnnb1*$^{flox/flox}$ *Akt/Nicd/Cre* iCCA lesions. GAPDH was used as a loading control.

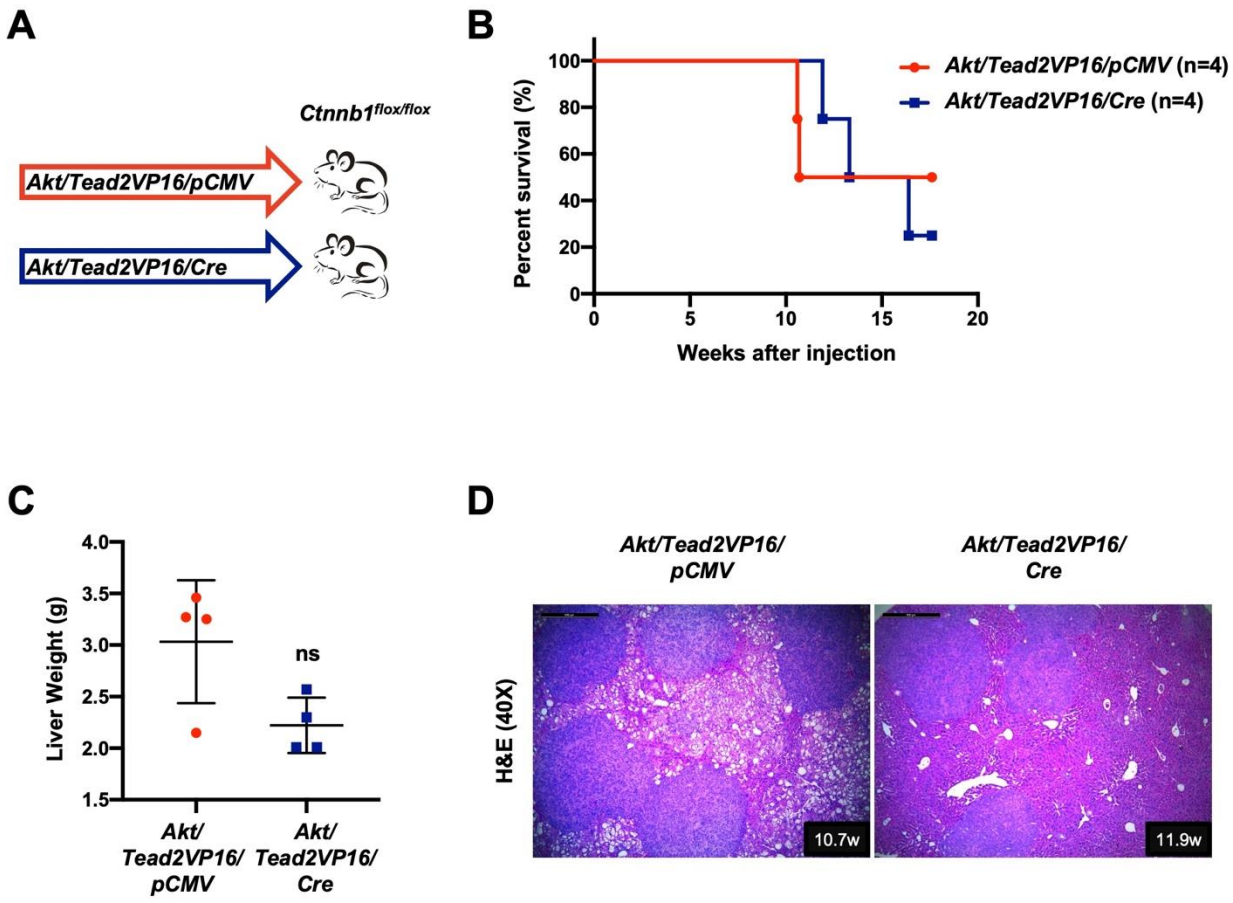
A
Ctnnb1flox/flox
Akt/Tead2VP16/pCMV
Akt/Tead2VP16/Cre
B
Akt/Tead2VP16/pCMV (n=4)
Akt/Tead2VP16/Cre (n=4)
Percent survival (%)
100
80
60
40
20
0
0
5
10
15
20
Weeks after injection
C
Liver Weight (g)
4.0
3.5
3.0
2.5
2.0
1.5
ns
Akt/ Tead2VP16/ pCMV
Akt/ Tead2VP16/ Cre
D
Akt/Tead2VP16/ pCMV
Akt/Tead2VP16/ Cre
H&E (40X)
10.7w
11.9w

Supplementary Figure 30. Deletion of β-catenin mildly delays *Akt/Tead2VP16* iCCA liver tumor development.

(A) Study design. *Ctnnb1*$^{flox/flox}$ mice were subjected to HTVi of either *Akt/Tead2VP16/pCMV* (n=4) or *Akt/Tead2VP16/Cre* (n=4) plasmids. (B) Survival curves showing the similar survival is observed in the indicated mice. (C) Liver weight of *Ctnnb1*$^{flox/flox}$ *Akt/Tead2VP16/pCMV* and *Akt/Tead2VP16/Cre* mice. Statistical significance: ns, not significant. (D) H&E of liver sections from *Ctnnb1*$^{flox/flox}$ *Akt/Tead2VP16/pCMV* (M10.7w.p.i) and *Ctnnb1*$^{flox/flox}$ *Akt/Tead2VP16/Cre* (F11.9w.p.i) mice revealing the tumor lesions are iCCA. Scale bar: 500 μm (40x). Abbreviations: H&E, hematoxylin and eosin staining; w.p.i, weeks post-injection.

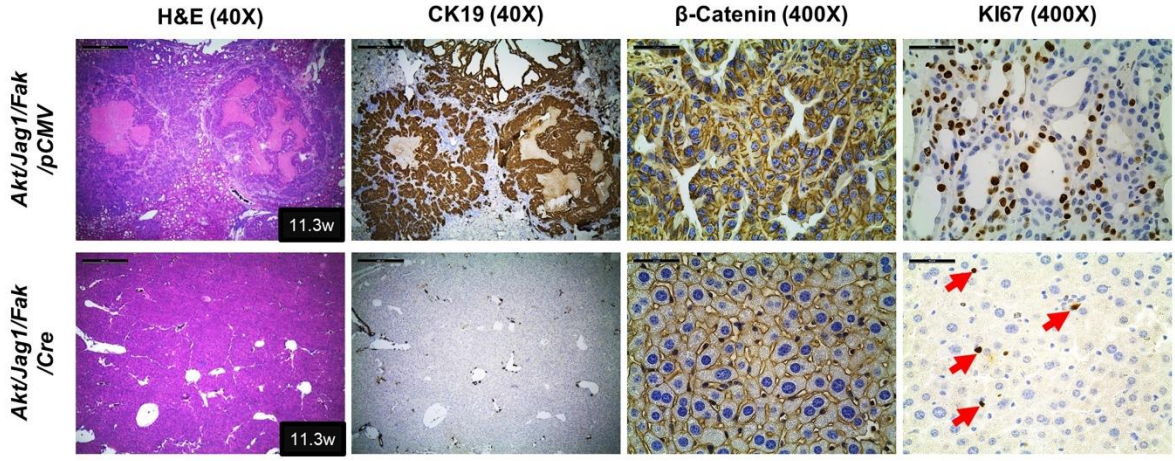
H&E (40X)
CK19 (40X)
β-Catenin (400X)
KI67 (400X)
Akt/Jag1/Fak /pCMV
Akt/Jag1/Fak /Cre
11.3w
11.3w

Supplementary Figure 31. Comparison of *Akt/Jag1/Fak* induced liver tumorigenesis in wildtype and *Ctnnb1* conditional knockout mice.

H&E and immunochemical staining of CK19, β-Catenin and KI67 in liver sections from *Ctnnb1*$^{flox/flox}$ *Akt/Jag1/Fak/pCMV* (F11.3w.p.i), and *Ctnnb1*$^{flox/flox}$ *Akt/Jag1/Fak/Cre* (F11.3w.p.i) mice. Scale bar: 500 μm (40x) and 50 μm (400x). Abbreviations: F, female; H&E: Hematoxylin and eosin; w.p.i, weeks post-injection.

A

Database	Group	N Matching Down Genes	UP in CCA	DOWN in CCA	P Value (UP vs DOWN)
NCI	siYZ vs siCon	2316	726 (31.4%)	353 (15.2%)	*P* < .05
TCGA	siYZ vs siCon	2352	720 (30.6%)	325 (13.8%)	*P* < .05

B

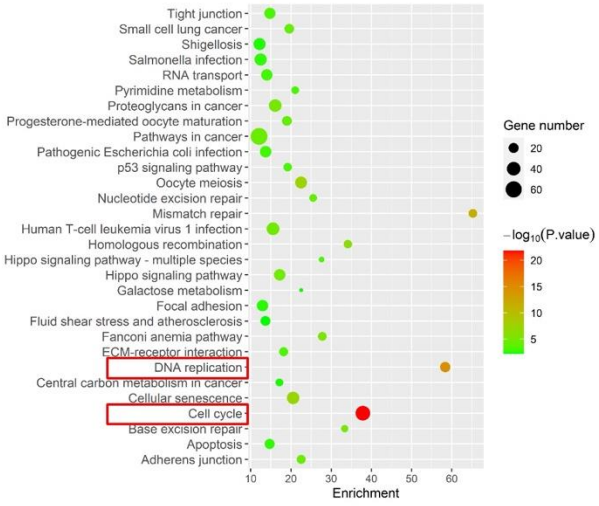

siYZ (DOWN) UP in NCI

C

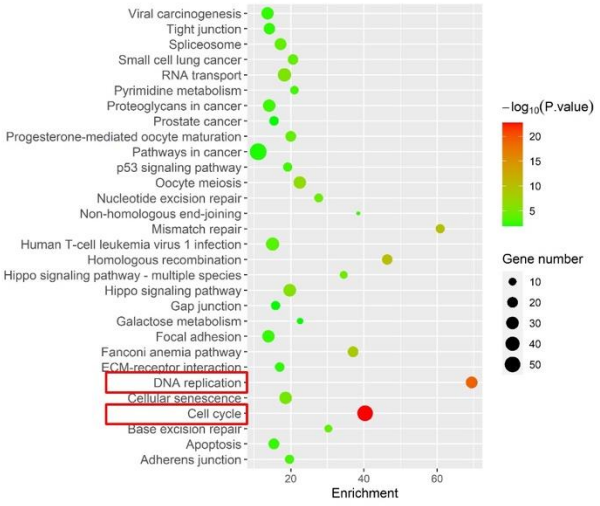

siYZ (DOWN) UP in TCGA

Supplementary Figure 32. A set of downregulated genes in siYT intrahepatic cholangiocarcinoma (iCCA) cell lines is upregulated in human iCCA specimens.

(A) Downregulated genes identified in siYT iCCA cells were matched with the National Cancer Institute (NCI) and The Cancer Genome Atlas (TCGA) CHOL datasets. Table showing the expression patterns of these downregulated genes by YAP/TAZ knockdown in human CCA specimens. (B, C) KEGG analysis of genes downregulated by siYT and upregulated in human iCCAs based on (B) the National Cancer Institute (NCI) or (C) The Cancer Genome Atlas (TCGA) CHOL dataset. Upregulated genes (down in siYT) in human iCCA specimens are associated with DNA replication, and cell cycle pathway. Genes were ranked by *P*-value.

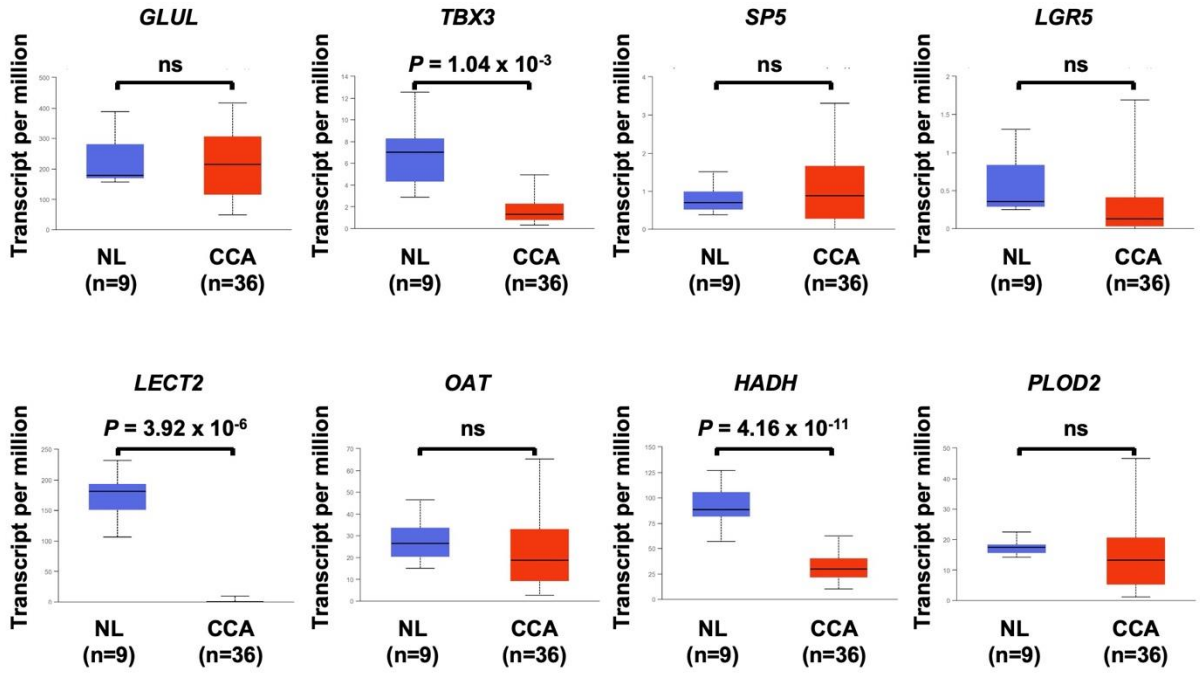
GLUL
ns
TBX3
P = 1.04 x 10-3
SP5
ns
LGR5
ns
LECT2
P = 3.92 x 10-6
OAT
ns
HADH
P = 4.16 x 10-11
PLOD2
ns
Transcript per million
NL (n=9)
CCA (n=36)

Supplementary Figure 33. The canonical Wnt signaling is not activated in human iCCA specimens.

Expression of canonical Wnt targets, including *GLUL, TBX3, SP5, LGR5, LECT2, OAT, HADH,* and *PLOD2* in iCCA specimens and surrounding non-tumorous livers based on The Cancer Genome Atlas (TCGA) CHOL database. Pictures were downloaded from UALCAN. Abbreviations: NL, non-tumorous surrounding liver; CCA: cholangiocarcinoma; ns: not significant.

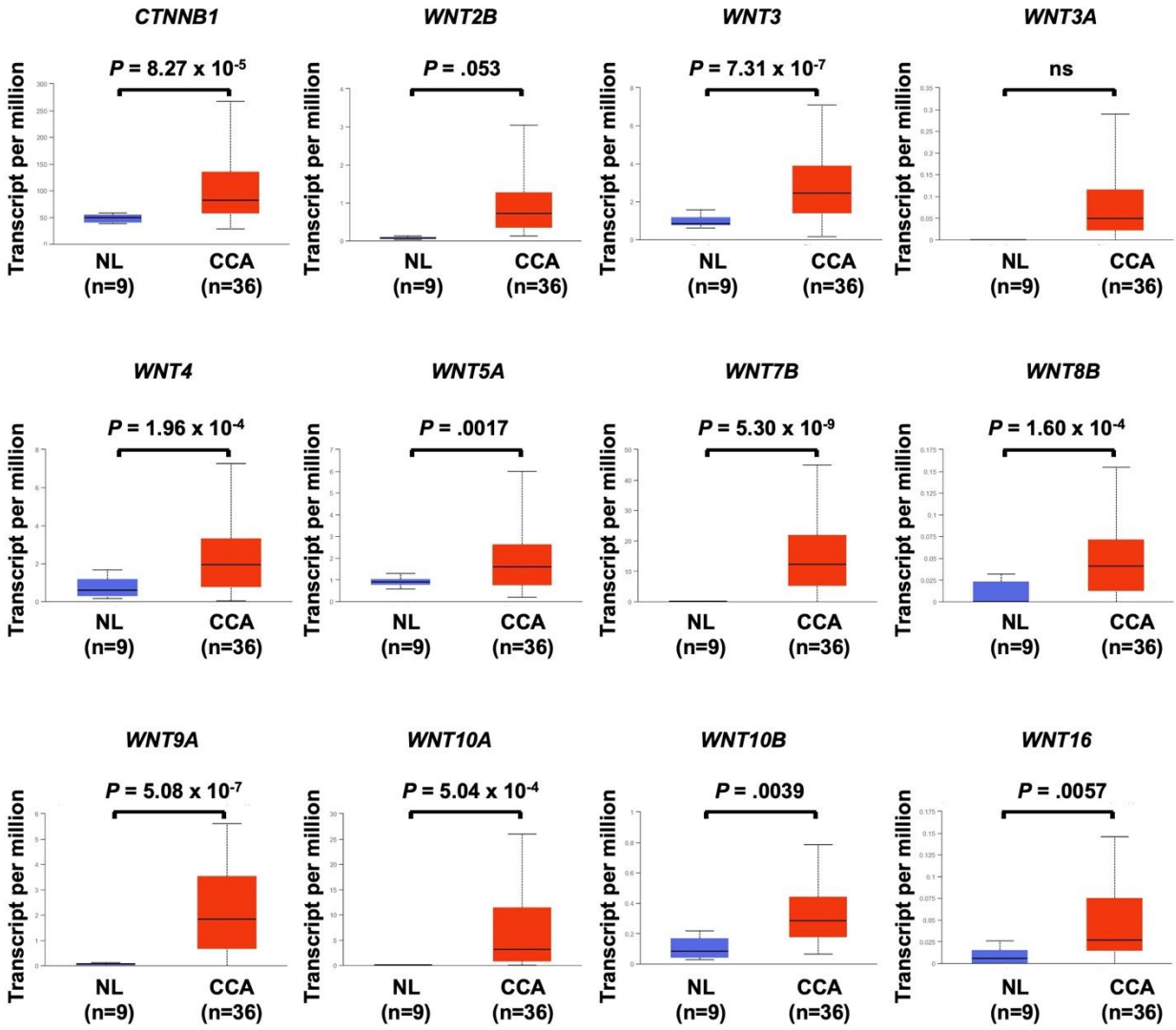
CTNNB1
P = 8.27 x 10-5
WNT2B
P = .053
WNT3
P = 7.31 x 10-7
WNT3A
ns
WNT4
P = 1.96 x 10-4
WNT5A
P = .0017
WNT7B
P = 5.30 x 10-9
WNT8B
P = 1.60 x 10-4
WNT9A
P = 5.08 x 10-7
WNT10A
P = 5.04 x 10-4
WNT10B
P = .0039
WNT16
P = .0057
Transcript per million
NL (n=9)
CCA (n=36)

Supplementary Figure 34. *CTNNB1* and multiple WNT ligand encoding genes are increased in human intrahepatic cholangiocarcinoma (iCCA) specimens.

Expression levels of *CTNNB1, WNT2B, WNT3, WNT3A, WNT4, WNT5A, WNT7B, WNT8B, WNT9A, WNT10A, WNT10B, and WNT16* genes in iCCA specimens and surrounding non-tumorous livers based on TCGA CHOL database. Pictures were downloaded from UALCAN. Abbreviations: NL, non-tumorous surrounding liver; CCA: cholangiocarcinoma; ns: not significant.

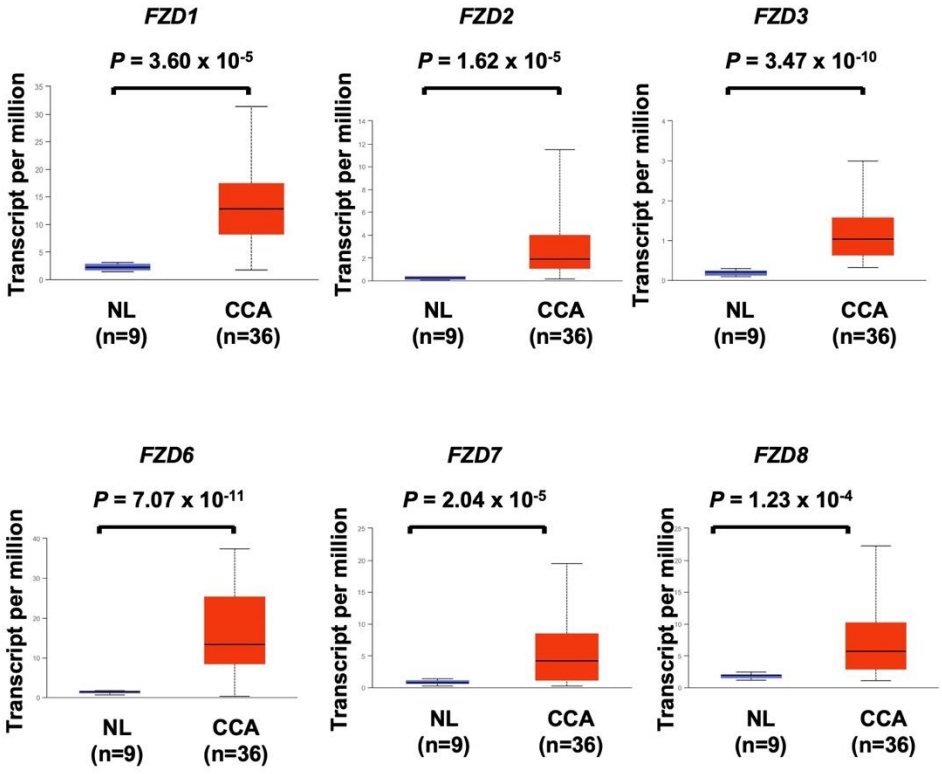
FZD1
P = 3.60 x 10-5
Transcript per million
NL (n=9)
CCA (n=36)
FZD2
P = 1.62 x 10-5
Transcript per million
NL (n=9)
CCA (n=36)
FZD3
P = 3.47 x 10-10
Transcript per million
NL (n=9)
CCA (n=36)
FZD6
P = 7.07 x 10-11
Transcript per million
NL (n=9)
CCA (n=36)
FZD7
P = 2.04 x 10-5
Transcript per million
NL (n=9)
CCA (n=36)
FZD8
P = 1.23 x 10-4
Transcript per million
NL (n=9)
CCA (n=36)

Supplementary Figure 35. Multiple frizzled (FZD) receptor encoding genes are increased in human intrahepatic cholangiocarcinoma (iCCA) specimens.

Expression levels of *FZD1, FZD2, FZD3, FZD6, FZD7,* and *FZD8* in human iCCA specimens and surrounding non-tumorous livers based on TCGA CHOL database. Pictures were downloaded from UALCAN. Abbreviations: NL, non-tumorous surrounding liver; CCA: cholangiocarcinoma; ns: not significant.

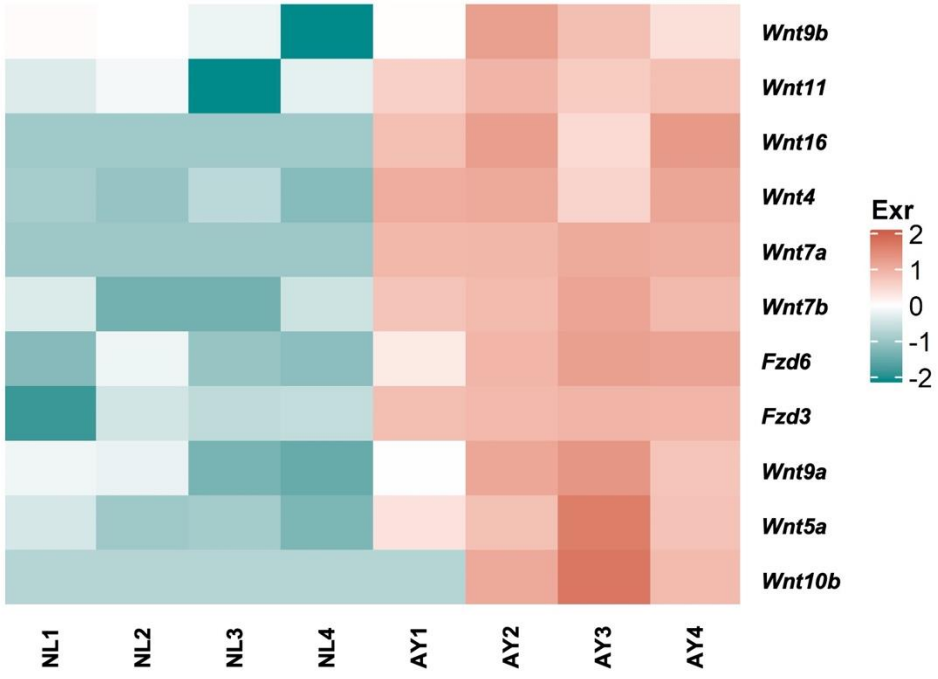
Wnt9b
Wnt11
Wnt16
Wnt4
Wnt7a
Wnt7b
Fzd6
Fzd3
Wnt9a
Wnt5a
Wnt10b
Exr
2
1
0
-1
-2
NL1
NL2
NL3
NL4
AY1
AY2
AY3
AY4

Supplementary Figure 36. Heatmap of the expression of WNT ligands and FZD receptors in normal livers and *Akt/Yap* tumor tissues.

Red, up-regulated; green, down-regulated. Abbreviations: NL, normal liver; AY, *Akt/Yap* iCCA.

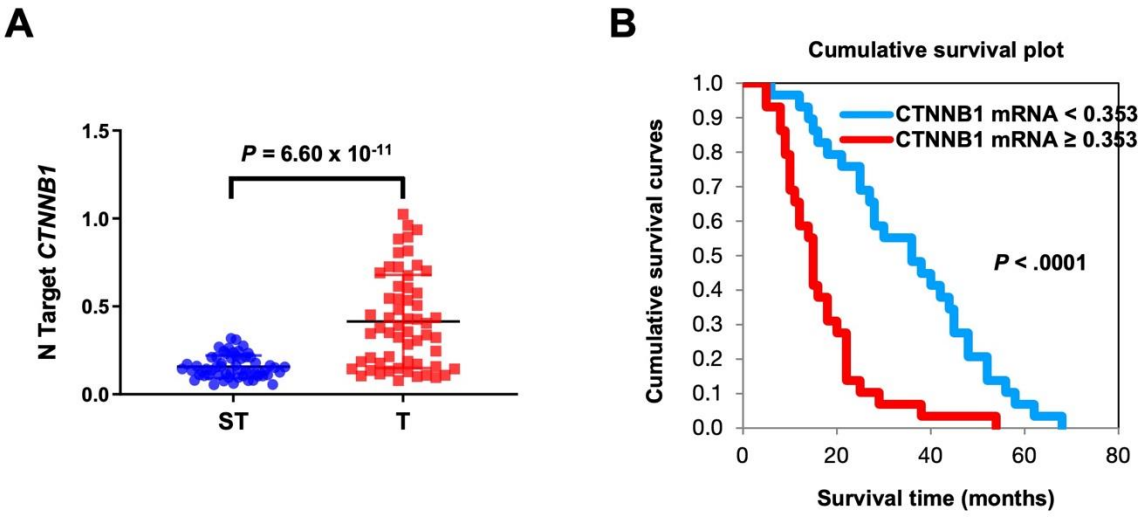
A
N Target CTNNB1
P = 6.60 x 10-11
1.5
1.0
0.5
0.0
ST
T
B
Cumulative survival plot
Cumulative survival curves
CTNNB1 mRNA < 0.353
CTNNB1 mRNA ≥ 0.353
P < .0001
1.0
0.9
0.8
0.7
0.6
0.5
0.4
0.3
0.2
0.1
0.0
0
20
40
60
80
Survival time (months)

Supplementary Figure 37. *CTNNB1* is overexpressed in human intrahepatic cholangiocarcinoma (iCCA) specimens and associated with a poor prognosis.

(A) Quantitative real-time RT-PCR analysis of *CTNNB1* mRNA levels in iCCA (T; n = 58) and corresponding non-tumorous surrounding liver tissues (ST; n = 58). Quantitative values were calculated using the PE Biosystems Analysis software and expressed as number target (N Target). N Target = $2^{-\Delta Ct}$, wherein the ΔCt value of each sample was calculated by subtracting the average Ct value of the gene of interest from the average Ct value of the *GAPDH* gene. (B) Kaplan–Meier survival curves of human iCCA specimens with high and low *CTNNB1* mRNA expression, indicating the poor prognosis of patients with elevated *CTNNB1* levels.

A

Database	Group	N Matching Down Genes	UP in CCA	DOWN in CCA	P Value (UP vs DOWN)
NCI	shβCat vs shCon	3049	876 (28.7%)	395 (13.0%)	*P* < .05
TCGA	shβCat vs shCon	3060	689 (22.5%)	331 (10.8%)	*P* < .05

B

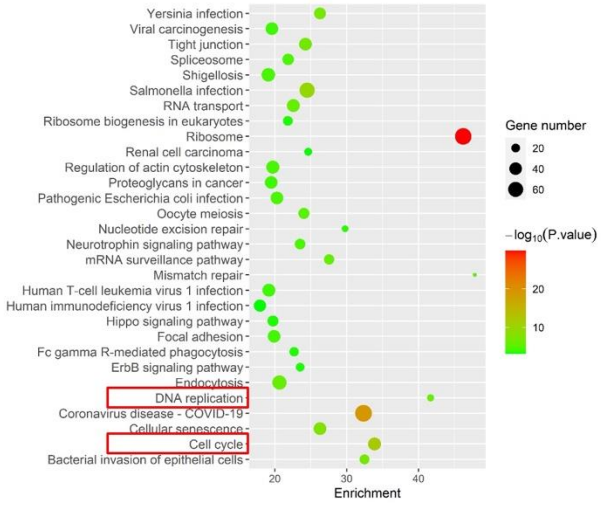

shβCat (DOWN) UP in NCI

C

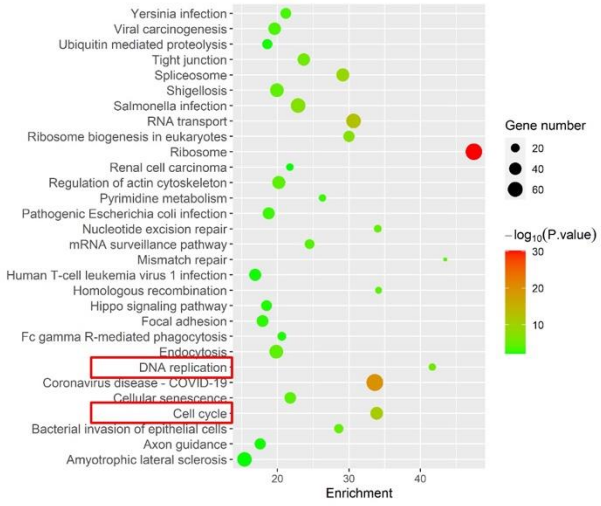

shβCat (DOWN) UP in TCGA

Supplementary Figure 38. A set of downregulated genes in shβCat iCCA cells are upregulated in human intrahepatic cholangiocarcinoma (iCCA) specimens.

(A) Downregulated genes identified in shβCatenin (shβCat) iCCA cells were matched with the National Cancer Institute (NCI) and The Cancer Genome Atlas (TCGA) CHOL datasets. Table showing the expression patterns of these downregulated genes by β-Catenin knockdown in human CCA specimens. (B, C) KEGG analysis of genes downregulated by shβCat and upregulated in human iCCAs based on (B) the National Cancer Institute (NCI) or (C) The Cancer Genome Atlas (TCGA) CHOL dataset. Upregulated genes (down in shβCat) in human iCCA specimens are associated with DNA replication, and cell cycle pathway. Genes were ranked by *P*-value.

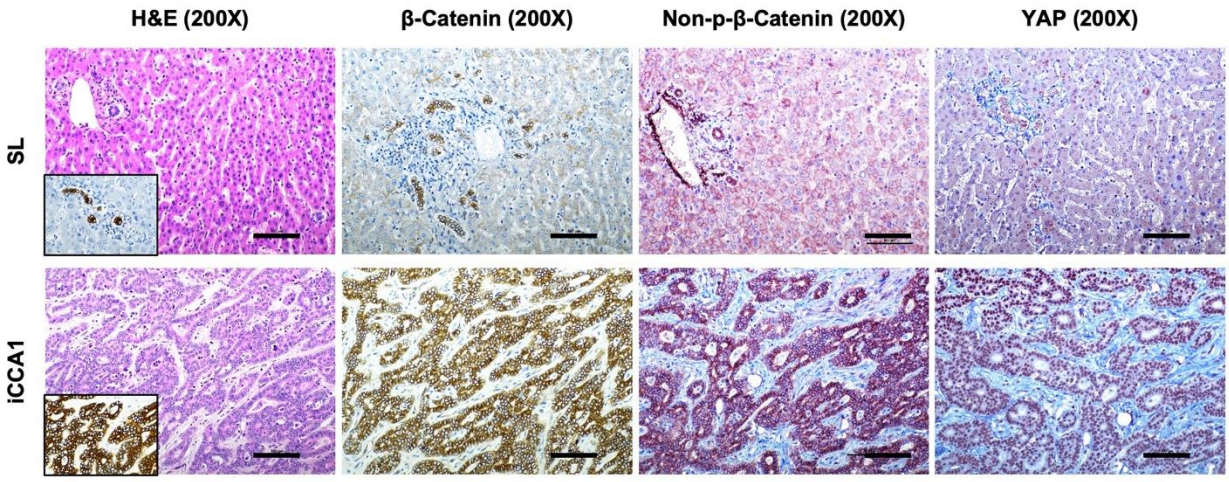
H&E (200X)
β-Catenin (200X)
Non-p-β-Catenin (200X)
YAP (200X)
SL
iCCA1

Supplementary Figure 39. Representative immunohistochemical analysis showing β-catenin staining patterns in the human surrounding non-tumorous liver and intrahepatic cholangiocarcinoma.

H&E and immunohistochemical staining for β-catenin, activated/non-phosphorylated β-catenin (Non-p-β-Catenin), and YAP in normal liver (upper panels), and iCCA (lower panels). CK19 was used as a biliary marker (insets). Scale bar: 100μm (200x). Abbreviations: SL, surrounding non-tumorous liver; iCCA, intrahepatic cholangiocarcinoma; H&E, hematoxylin and eosin staining.

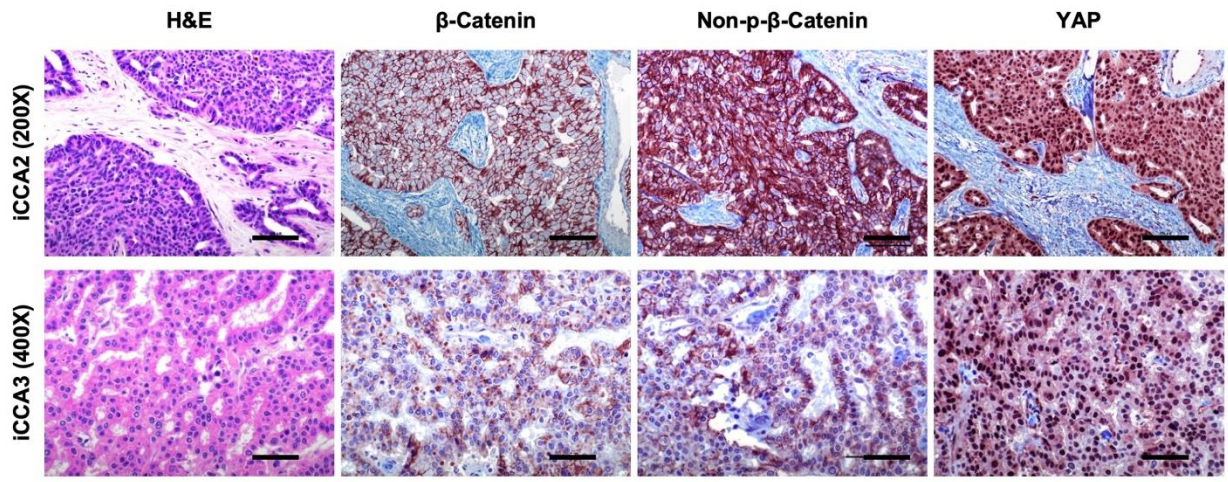
H&E
β-Catenin
Non-p-β-Catenin
YAP
iCCA2 (200X)
iCCA3 (400X)

Supplementary Figure 40. Representative immunohistochemical analysis showing β-Catenin staining patterns in human intrahepatic cholangiocarcinoma (iCCA) specimens. H&E and immunohistochemical staining for β-Catenin, activated/non-phosphorylated β-Catenin (Non-p-β-Catenin), and YAP in human iCCA specimens (upper panels, iCCA2; lower panels, iCCA3). Scale bar: 100µm (200), 50 µm (400x). Abbreviations: SL, surrounding non-tumorous liver; iCCA, intrahepatic cholangiocarcinoma; H&E, hematoxylin and eosin staining.

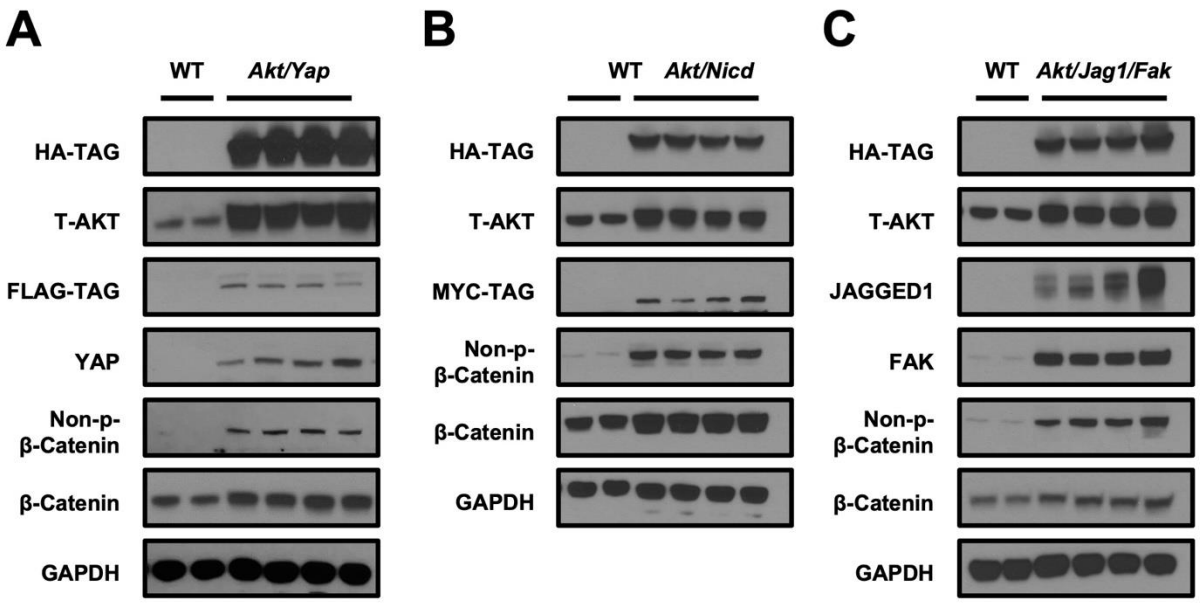
A
WT
Akt/Yap
HA-TAG
T-AKT
FLAG-TAG
YAP
Non-p-β-Catenin
β-Catenin
GAPDH
B
WT
Akt/Nicd
HA-TAG
T-AKT
MYC-TAG
Non-p-β-Catenin
β-Catenin
GAPDH
C
WT
Akt/Jag1/Fak
HA-TAG
T-AKT
JAGGED1
FAK
Non-p-β-Catenin
β-Catenin
GAPDH

Supplementary Figure 41. Activated/non-phosphorylated β-Catenin (Non-p-β-Catenin) is overexpressed in *Akt/Yap, Akt/Nicd* and *Akt/Jag1/Fak* intrahepatic cholangiocarcinoma (iCCA) lesions.

(A-C) Western blotting analysis of β-Catenin and Non-p-β-Catenin$^{S33/S37/T41}$ levels in livers from *FVB/N* wildtype mice (WT) or *FVB/N* mice injected with (A) Akt and Yap plasmids (*Akt/Yap*), or (B) Akt and Nicd plasmids (*Akt/Nicd*), or (C) Akt, Jag1, and Fak plasmids (*Akt/Jag1/Fak*). GAPDH was used as a loading control.

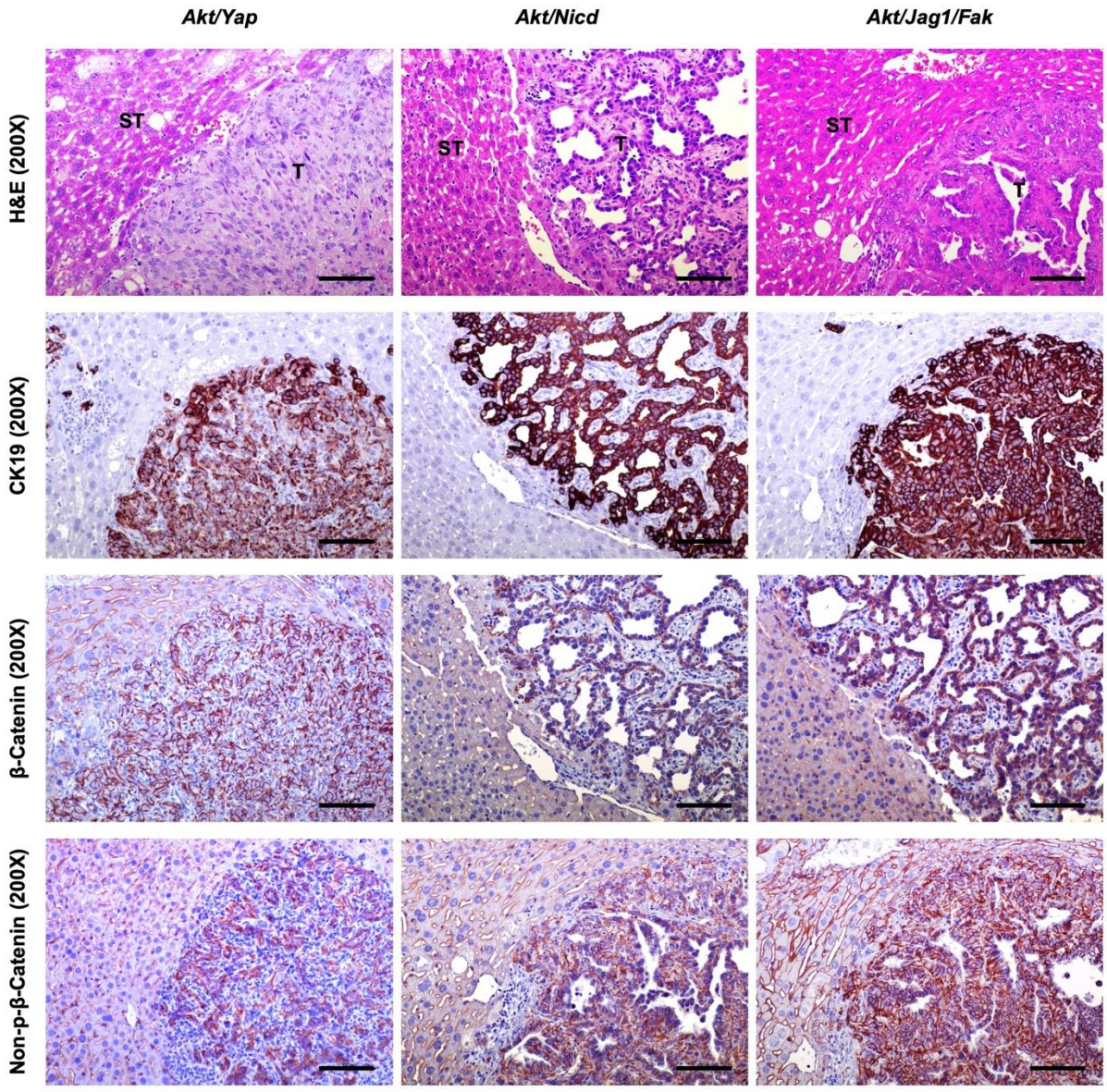
Akt/Yap
Akt/Nicd
Akt/Jag1/Fak
H&E (200X)
CK19 (200X)
β-Catenin (200X)
Non-p-β-Catenin (200X)
ST
T

Supplementary Figure 42. Activated/non-phosphorylated β-Catenin (Non-p-β-Catenin) is overexpressed in *Akt/Yap, Akt/Nicd*, and *Akt/Jag1/Fak* intrahepatic cholangiocarcinoma (iCCA) lesions.

(A-C) Immunohistochemical patterns of β-Catenin and Non-p-β-Catenin$^{S33/S37/T41}$ proteins in livers from *FVB/N* mice injected with Akt and Yap plasmids (*Akt/Yap*), Akt and Nicd plasmids (*Akt/Nicd*), and Akt, Jag1, and Fak plasmids (*Akt/Jag1/Fak*). Note the more pronounced immunoreactivity (both membranous and cytoplasmic) for β-Catenin and Non-p-β-Catenin$^{S33/S37/T41}$ in the tumor lesions (T) of the three mouse models compared with non-tumorous surrounding livers (ST). CK19 staining was used as a biliary cell marker. Original magnification: 200X; scale bar: 100 µm.

A

	baseMean	log2FoldChange *YAP/AKT* CAF vs qHSC	lfcSE	stat	pvalue	padj
Wnt11	1255.37194	11.5655197	0.84607353	-13.669639	1.54E-42	2.95E-40
Wnt16	123.40583	8.028901453	0.72455193	-11.081195	1.55E-28	1.34E-26
Wnt7b	10.2228005	6.902691416	1.33819407	-5.158214	2.49E-07	2.53E-06
Wnt7a	7.0326439	6.360778976	1.39377143	-4.5637174	5.03E-06	4.02E-05
Wnt10b	3.31656617	5.273611083	1.40741939	-3.7470075	0.00017896	0.00101488
Wnt9a	226.348575	4.19220183	0.42320306	-9.9058872	3.92E-23	2.39E-21
Wnt9b	31.1346418	3.70734194	1.21065463	-3.0622622	0.00219671	0.00948937
Wnt5b	34.8673085	3.61557097	0.68160118	-5.3045257	1.13E-07	1.23E-06
Wnt5a	1219.08529	3.507423969	0.24158791	-14.51821	9.29E-48	2.33E-45
Wnt2b	20.5134084	3.359148514	0.69873826	-4.8074489	1.53E-06	1.35E-05
Wnt10a	0.77393808	3.038648727	2.17336442	-1.3981313	0.16207366	0.35519516
Wnt8a	0.53140672	2.641312747	3.46070471	-0.7632297	0.4453264	0.72358081
Wnt1	0.50657358	1.529336339	2.97291684	-0.5144228	0.60695639	0.86790987
Wnt6	4.61799697	1.11415206	1.28126947	-0.8695689	0.38453605	0.65734614
Wnt3	0.11605632	0.937908835	3.53381154	-0.26541	0.79069365	0.91726515

B

	baseMean	log2FoldChange *KRAS/SGP19* CAF vs qHSC	lfcSE	stat	pvalue	padj
Wnt11	332.86546	9.655498443	0.76909008	-12.554444	3.76E-36	3.19E-34
Wnt16	7.3843069	3.827581524	0.984075	-3.8895222	0.00010044	0.00059503
Wnt7b	6.8194447	6.40611918	1.3956808	-4.5899601	4.43E-06	3.45E-05
Wnt7a	2.4436066	4.911960842	2.00442261	-2.4505615	0.01426336	0.04778511
Wnt10b	4.3690572	5.756012297	1.52469702	-3.7751843	0.00015989	0.00090605
Wnt9a	151.3534	3.605364965	0.33047355	-10.909693	1.04E-27	5.70E-26
Wnt9b	7.0807807	1.041449368	1.07947646	-0.9647726	0.3346587	0.5793428
Wnt5b	19.143788	2.698929369	0.75625741	-3.5687973	0.00035862	0.00187471
Wnt5a	820.98723	2.967380474	0.26840935	-11.055429	2.06E-28	1.17E-26
Wnt2b	39.955441	4.439373336	0.56657154	-7.8355036	4.67E-15	1.05E-13
Wnt10a	0.8193738	3.349338817	3.27160809	-1.0237592	0.30594903	0.54546471
Wnt8a	0.2304375	1.600543899	3.781982	-0.4232024	0.67214759	0.86846141
Wnt1	1.8665591	3.69873716	1.80910113	-2.0445165	0.04090255	0.11392151
Wnt6	7.1727169	1.753371848	1.18084564	-1.4848442	0.13758509	0.30084481
Wnt3	0.1199346	0.86756188	3.81693853	-0.2272926	0.82019623	0.90144855

Supplementary Figure 43. Multiple WNT ligand encoding genes are increased in cancer-associated fibroblasts.

(A-B) Fold regulation of Wnts mRNA in cancer-associated fibroblasts (CAF) from (A) *Akt/Yap* and (B) *Kras/sgp19* iCCA models compared with quiescent hepatic stellate cells (qHSC).

A

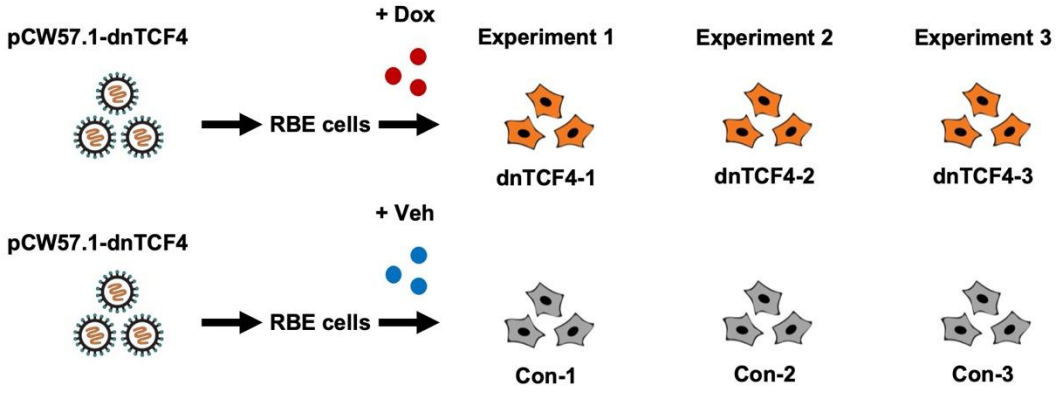

B

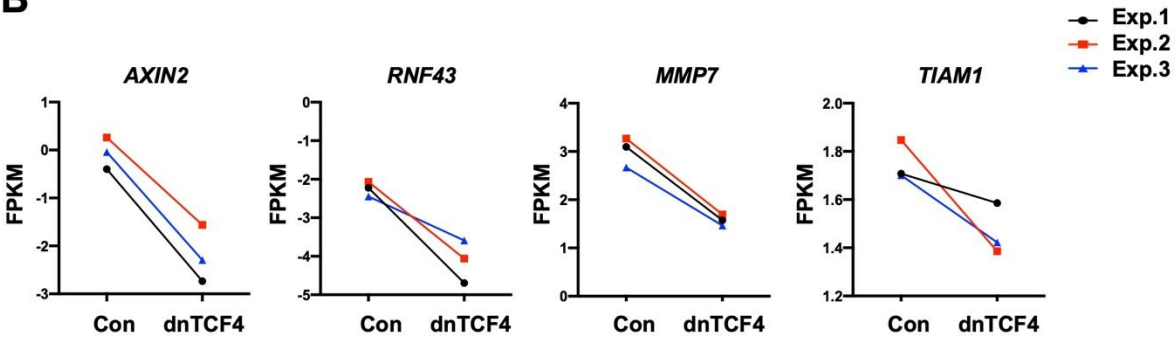

C

Group	N Genes	Direction	FC	P Value
dnTCF4 vs Con	167	Down	>1.3	*P* < .05
dnTCF4 vs Con	143	Up	>1.3	*P* < .05

Supplementary Figure 44. RNA sequencing in dnTCF4 overexpressed iCCA cell lines.

(A) Study design of RNA sequencing. Human RBE cells were transfected with doxycycline-inducible pCW57.1-dnTCF4 plasmid by lentiviral transduction, followed by incubation for 48 h with 5μg/ml doxycycline (dnTCF4, n=3) or vehicle control (Con, n=3). The obtained cells were prepared for RNA sequencing. (B) Fragments per kilobase of transcript per million mapped reads (FPKM) results of *AXIN2, RNF43, MMP7,* and *TCF4* expression. (C) Significant downregulated and upregulated genes in dnTCF4 overexpression RBE cells are shown in Table. Abbreviations: Dox, doxycycline; Veh, Vehicle; FC, fold change.

A

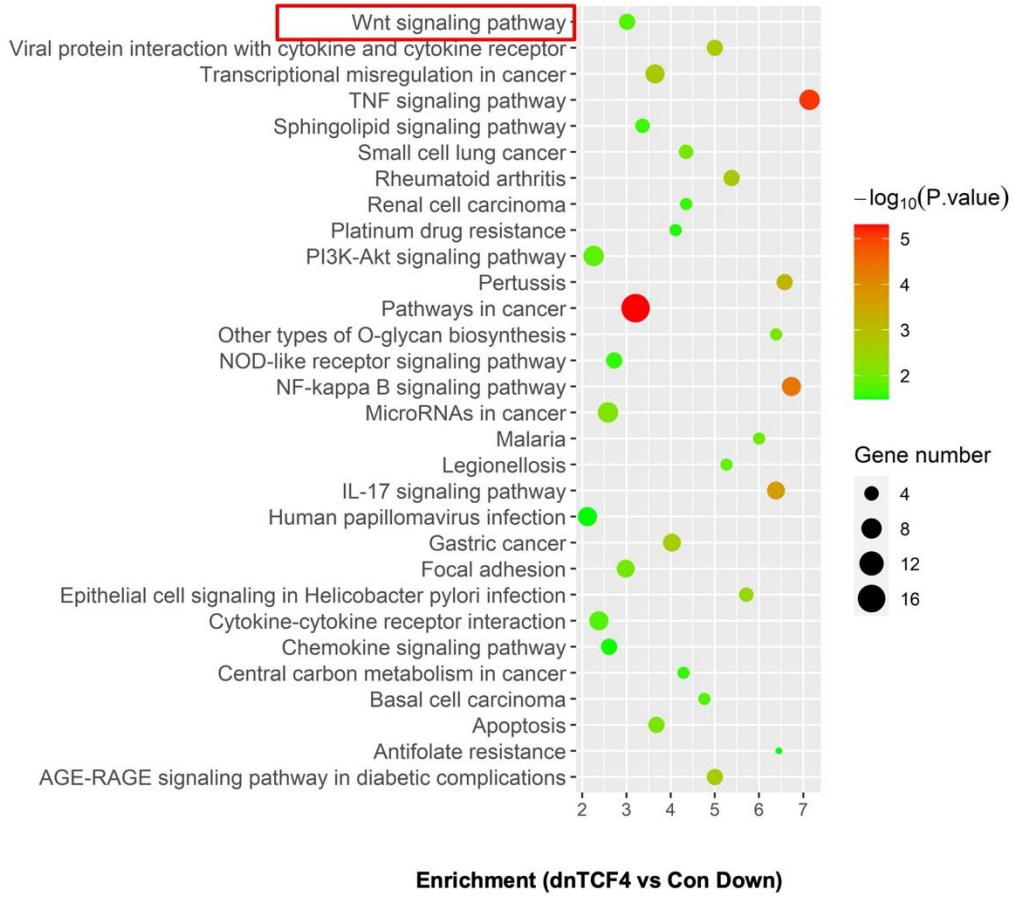
Wnt signaling pathway
Viral protein interaction with cytokine and cytokine receptor
Transcriptional misregulation in cancer
TNF signaling pathway
Sphingolipid signaling pathway
Small cell lung cancer
Rheumatoid arthritis
Renal cell carcinoma
Platinum drug resistance
PI3K-Akt signaling pathway
Pertussis
Pathways in cancer
Other types of O-glycan biosynthesis
NOD-like receptor signaling pathway
NF-kappa B signaling pathway
MicroRNAs in cancer
Malaria
Legionellosis
IL-17 signaling pathway
Human papillomavirus infection
Gastric cancer
Focal adhesion
Epithelial cell signaling in Helicobacter pylori infection
Cytokine-cytokine receptor interaction
Chemokine signaling pathway
Central carbon metabolism in cancer
Basal cell carcinoma
Apoptosis
Antifolate resistance
AGE-RAGE signaling pathway in diabetic complications
2
3
4
5
6
7
Enrichment (dnTCF4 vs Con Down)
−log10(P.value)
5
4
3
2
Gene number
4
8
12
16

B

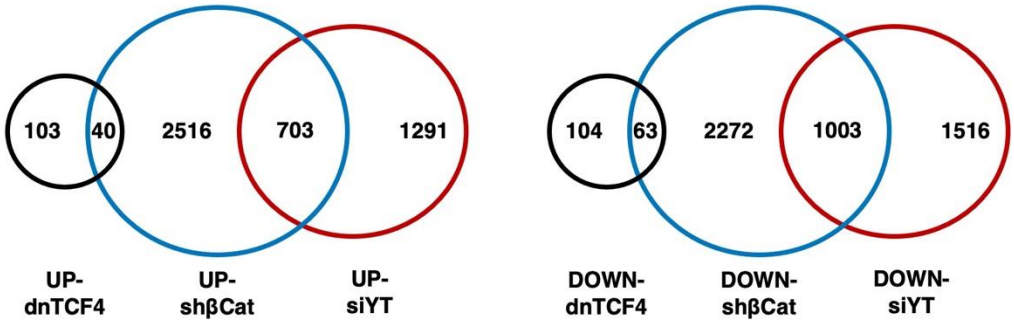
103
40
2516
703
1291
UP-
dnTCF4
UP-
shβCat
UP-
siYT
104
63
2272
1003
1516
DOWN-
dnTCF4
DOWN-
shβCat
DOWN-
siYT

Supplementary Figure 45. Comparison of the transcriptomes in dnTCF4, shβCat and siYT RBE cells.

(A) KEGG analysis of downregulated genes in dnTCF4 overexpressed RBE cells. Blocking β-Catenin/TCF4 interaction in RBE leads to the downregulation of genes enriched in the Wnt signaling pathway (Red inserts). Genes were ranked by *P*-value. (B) Venn diagram showing the overlapping upregulated and downregulated gene number in the dnTCF4 (in black), shβCat (in blue) and siYT (in red) RBE cell lines.

A

Group	N Genes	Direction	FC	P Value
BAY vs AY	664	Down	>2.0	*P* < .05
BAY vs AY	393	Up	>2.0	*P* < .05

B

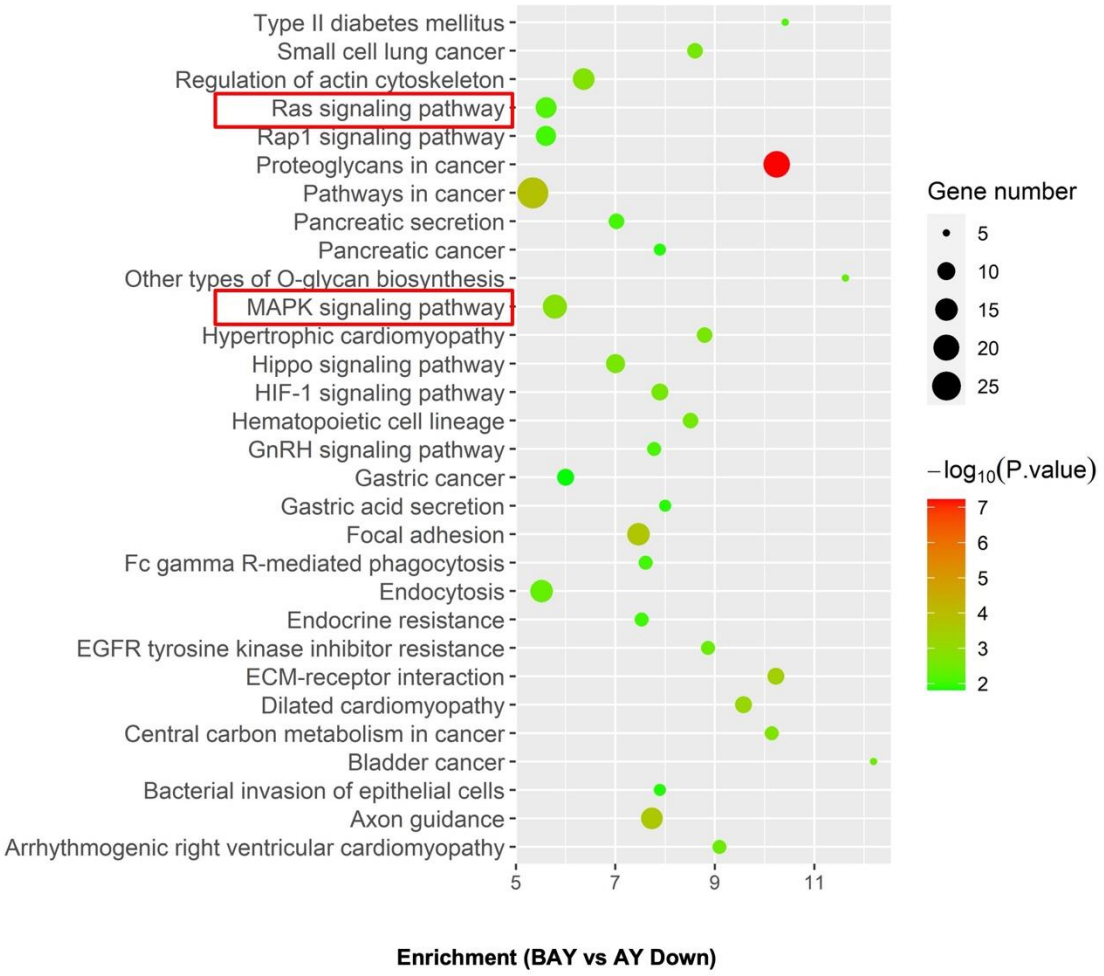

Supplementary Figure 46. RNA sequencing in *Ctnnb1* deleted *Akt/Yap* and *Akt/Yap* iCCA lesions.

(A) Significant downregulated and upregulated genes in *Ctnnb1* deleted *Akt/Yap* iCCAs compared with *Akt/Yap* iCCAs were shown in Table. (B) KEGG analysis of downregulated genes in *Ctnnb1* deleted *Akt/Yap* iCCAs. Deletion of *Ctnnb1* in *Akt/Yap* iCCAs leads to downregulation of genes enriched in the Ras signaling pathway and MAPK signaling pathway (Red inserts). Genes were ranked by *P*-value. Abbreviations: BAY, *Ctnnb1*$^{flox/flox}$ *Akt/Yap/Cre* iCCA; AY, *Akt/Yap* iCCA; FC, fold change.

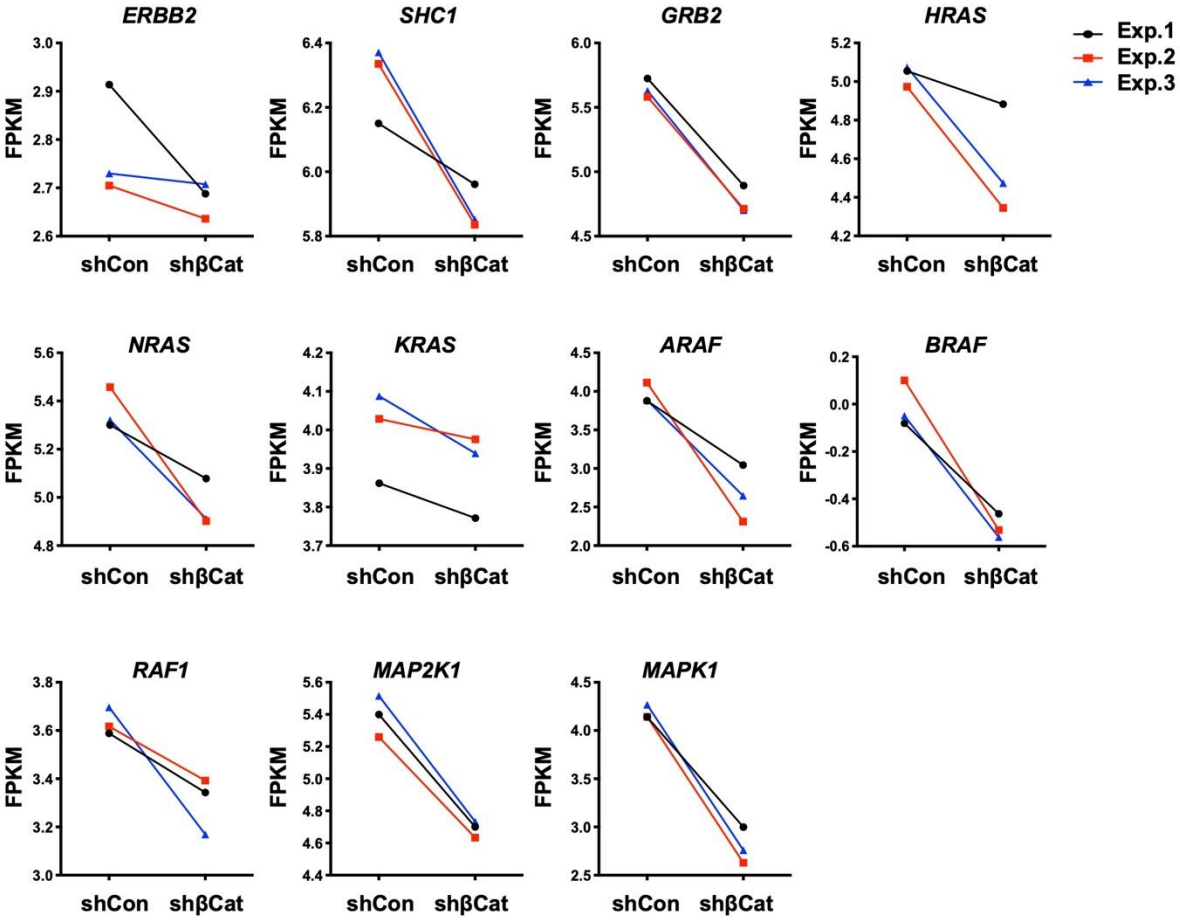
ERBB2
SHC1
GRB2
HRAS
NRAS
KRAS
ARAF
BRAF
RAF1
MAP2K1
MAPK1
FPKM
shCon
shβCat
Exp.1
Exp.2
Exp.3

Supplementary Figure 47. Silencing of β-Catenin in RBE cells leads to the downregulation of genes involved in the Ras/MAPK signaling pathway.

Fragments per kilobase of transcript per million mapped reads (FPKM) results of *ERBB2, SHC1, GRB2, HRAS, NRAS, KRAS, ARAF, BRAF, RAF1, MAP2K1,* and *MAPK1* expression. RNA sequencing in *Ctnnb1* deleted *Akt/Yap* and *Akt/Yap* iCCA lesions.

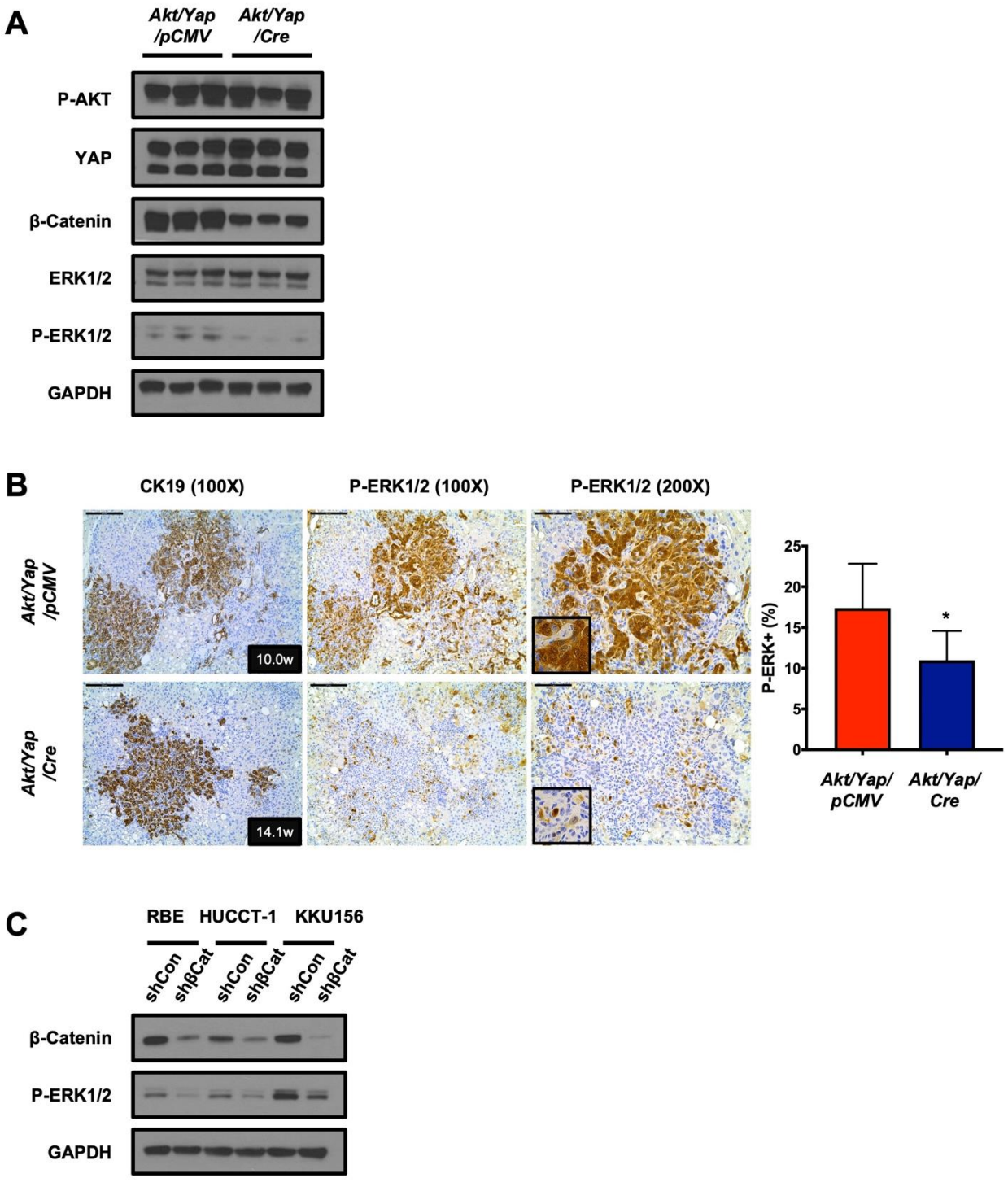
A
Akt/Yap /pCMV
Akt/Yap /Cre
P-AKT
YAP
β-Catenin
ERK1/2
P-ERK1/2
GAPDH
B
CK19 (100X)
P-ERK1/2 (100X)
P-ERK1/2 (200X)
Akt/Yap /pCMV
Akt/Yap /Cre
10.0w
14.1w
P-ERK+ (%)
25
20
15
10
5
0
*
Akt/Yap/ pCMV
Akt/Yap/ Cre
C
RBE
HUCCT-1
KKU156
shCon
shβCat
shCon
shβCat
shCon
shβCat
β-Catenin
P-ERK1/2
GAPDH

Supplementary Figure 48. β-Catenin knockdown inhibits p-ERK expression in iCCA.

(A) Western blot analysis and (B) immunohistochemistry were performed to detect p-ERK1/2 levels in *Ctnnb1*$^{flox/flox}$ *Akt/Yap/pCMV* and *Ctnnb1*$^{flox/flox}$ *Akt/Yap/Cre* iCCA lesions. GAPDH was used as a loading control. Statistical significance: **P* < .05. (C) Western blot analysis of p-ERK1/2 in human iCCA cells transfected with pLKO.1-shCon (shCon) or pLKO.1-shβ-Catenin (shβCat). Scale bar: 100 μm (100x) and 100 μm (200X). Silencing of β-Catenin in RBE cells leads to the downregulation of genes involved in the Ras/MAPK signaling pathway.

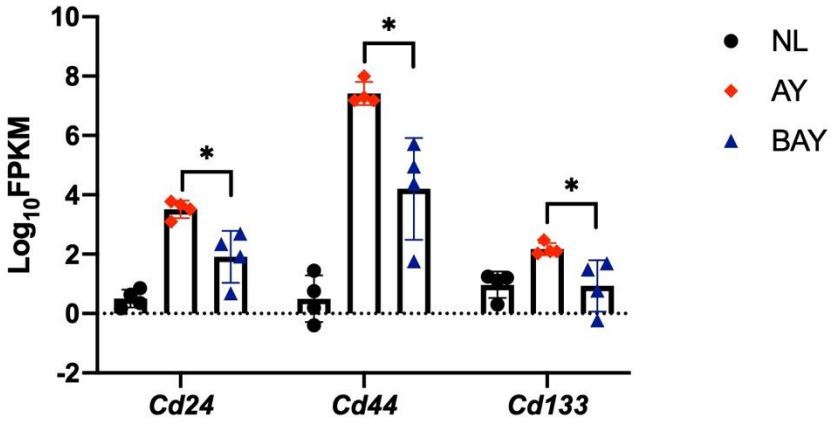
10
8
6
4
2
0
-2
Log10FPKM
*
*
*
Cd24
Cd44
Cd133
NL
AY
BAY

Supplementary Figure 49. Expression pattern of cholangiocarcinoma stem cell markers in three different sample sets.

The expression of *Cd24, Cd44*, and *Cd133* in NL, AY, and BAY samples based on the RNA Sequencing data. Statistical significance: **P* < .05. Abbreviations: NL, normal liver; AY, *Akt/Yap* iCCA; BAY, *Ctnnb1*$^{flox/flox}$ *Akt/Yap/Cre* iCCA.

2. Supplementary Tables

Supplementary Table 1. Plasmids used in the experiments

Study	Plasmids
In vitro	pT3-EF1a-HA-myr-Akt, pT3-EF1α-Flag-YapS127A, pT3-EF1α-Flag-YapS94A, pT3-EF1α, pT3-EF1α-dnTEAD2, pT3-EF1α-MYC-VGLL4, pT3-EF5α-Tead2VP16, pT3-EF1α-Flag-YapΔ(P+TBD), pT3-EF1α-Flag-YapΔWW, pT3-EF1α-Flag-YapΔSH3, pT3-EF1α-Flag-YapΔ(TAD+PDZ), pT3-EF1α-Flag-YapΔPDZ, pT3-EF1α-Myc-mNICD (NICD), pT3-EF1α-Tead2VP16, pT3-EF1α-MYC-AXIN2, pT3-EF1α-JAG1, pT3-EF1α-FAK, pCMV, pCMV-Cre and pCMV-sleeping beauty transposase (pCMV/SB)
In vivo	psPAX2, pMD2.G, plenti-EGFP, plenti-dnTEAD2, pCW57.1-dnTCF4, plenti-FLAG-β-Catenin WT and pT3-EF1α-Myc-β-Catenin WT, pLKO.1-sc and pLKO.1-shβ-Catenin

Supplementary Table 2. Plasmid dosages used for iCCA murine models

Mouse strain	iCCA murine model	Plasmid dosages (μg)
FVB/N	*Akt/Yap*	Akt(20)+YapS127A(20)+SB(1.6)
FVB/N	*Akt/YapS94A*	Akt(20)+YapS94A(20)+SB(1.6)
FVB/N	*Akt/Yap/pT3*	Akt(20)+YapS127A(20)+pT3(60)+SB(4.0)
FVB/N	*Akt/Yap/dnTEAD2*	Akt(20)+YapS127A(20)+dnTEAD2(60)+SB(4.0)
FVB/N	*Akt/Yap/VGLL4*	Akt(20)+YapS127A(20)+VGLL4(60)+SB(4.0)
FVB/N	*Akt/Tead2VP16*	Akt(20)+Tead2VP16-5α(20)+SB(1.6)
FVB/N	*Akt/YapΔWW*	Akt(20)+YapΔWW(20)+SB(1.6)
FVB/N	*Akt/YapΔSH3*	Akt(20)+YapΔSH3(20)+SB(1.6)
FVB/N	*Akt/YapΔPDZ*	Akt(20)+YapΔPDZ(20)+SB(1.6)
FVB/N	*Akt/Yap/Cre*	Akt(20)+YapS127A(20)+Cre(60)+SB(4.0)
FVB/N	*Akt/Yap/Axin2*	Akt(20)+YapS127A(20)+AXIN2(60)+SB(4.0)
Ctnnb1$^{flox/flox}$	*Akt/Yap/pCMV*	Akt(20)+YapS127A(20)+pCMV(60)+SB(4.0)
Ctnnb1$^{flox/flox}$	*Akt/Yap/Cre*	Akt(20)+YapS127A(20)+Cre(60)+SB(4.0)
Yap$^{flox/flox}$	*Akt/Nicd/pCMV*	Akt(20)+NICD(20)+pCMV(60)+SB(4.0)
Yap$^{flox/flox}$	*Akt/Nicd/Cre*	Akt(20)+NICD(20)+Cre(60)+SB(4.0)
Ctnnb1$^{flox/flox}$	*Akt/Nicd/pCMV*	Akt(20)+NICD(20)+pCMV(60)+SB(4.0)
Ctnnb1$^{flox/flox}$	*Akt/Nicd/Cre*	Akt(20)+NICD(20)+Cre(60)+SB(4.0)
Ctnnb1$^{flox/flox}$	*Akt/Tead2VP16/pCMV*	Akt(20)+Tead2VP16-1α(20)+pCMV(60)+SB(4.0)
Ctnnb1$^{flox/flox}$	*Akt/Tead2VP16/Cre*	Akt(20)+Tead2VP16-1α(20)+Cre(60)+SB(4.0)
Ctnnb1$^{flox/flox}$	*Akt/Jag1/Fak/pCMV*	Akt(20)+JAG1(20)+FAK(30)+pCMV(60)+SB(5.2)
Ctnnb1$^{flox/flox}$	*Akt/Jag1/Fak/Cre*	Akt(20)+JAG1(20)+FAK(30)+Cre(60)+SB(5.2)

Supplementary Table 3. Basic information of iCCA murine models

Mouse strain	iCCA murine model	Sex	Weeks post-injection	Body weight (g)	Liver weight (g)	Macroscopic view
FVB/N	*Akt/Yap*	M	2.5	23.9	2.0	Nodules
FVB/N	*Akt/Yap*	M	3.0	20.8	1.8	Nodules
FVB/N	*Akt/Yap*	M	3.5	25.7	2.0	Nodules
FVB/N	*Akt/Yap*	M	5.7	27.6	1.8	Tumors
FVB/N	*Akt/Yap*	F	5.8	21.2	2.2	Tumors
FVB/N	*Akt/Yap*	M	6.0	30.4	2.9	Tumors
FVB/N	*Akt/Yap*	M	6.0	27.3	2.1	Tumors
FVB/N	*Akt/Yap*	M	7.1	27.3	2.8	Tumors
FVB/N	*Akt/Yap*	F	7.6	22.6	3.2	Tumors
FVB/N	*Akt/Yap*	M	7.9	30.8	5.3	Tumors
FVB/N	*Akt/Yap*	M	9.1	35.5	5.8	Tumors
FVB/N	*Akt/Yap*	F	9.6	27.9	4.5	Tumors
FVB/N	*Akt/Yap*	F	9.6	32.8	5.6	Tumors
FVB/N	*Akt/Yap*	M	10.4	30.3	3.5	Tumors
FVB/N	*Akt/Yap*	M	10.8	32.5	4.2	Tumors
FVB/N	*Akt/Yap*	M	10.8	28.7	3.6	Tumors
FVB/N	*Akt/Yap*	M	11.0	31.9	3.7	Tumors
FVB/N	*Akt/Yap*	M	11.0	34.2	7.7	Tumors
FVB/N	*Akt/YapS94A*	M	5.7	25.5	2.0	Normal
FVB/N	*Akt/YapS94A*	M	6.0	26.3	2.0	Normal
FVB/N	*Akt/YapS94A*	M	7.0	30.0	2.2	Normal
FVB/N	*Akt/YapS94A*	M	7.0	30.7	2.5	Normal
FVB/N	*Akt/YapS94A*	M	8.6	21.4	1.7	Normal
FVB/N	*Akt/YapS94A*	M	8.6	21.9	1.3	Normal
FVB/N	*Akt/YapS94A*	M	10.4	33.6	2.5	Normal
FVB/N	*Akt/YapS94A*	M	10.8	31.4	2.0	Normal
FVB/N	*Akt/YapS94A*	M	10.8	29.1	1.9	Normal
FVB/N	*Akt/YapS94A*	M	11.0	33.2	1.9	Normal
FVB/N	*Akt/YapS94A*	F	21.1	24.1	1.7	Normal
FVB/N	*Akt/Yap/pT3*	M	5.0	28.8	2.2	Nodules
FVB/N	*Akt/Yap/pT3*	M	6.9	26.4	2.5	Tumors
FVB/N	*Akt/Yap/pT3*	F	6.9	23.7	4.8	Tumors
FVB/N	*Akt/Yap/pT3*	M	7.6	31.3	4.6	Tumors
FVB/N	*Akt/Yap/pT3*	F	8.0	25.2	5.5	Tumors
FVB/N	*Akt/Yap/pT3*	M	9.1	36.4	4.3	Tumors
FVB/N	*Akt/Yap/pT3*	F	9.4	26.5	4.9	Tumors
FVB/N	*Akt/Yap/pT3*	F	9.4	24.5	5.1	Tumors
FVB/N	*Akt/Yap/pT3*	M	9.7	30.1	5.5	Tumors
FVB/N	*Akt/Yap/pT3*	M	9.8	27.6	2.9	Tumors
FVB/N	*Akt/Yap/pT3*	M	10.3	30.0	4.8	Tumors
FVB/N	*Akt/Yap/pT3*	M	10.7	31.2	3.9	Tumors
FVB/N	*Akt/Yap/pT3*	M	10.7	31.9	4.1	Tumors
FVB/N	*Akt/Yap/pT3*	M	10.8	35.3	5.2	Tumors
FVB/N	*Akt/Yap/pT3*	M	7.7	31.9	3.02	Tumors

FVB/N	*Akt/Yap/pT3*	F	8.1	25.69	6.11	Tumors
FVB/N	*Akt/Yap/pT3*	F	10.7	32	8.59	Tumors
FVB/N	*Akt/Yap/dnTEAD2*	M	4.0	25.4	1.7	Nodules
FVB/N	*Akt/Yap/dnTEAD2*	M	5.0	26.0	1.8	Nodules
FVB/N	*Akt/Yap/dnTEAD2*	M	11.4	31.5	2.0	Nodules
FVB/N	*Akt/Yap/dnTEAD2*	M	17.4	31.6	2.6	Tumors
FVB/N	*Akt/Yap/dnTEAD2*	M	17.4	31.4	3.7	Tumors
FVB/N	*Akt/Yap/dnTEAD2*	M	17.85	33.2	5.2	Tumors
FVB/N	*Akt/Yap/dnTEAD2*	M	18.0	32.8	6.9	Tumors
FVB/N	*Akt/Yap/dnTEAD2*	M	21.9	33.6	4.0	Tumors
FVB/N	*Akt/Yap/VGLL4*	M	10.7	33.9	2.3	Normal
FVB/N	*Akt/Yap/VGLL4*	F	17.8	25.8	5.4	Tumors
FVB/N	*Akt/Yap/VGLL4*	F	17.8	21.0	6.5	Tumors
FVB/N	*Akt/Yap/VGLL4*	F	17.8	31.7	4.6	Tumors
FVB/N	*Akt/Yap/VGLL4*	M	19.4	30.9	1.8	Normal
FVB/N	*Akt/Yap/VGLL4*	M	19.4	43.6	2.5	Nodules
FVB/N	*Akt/TEAD2vp16*	M	3.0	22.8	1.8	Normal
FVB/N	*Akt/TEAD2vp16*	M	3.5	28.5	2.6	Normal
FVB/N	*Akt/TEAD2vp16*	M	4.0	28.8	1.9	Normal
FVB/N	*Akt/TEAD2vp16*	M	4.0	26.3	1.6	Normal
FVB/N	*Akt/TEAD2vp16*	M	5.7	26.6	2.0	Normal
FVB/N	*Akt/TEAD2vp16*	M	5.7	27.9	2.0	Normal
FVB/N	*Akt/TEAD2vp16*	M	6.0	28.8	2.4	Normal
FVB/N	*Akt/TEAD2vp16*	M	6.5	25.3	1.9	Normal
FVB/N	*Akt/TEAD2vp16*	M	7.1	28.1	2.1	Normal
FVB/N	*Akt/TEAD2vp16*	M	7.9	30.6	2.4	Nodules
FVB/N	*Akt/TEAD2vp16*	M	7.9	31.8	2.7	Nodules
FVB/N	*Akt/TEAD2vp16*	M	9.0	30.5	2.3	Tumors
FVB/N	*Akt/TEAD2vp16*	M	9.1	36.3	2.9	Tumors
FVB/N	*Akt/TEAD2vp16*	M	9.1	38.4	2.9	Tumors
FVB/N	*Akt/TEAD2vp16*	M	10.4	29.8	2.5	Tumors
FVB/N	*Akt/TEAD2vp16*	M	10.4	31.0	2.2	Tumors
FVB/N	*Akt/TEAD2vp16*	M	10.4	27.9	2.8	Tumors
FVB/N	*Akt/TEAD2vp16*	F	10.6	27.1	3.8	Tumors
FVB/N	*Akt/TEAD2vp16*	M	10.8	32.5	2.5	Tumors
FVB/N	*Akt/TEAD2vp16*	F	14.1	29.8	7.4	Tumors
FVB/N	*Akt/TEAD2vp16*	F	15.1	28.8	5.9	Tumors
FVB/N	*Akt/TEAD2vp16*	F	18.1	28.2	6.2	Tumors
FVB/N	*Akt/Yap-ΔWW*	M	3.0	25.3	5.2	Tumors
FVB/N	*Akt/Yap-ΔWW*	M	3.0	25.4	5.2	Tumors
FVB/N	*Akt/Yap-ΔWW*	F	3.6	19.7	3.6	Tumors
FVB/N	*Akt/Yap-ΔWW*	F	4.0	26.3	4.1	Tumors
FVB/N	*Akt/Yap-ΔWW*	F	4.0	25.2	4.8	Tumors
FVB/N	*Akt/Yap-ΔSH3*	M	8.7	32.4	5.2	Tumors

FVB/N	*Akt/Yap-ΔSH3*	M	9.9	29.3	3.2	Tumors
FVB/N	*Akt/Yap-ΔSH3*	M	9.9	28.8	5.7	Tumors
FVB/N	*Akt/Yap-ΔSH3*	M	9.9	29.6	5.3	Tumors
FVB/N	*Akt/Yap-ΔSH3*	M	11.3	31.6	5.5	Tumors
FVB/N	*Akt/Yap-ΔPDZ*	F	5.28	21.9	3.3	Tumors
FVB/N	*Akt/Yap-ΔPDZ*	F	5.8	23.5	2.8	Tumors
FVB/N	*Akt/Yap-ΔPDZ*	F	6.0	29.5	3.6	Tumors
FVB/N	*Akt/Yap-ΔPDZ*	F	6.0	20.5	5.0	Tumors
FVB/N	*Akt/Yap/Cre*	F	7.6	Died (ascites, tumors)		
FVB/N	*Akt/Yap/Cre*	F	10.1	29	4.7	Tumors
FVB/N	*Akt/Yap/Cre*	F	10.1	23.3	5.2	Tumors
FVB/N	*Akt/Yap/Axin2*	M	7.7	32.5	2.5	Normal
FVB/N	*Akt/Yap/Axin2*	M	7.7	36.5	2.38	Nodules
FVB/N	*Akt/Yap/Axin2*	F	9.4	30.22	2.06	Tumors
FVB/N	*Akt/Yap/Axin2*	F	11.4	23.18	1.72	Tumors
FVB/N	*Akt/Yap/Axin2*	F	11.4	29.07	2.26	Tumors
Ctnnb1$^{flox/flox}$	*Akt/Yap/pCMV*	F	6.9	24.7	7.6	Tumors
Ctnnb1$^{flox/flox}$	*Akt/Yap/pCMV*	F	6.9	25.2	9.0	Tumors
Ctnnb1$^{flox/flox}$	*Akt/Yap/pCMV*	F	7.1	28.2	4.8	Tumors
Ctnnb1$^{flox/flox}$	*Akt/Yap/pCMV*	M	8.9	31.2	6.5	Tumors
Ctnnb1$^{flox/flox}$	*Akt/Yap/pCMV*	M	9.3	31.0	6.7	Tumors
Ctnnb1$^{flox/flox}$	*Akt/Yap/pCMV*	F	9.3	28.2	8.7	Tumors
Ctnnb1$^{flox/flox}$	*Akt/Yap/pCMV*	F	9.3	28.3	11.1	Tumors
Ctnnb1$^{flox/flox}$	*Akt/Yap/pCMV*	M	9.8	34.3	5.8	Tumors
Ctnnb1$^{flox/flox}$	*Akt/Yap/pCMV*	F	10.0	26.2	7.0	Tumors
Ctnnb1$^{flox/flox}$	*Akt/Yap/pCMV*	F	10.0	26.5	8.1	Tumors
Ctnnb1$^{flox/flox}$	*Akt/Yap/pCMV*	F	10.0	30.0	9.8	Tumors
Ctnnb1$^{flox/flox}$	*Akt/Yap/Cre*	F	7.6	23.9	1.7	Normal
Ctnnb1$^{flox/flox}$	*Akt/Yap/Cre*	M	8.9	29.8	1.8	Normal
Ctnnb1$^{flox/flox}$	*Akt/Yap/Cre*	M	9.3	30.2	1.5	Nodules
Ctnnb1$^{flox/flox}$	*Akt/Yap/Cre*	M	9.8	31.3	1.5	Nodules
Ctnnb1$^{flox/flox}$	*Akt/Yap/Cre*	F	14.1	31.1	1.8	Tumors
Ctnnb1$^{flox/flox}$	*Akt/Yap/Cre*	F	15.3	23.7	1.1	Tumors
Ctnnb1$^{flox/flox}$	*Akt/Yap/Cre*	F	20.9	31.4	1.6	Tumors
Ctnnb1$^{flox/flox}$	*Akt/Yap/Cre*	F	20.9	29.6	5.0	Tumors
Ctnnb1$^{flox/flox}$	*Akt/Yap/Cre*	M	22.6	37.8	1.8	Tumors
Ctnnb1$^{flox/flox}$	*Akt/Yap/Cre*	M	22.6	30.7	2.2	Tumors
Ctnnb1$^{flox/flox}$	*Akt/Yap/Cre*	M	22.6	37.4	2.1	Normal
Ctnnb1$^{flox/flox}$	*Akt/Yap/Cre*	F	26.2	28.8	4.3	Tumors
Ctnnb1$^{flox/flox}$	*Akt/Yap/Cre*	F	26.6	28.5	5.9	Tumors
Ctnnb1$^{flox/flox}$	*Akt/Yap/Cre*	F	26.6	30.7	6.8	Tumors
Yap$^{flox/flox}$	*Akt/Nicd/pCMV*	F	3.4	24.3	3.1	Tumors
Yap$^{flox/flox}$	*Akt/Nicd/pCMV*	F	3.4	26.2	3.83	Tumors

Yap$^{flox/flox}$	*Akt/Nicd/pCMV*	M	3.8	25.5	10.5	Tumors
Yap$^{flox/flox}$	*Akt/Nicd/pCMV*	M	4.1	Died (high tumor burden)		
Yap$^{flox/flox}$	*Akt/Nicd/pCMV*	M	4.1	Died (high tumor burden)		
Yap$^{flox/flox}$	*Akt/Nicd/pCMV*	M	4.1	Died (high tumor burden)		
Yap$^{flox/flox}$	*Akt/Nicd/pCMV*	M	4.2	Died (high tumor burden)		
Yap$^{flox/flox}$	*Akt/Nicd/Cre*	F	3.4	24.4	1.34	Normal
Yap$^{flox/flox}$	*Akt/Nicd/Cre*	M	5.9	Died (high tumor burden)		
Yap$^{flox/flox}$	*Akt/Nicd/Cre*	M	6.0	31.2	10	Tumors
Yap$^{flox/flox}$	*Akt/Nicd/Cre*	M	6.0	29.5	6.5	Tumors
Yap$^{flox/flox}$	*Akt/Nicd/Cre*	M	6.4	30	7.5	Tumors
Yap$^{flox/flox}$	*Akt/Nicd/Cre*	M	7.6	28.4	5.7	Tumors
Ctnnb1$^{flox/flox}$	*Akt/Nicd/pCMV*	M	4.2	27.2	4.22	Tumors
Ctnnb1$^{flox/flox}$	*Akt/Nicd/pCMV*	M	4.2	29	5.0	Tumors
Ctnnb1$^{flox/flox}$	*Akt/Nicd/pCMV*	M	5.0	Died (high tumor burden)		
Ctnnb1$^{flox/flox}$	*Akt/Nicd/pCMV*	F	5.14	22	4.0	Tumors
Ctnnb1$^{flox/flox}$	*Akt/Nicd/pCMV*	M	5.28	Died (high tumor burden)		
Ctnnb1$^{flox/flox}$	*Akt/Nicd/pCMV*	F	5.86	Died (high tumor burden)		
Ctnnb1$^{flox/flox}$	*Akt/Nicd/pCMV*	M	6.0	35.7	6.1	Tumors
Ctnnb1$^{flox/flox}$	*Akt/Nicd/Cre*	M	6.0	31.5	2.95	Tumors
Ctnnb1$^{flox/flox}$	*Akt/Nicd/Cre*	M	6.0	Died (high tumor burden)		
Ctnnb1$^{flox/flox}$	*Akt/Nicd/Cre*	M	6.3	32	12	Tumors
Ctnnb1$^{flox/flox}$	*Akt/Nicd/Cre*	M	6.3	30.56	8.28	Tumors
Ctnnb1$^{flox/flox}$	*Akt/Nicd/Cre*	F	6.4	25.8	2.57	Tumors
Ctnnb1$^{flox/flox}$	*Akt/Nicd/Cre*	F	6.4	26.2	5.9	Tumors
Ctnnb1$^{flox/flox}$	*Akt/Nicd/Cre*	M	7.2	28.74	4.81	Tumors
Ctnnb1$^{flox/flox}$	*Akt/Nicd/Cre*	M	7.2	31.7	7.8	Tumors
Ctnnb1$^{flox/flox}$	*Akt/Tead2VP16/pCMV*	F	10.6	30.36	3.25	Died (ascites, tumors)
Ctnnb1$^{flox/flox}$	*Akt/Tead2VP16/pCMV*	M	10.7	31.8	3.46	Died (ascites, tumors)
Ctnnb1$^{flox/flox}$	*Akt/Tead2VP16/pCMV*	M	17.6	33.18	3.27	Tumors
Ctnnb1$^{flox/flox}$	*Akt/Tead2VP16/pCMV*	F	17.6	28.77	2.15	Tumors
Ctnnb1$^{flox/flox}$	*Akt/Tead2VP16/Cre*	F	11.9	32.92	2.01	Died (ascites, tumors)
Ctnnb1$^{flox/flox}$	*Akt/Tead2VP16/Cre*	M	13.3	31.9	2.57	Died (ascites, tumors)
Ctnnb1$^{flox/flox}$	*Akt/Tead2VP16/Cre*	F	16.4	33.5	2.3	Died (ascites, tumors)
Ctnnb1$^{flox/flox}$	*Akt/Tead2VP16/Cre*	F	17.6	34.86	2.01	Tumors
Ctnnb1$^{flox/flox}$	*Akt/Jag1/Fak/pCMV*	F	11.3	26.6	8.37	Tumors
Ctnnb1$^{flox/flox}$	*Akt/Jag1/Fak/pCMV*	F	11.3	26.4	6.5	Tumors
Ctnnb1$^{flox/flox}$	*Akt/Jag1/Fak/pCMV*	M	13.1	31.1	4.1	Tumors
Ctnnb1$^{flox/flox}$	*Akt/Jag1/Fak/pCMV*	M	13.1	31.2	3.51	Tumors

Ctnnb1$^{flox/flox}$	*Akt/Jag1/Fak/Cre*	F	11.3	24.2	1.3	Nodules
Ctnnb1$^{flox/flox}$	*Akt/Jag1/Fak/Cre*	F	11.3	22.7	1.1	Normal
Ctnnb1$^{flox/flox}$	*Akt/Jag1/Fak/Cre*	M	13.8	16.0	0.8	Normal
Ctnnb1$^{flox/flox}$	*Akt/Jag1/Fak/Cre*	F	28.0	23.0	1.86	Tumors
Ctnnb1$^{flox/flox}$	*Akt/Jag1/Fak/Cre*	F	35.0	25.7	1.85	Tumors
Ctnnb1$^{flox/flox}$	*Akt/Jag1/Fak/Cre*	F	35.0	25.1	1.5	Tumors

Supplementary Table 4. Clinicopathological features of iCCA patients

Variables	
No. of patients	58
Male	35
Female	23
Age (years)	
<60	15
≥60	43
Etiology	
HBV	12
HCV	8
Hepatolithiasis	11
PSC	2
NA	25
Liver cirrhosis	
Yes	23
No	35
Tumor differentiation	
Well	28
Moderately	22
Poorly	8
Tumor size (cm)	
<5	38
>5	20
Tumor number	
Single	43
Multiple	15
Prognosis	
Better (≥ 3 years)	12
Poorer (< 3 years)	46
Lymph node metastasis	
Yes	23
No	35

Lung metastasis	
Yes	12
No	46

Abbreviations: NA, not available; PSC, primary sclerosing cholangitis

Supplementary Table 5. Primary antibodies information for immunohistochemistry

Antibody	Species	Dilution	Company	Catalog Number
CK19	Rabbit	1:1000	Abcam	Ab133496
HA	Rabbit	1:100	Cell Signaling Technology	3724
Ki-67	Rabbit	1:150	Thermo Fisher Scientific	MA5-14520
β-Catenin	Mouse	1:200	BD Biosciences	BD610153
YAP	Rabbit	1:100	Cell Signaling Technology	14074
CD31	Rabbit	1:100	Cell Signaling Technology	77699
Vimentin	Rabbit	1:200	Cell Signaling Technology	5741
Non-phospho-β-Catenin $^{Ser33/37/Thr41}$	Rabbit	1:400	Cell Signaling Technology	8814
P-ERK1/2	Rabbit	1:500	Cell Signaling Technology	4370
Second antibody Goat anti-Rabbit		1:500	Invitrogen	B2770
Second antibody Goat anti-Mouse		1:250	Vector Laboratories	BMK2202

Supplementary Table 6. Primary antibodies information for Western blot analysis

Antibody	Species	Dilution	Company	Catalog Number
YAP	Rabbit	1:1000	Cell Signaling Technology	14074
β-Catenin	Mouse	1:2000	BD Biosciences	BD610153
Pan-TEADs	Rabbit	1:1000	Cell Signaling Technology	13295
FLAG-Tag	Rabbit	1:1000	Cell Signaling Technology	14793
MYC-Tag	Mouse	1:1000	Cell Signaling Technology	2276
HA-Tag	Rabbit	1:1000	Cell Signaling Technology	3724
T-AKT	Rabbit	1:2000	Cell Signaling Technology	9272
p-AKT^{Ser473}	Rabbit	1:1000	Cell Signaling Technology	3787
p-AKT^{Thr308}	Rabbit	1:1000	Cell Signaling Technology	9275
4EBP1	Rabbit	1:1000	Cell Signaling Technology	9644
p-4EBP1$^{Thr37/ Thr46}$	Rabbit	1:2000	Cell Signaling Technology	2855
p-RPS6	Rabbit	1:1000	Cell Signaling Technology	4858
NOTCH2	Rabbit	1:2000		5732
JAGGED1	Rabbit	1:1000	Abcam	Ab109536
SURVIVIN	Rabbit	1:1000	Cell Signaling Technology	2808
PCNA	Mouse	1:2000	Cell Signaling Technology	2586
HISTONE H3	Rabbit	1:2000	Cell Signaling Technology	4499
β-Tubulin	Rabbit	1:1000	Abcam	Ab6046

ERK	Rabbit	1:1000	Cell Signaling Technology	9102
P-ERK	Rabbit	1:1000	Cell Signaling Technology	4370
FAK	Rabbit	1:1000	Cell Signaling Technology	3285
Non-phospho-β-Catenin $^{Ser33/37/Thr41}$	Rabbit	1:1000	Cell Signaling Technology	4270
GAPDH	Rabbit	1:2000	Cell Signaling Technology	5174
Second antibodies Goat anti-Rabbit		1:500	Abcam	ab205718
Second antibodies Goat anti-mouse		1:500	Invitrogen	MA511306

Supplementary Table 7. Primary antibodies information for immunofluorescence

Antibody	Species	Dilution	Company	Catalog Number
YAP	Rabbit	1:100	Cell Signaling Technology	14074
β-Catenin	Mouse	1:200	BD Biosciences	610153
CK19	Rabbit	1:200	Abcam	Ab133496
CD31	Rabbit	1:100	Cell Signaling Technology	77699
Vimentin	Rabbit	1:100	Cell Signaling Technology	5741
Pan-TEADs	Rabbit	1:1000	Cell Signaling Technology	13295
Goat anti-Rabbit Secondary antibody, Alexa Fluor 488		1:1000	Invitrogen	A21295
Goat anti-Rabbit Secondary antibody, Alexa Fluor 594		1:1000	Invitrogen	A11012
Goat anti-Mouse Secondary antibody, Alexa Fluor 488		1:1000	Invitrogen	A11001
Goat anti-Mouse Secondary antibody, Alexa Fluor 568		1:1000	Invitrogen	A11004

Supplementary Table 8. Primers sequences used for qRT-PCR analysis

Gene	Forward sequence (5'-3')	Reverse sequence (5'-3')
18s rRNA	CGGCTACCACATCCAAGGAA	5'-GCTGGAATTACCGCGGCT-3'
Human-*CTGF*	CAGCATGGACGTTCGTCTG	AACCACGGTTTGGTCCTTGG
Human-*CYR61*	GGTCAAAGTTACCGGGCAGT	GGAGGCATCGAATCCCAGC

Human-*YAP1*	TAGCCCTGCGTAGCCAGTTA	TCATGCTTAGTCCACTGTCTGT
Human-*WWTR1*	TCCCAGCCAAATCTCGTGATG	AGCGCATTGGGCATACTCAT
Human-*CTNNB1*	AAAGCGGCTGTTAGTCACTGG	CGAGTCATTGCATACTGTCCAT
Human-*AXIN2*	TACACTCCTTATTGGGCGATCA	TTGGCTACTCGTAAAGTTTTGGT
Human-*CRIM1*	AGTTTCCAAGTCAGGATATGTGC	AGCATAACCCTCGATCAGAACA
Human-*CCDC80*	GACCCCGTTTCACTATGCTGT	GGCGAGCTAGTCTCAACACG
Human-*ABCB1*	TTGCTGCTTACATTCAGGTTTCA	AGCCTATCTCCTGTCGCATTA
Human-*AREG*	GTGGTGCTGTCGCTCTTGATA	CCCCAGAAAATGGTTCACGCT
Mouse-*Ctgf*	GGGCCTCTTCTGCGATTTC	ATCCAGGCAAGTGCATTGGTA
Mouse-*Cyr61*	CTGCGCTAAACAACTCAACGA	GCAGATCCCTTTCAGAGCGG
Mouse-*Notch2*	ATGTGGACGAGTGTCTGTTGC	GGAAGCATAGGCACAGTCATC
Mouse-*Jagged 1*	CCTCGGGTCAGTTTGAGCTG	CCTTGAGGCACACTTTGAAGTA
Mouse-*Ccdn1*	CGTGGCCTCTAAGATGAAGGA	CCTCGGGCCGGATAGAGTAG
Mouse-*Myc*	TGTACCTCGTCCGATTCC	CATCTTCTTGCTCTTCTTCAG
Mouse-*Hes1*	AAAGCCTATCATGGAGAAGAGGCG	GGAATGCCGGGAGCTATCTTTCTT
Mouse-*Hey1*	GCGCGGACGAGAATGGAAA	TCAGGTGATCCACAGTCATCTG
Mouse-*Hey2*	AAGCGCCCTTGTGAGGAAAC	GGTAGTTGTCGGTGAATTGGAC

3. Supplementary Material

The analysis included data from 58 patients with human intrahepatic cholangiocarcinoma (all with survival data). The variables have been analyzed using the Statistical Package for Social Science (SPSS, version 22.0, Chicago, IL, USA).

Descriptive statistics

Sex	Number (%)	Mean age (SD)	Mean survival (SD)
Male	35 (60.3)	64.5 (13.0)	25.0 (15.7)
Female	23 (39.7)	66.3 (9.0)	28.2 (17.9)
Total	58	65.3 (11.6)	26.3 (16.5)

Mean survival is 26.3 months (SD 16.5)

(Differences between males and females are not statistically significant)

Sex	Number (%)	Mean CTNNB1 mRNA (SD)
Male	35 (60.3)	0.420 (0.287)
Female	23 (39.7)	0.393 (0.236)
Total	58	0.409 (0.266)

(The difference is not statistically significant)

***CTNNB1* mRNA in human intrahepatic cholangiocarcinoma**

Low and high *CTNNB1 mRNA* values were recoded into binary variables (0/1) using the median values (*CTNNB1* mRNA = 0.353) as the cut-off. The whole dataset was then divided into 29 subjects with values of *CTNNB1* mRNA below the median and 29 subjects above the median. Statistical comparison between the two groups was performed using the log-rank test:

Marker	Number of subjects (%)	Mean survival in months (SD)	Log-rank test
CTNNB1 mRNA < 0.353	29 (50.0)	35.7 (16.4)	–
CTNNB1 mRNA ≥ 0.353	29 (50.0)	16.9 (10.3)	<0.0001
Total	58	26.3 (16.5)	

Conclusion 1: *patients with CTNNB1 mRNA values above the median 0.353 survive on average shorter than patients with CTNNB1 mRNA below 0.353 (see Kaplan-Meier curve)*

Survival analysis (univariate)

Variable	Survival (months) (SD)	*P*-value
Age (years)		
< 65	25.3 (16.4)	0.680
≥ 65	27.1 (16.9)	
Sex		
Female	28.2 (17.9)	0.474
Male	25.0 (15.7)	
Cirrhosis		
Yes	26.6 (17.0)	0.831
No	25.7 (16.1)	
Etiology		
HBV	23.0 (19.3)	0.496[#]
HCV	31.9 (13.4)	
Hepatolithiasis	28.1 (15.2)	
PSC	10.0 (2.8)	
Diameter		
< 5 cm	26.7 (17.6)	0.784
≥ 5 cm	25.5 (14.9)	
Lymph Node Metastasis		
No	33.0 (17.0)	**0.007**
Yes	19.4 (15.3)	
Lung Metastasis		
No	30.3 (16.2)	**<0.0001**
Yes	10.8 (4.5)	
Differentiation		
Well	25.7 (18.7)	0.326[#]
Moderately	24.1 (13.2)	
Poorly	34.2 (16.5)	
Tumor number		
Single	29.3 (16.1)	**0.016**
Multiple	17.5 (15.0)	
CTNNB1 mRNA		
< 0.353	35.7 (16.4)	**<0.0001**
≥ 0.353	16.9 (10.3)	

[#]One-way ANOVA

A significant difference in survival was found in the univariate analysis for lymph node metastasis, lung metastasis, tumor number, and CTNNB1 mRNA above the median.

Multivariable Cox regression analysis

A multivariable Cox proportional hazard model was created with survival as the outcome variable. CTNNB1 mRNA was included as a predictor together with the covariates (full model). Hazard ratios (HRs) and their 95% confidence intervals were calculated, and the Wald test was used for model testing.

Covariates	Full model (HR[#] and 95% CI)
Age ≥ 65 yrs	1.483 (0.765–2.875)
Male sex	0.958 (0.435–2.110)
Cirrhosis (y/n)	2.351 (0.936–5.903)
Etiology	
HBV	Reference
HCV	0.986 (0.242–4.021)
Hepatolithiasis	1.038 (0.337–3.202)
PSC	4.260 (0.735–24.70)
Size ≥ 5 cm	1.075 (0.472–2.449)
Lymph Node Metastasis	
No	Reference
Yes	2.771 (0.908–8.456)
Lung Metastasis	
No	Reference
Yes	3.028 (0.975–9.404)
Differentiation	
Well	Reference
Moderately	1.512 (0.656–3.484)
Poorly	1.062 (0.303–3.722)
Tumor number	
Single	Reference
Multiple	0.734 (0.248–2.168)
CTNNB1 mRNA ≥ 0.353 (median value)	8.481 (2.920–24.63) **

*p<0.05; **p<0.001

Conclusion: *Only CTNNB1 mRNA levels above the median were independent predictors of reduced survival in the whole model. The other variables did not show significant associations.*

4. Materials and Methods

Constructs and Reagents

Plasmids used for animal studies, including pT3-EF1a-HA-myr-Akt, pT3-EF1α-Flag-YapS127A, pT3-EF1α-Flag-YapS94A, pT3-EF1α, pT3-EF1α-dnTEAD2, pT3-EF5α-Tead2VP16, pT3-EF1α-Tead2VP16, pCMV, pCMV-Cre, pT3-EF1α-Myc-mNICD (NICD), pT3-EF1α-JAG1, pT3-EF1α-FAK, and pCMV-sleeping beauty transposase (pCMV/SB), were previously described [4-7]. Truncated Yap inserts, including YapΔ(P+TBD), YapΔWW, YapΔSH3, YapΔ(TAD+PDZ), and YapΔPDZ were obtained via overlap extension PCR and cloned into the pT3-EF1a vector. The AAV9.VGLL4-GFP construct was kindly provided by Dr. Zhiqiang Lin from Masonic Medical Research Institute (Utica, NY). The Myc-AXIN2 (#21279) construct was purchased from Addgene (Cambridge, MA). The VGLL4 and Myc-AXIN2 were then cloned into the pT3-EF1a vector to generate pT3-EF1α-MYC-VGLL4 and pT3-EF1α-MYC-AXIN2 plasmids. For cell studies, plasmids used in this project, including psPAX2(#12260), pMD2.G(#12259), plenti-EGFP (#17448), pLKO.1-sc (#10879) and pLKO.1-shβ-Catenin (#18803), were purchased from Addgene. Additional plasmids include plenti-dnTEAD2, pCW57.1-dnTCF4, plenti-FLAG-β-Catenin WT and pT3-EF1α-Myc-β-Catenin WT. All plasmids were extracted using the Endotoxin Free Prep Kit (Sigma-Aldrich, St. Louis, MO, USA).

Histology, Hematoxylin-Eosin (H&E), and Immunohistochemistry (IHC)

Mouse liver tissues were fixed in 10% Neutral Buffered Formalin (ThermoFisher Scientific, Waltham, MA) at 4°C overnight and then processed for paraffin embedding. Paraffined tissues were cut into sections at a thickness of 5 μm for H&E or IHC staining. For H&E, sections were deparaffinized in xylene and stained with hematoxylin and eosin (ThermoFisher Scientific) following the standard protocol. For IHC, sections were heated in an oven at 60°C overnight. First, sections were deparaffinized in xylene, hydrated in 100%, 95%, 70%, and 50% alcohols, followed by antigen retrieval in 10mM sodium citrate buffer (pH 6.0). Next, sections were blocked in 10%

goat serum and Avidin-Biotin blocking kit (Vector Laboratories, Burlingame, CA) and then incubated with primary antibodies at 4°C overnight. The following day, sections were subjected to 3% H2O2 to quench endogenous peroxidase activity, followed by incubation with secondary antibody at RT for 30min. Every step should be followed by washing three times in PBS for 5 min each. The Vectastain Elite ABC Kit (Vector Laboratories) and DAB substrate (Dako North America, Carpinteria, CA) were used to visualize the signal. Subsequently, sections were immersed in hematoxylin, dehydrated in graded alcohols, and covered-slipped with ClearMount mounting medium (StatLab, Lodi, CA). Antibodies used for IHC are listed in Sup. Table 5.

Protein Extraction and Western blotting (WB)

Cell pellets or mouse liver tissues were homogenized and lysed in M-PER Mammalian Protein Extraction Reagent (Thermo Fisher Scientific) with the Halt™ Protease and Phosphatase Inhibitor Cocktail (Thermo Fisher Scientific) at a ratio of 100:1. Protein concentration was calculated using the Pierce BCA Protein Assay Kit (ThermoFisher Scientific). Next, proteins were denatured in sample buffer (Laemmli Sample buffer: β-ME=19:1) at 95°C for 5min and separated by sodium dodecyl sulfate–polyacrylamide gel electrophoresis. The gel was subsequently transferred onto nitrocellulose membranes (Bio-Rad Laboratories, Hercules, CA). The membranes were blocked in 10% nonfat milk diluted in Tris-buffered saline containing 0.1% Tween-20 (TBST) at room temperature for 1 hour and followed by incubation with primary antibodies at 4°C overnight. The following day, the membranes were incubated with horseradish peroxidase-conjugated secondary antibody (Jackson ImmunoResearch Laboratories Inc., West Grove, PA) at room temperature for 1 hour. After washing with TBST, membranes were developed with the Clarity Western ECL Substrate (Bio-Rad Laboratories). Antibodies used for WB are listed in Sup. Table 6.

RNA Extraction and Quantitative reverse transcription real-time polymerase chain reaction

Total RNA extraction from mouse liver tissues or cells was performed using the Quick RNA Miniprep Kit (Zymo Research, Irvine, CA). RNA was converted to cDNA using the iScript™ Reverse Transcription Supermix (Bio-Rad). qRT-PCR was performed on the QuantStudio™6 Flex system (Applied Biosystems, Waltham, MA). Reactions were performed as follows: 1.0 ul primer mix, 5ul TaqMan Universal PCR Master Mix (ThermoFisher Scientific), 2.5ul cDNA (100 ng), and 2.1ul d2H2O. Cycling conditions were: polymerase activation at 95°C for 10 min, 40 cycles: denaturation at 95°C for 15 s, and extension at 60°C for 1 min. Primers for qRT-PCR were ordered from Integrated DNA Technologies (Coralville, IA) and listed in Sup. Table 8.

Immunofluorescence

Deparaffinized liver tissue sections or cells plated in cover glasses were fixed with 4% formaldehyde (pH 7.4) for 15 min at room temperature. Next, sections or cells were treated with 0.1% Triton™ X-100 in PBS for 5 min at room temperature for permeabilization and blocked in 10% goat serum for 1 hour. After blocking, sections or cells were incubated with primary antibodies overnight at 4°C and subsequently incubated with the fluorochrome-conjugated secondary antibody for 1 hour at room temperature. Every step was followed by washing three times in PBS for 5 min each. Finally, sections or cells were counterstained with DAPI (Millipore) for imaging. Antibodies detailed information is listed in Sup. Table 7.

Colony formation assay

Stable lentivirus transfected RBE, HUCCT-1, and KKU156 cells were plated in triplicate at densities of 1000 to 2000 cells per well in a 6-well culture plate, respectively. Cells were cultured with puromycin-containing DMEM medium for two weeks. Cell colonies were fixed, stained with 0.2% crystal violet solution, and counted for quantification.

Co-immunoprecipitation (co-IP)

RBE and KKU156 cells were transfected with pT3-EF1α-Flag-YapS127A plasmid. RBE cells overexpressed with Flag tagged wildtype β-Catenin were obtained by lentiviral transduction of plenti-Flag-β-Catenin-WT plasmid. Cells were lysed in IP Lysis Buffer (#26149, ThermoFisher Scientific) containing Halt™ Protease and Phosphatase Inhibitor Cocktail (#78446, ThermoFisher Scientific). Akt/Yap iCCA tumors and human iCCA tissues obtained from West China Hospital were homogenized and lysed in IP Lysis Buffer. Lysates were subjected to immunoprecipitation with the indicated antibody using the Pierce Co-Immunoprecipitation Kit (#26149, ThermoFisher Scientific), following the manufacturer's instructions. YAP (#14074, Cell Signaling Technology), β-Catenin (#610153, BD Biosciences) and FLAG (#AF519, Beyotime) antibodies were used to immunoprecipitate the antigen (bait protein). Rabbit or mouse IgG was used as a control. Co-precipitating proteins were detected by Western blotting. Human surrounding non-tumorous livers and iCCA tissues obtained from Pittsburgh Liver Research Center were homogenized in RIPA buffer premixed with fresh protease and phosphatase inhibitor cocktails. The concentration of the protein was determined by the bicinchoninic acid assay. For immunoprecipitation, 1mg of human liver lysate was precleared with 40µl of Protein A/G PLUS-Agarose (sc-2003, Santa Cruz Biotechnology) for 2 hours at 4°C. After centrifugation (3,000 rpm, 1 minute), the supernatant was incubated with YAP antibody (#14074, Cell Signaling Technology, 1:100) or control IgG overnight at 4°C. The next day, samples were incubated with 40µl of Protein A/G PLUS-Agarose for 2 hours at 4°C. The pellet was collected, washed with RIPA buffer for three times, resuspended in 20µl of loading buffer, and subjected to western blotting.

For the Yap structure-function study, HEK-293FT cells were co-transfected pT3-EF1α-Myc-β-Catenin WT plasmid with either full length or truncated Flag-YapS127A mutants and lysed in IP Lysis Buffer (ThermoFisher Scientific). *Akt/Yap*, *Akt/Yap*Δ*WW*, *Akt/Yap*Δ*SH3*, or *Akt/Yap*Δ*PDZ* iCCA tumors were homogenized and lysed in IP Lysis Buffer. Following the manufacturer's

instructions, lysates were subjected to immunoprecipitation with Anti-FLAG M2 magnetic beads (M8823, Sigma-Aldrich).

For YAP/β-Catenin cytoplasmic and nuclear interaction detection, *Akt/Yap* iCCA tumors were homogenized and isolated using the NE-PER™ Nuclear and Cytoplasmic Extraction Reagents (#78833, ThermoFisher Scientific), following the manufacturer's instructions. The cytoplasmic and nuclear fractions were next subjected to immunoprecipitation with anti-FLAG M2 magnetic beads. Next, binding proteins were eluted in elution buffer and followed by western blotting analysis.

RNA Sequencing Analysis

Human RBE cells were subjected to transfection with lentivirus (pLKO.1-shCon or pLKO.1-shβ-Catenin; pCW57.1-dnTCF4 followed by incubation with vehicle or doxycycline) and *siRNA* (*siCon* or *siYAP/TAZ*). Total RNA was extracted from RBE cells, murine normal liver (NL), *Akt/Yap* (AY), *Akt/Tead2VP16* (AT) and *Ctnnb1*$^{flox/flox}$ *Akt/Yap/Cre* (BAY) tumor tissues. RNA sample quality was detected using Bioanalyzer (Agilent, Santa Clara, CA). Values of RNA integrity number (RIN) above 6.8 are required for RNA Sequencing. RNA samples that met the standard were submitted for RNA sequencing. Library preparation and sequencing were performed by Novogene (Sacramento, CA). Reads quality was controlled by fastqc (v0.11.7). The controlled reads were then aligned to the respective genome (human reference genome version 38 [hg38], Mus Musculus [GRCm38/mm10]). Genes' Ensembl IDs were converted to Entrez ID by the Bioconductor Package Maintainer org.Hs.eg.db (version 3.8.2). After removing the duplicated genes, the fragments per kilobase of transcript per million mapped reads were calculated and analyzed using the Edge R package (version 3.28.1). The Venn diagram and heatmap were generated by the VennDiagram package and ComplexHeatmap package, respectively.

References

1. Callus BA, Finch-Edmondson ML, Fletcher S, et al. YAPping about and not forgetting TAZ. FEBS Lett 2019;593:253-276.
2. Kulman JD, Harris JE, Xie L, et al. Proline-rich Gla protein 2 is a cell-surface vitamin K-dependent protein that binds to the transcriptional coactivator Yes-associated protein. Proc Natl Acad Sci U S A 2007;104:8767-72.
3. **Chang L, Azzolin L, Di Biagio D,** et al. The SWI/SNF complex is a mechanoregulated inhibitor of YAP and TAZ. Nature 2018;563:265-269.
4. **Zhang S, Song X, Cao D, Xu Z,** et al. Pan-mTOR inhibitor MLN0128 is effective against intrahepatic cholangiocarcinoma in mice. J Hepatol 2017;67:1194-1203.
5. **Fan B, Malato Y, Calvisi DF,** et al. Cholangiocarcinomas can originate from hepatocytes in mice. J Clin Invest 2012;122:2911-5.
6. **Zhang J, Liu P,** Tao J, et al. TEA Domain Transcription Factor 4 Is the Major Mediator of Yes-Associated Protein Oncogenic Activity in Mouse and Human Hepatoblastoma. Am J Pathol 2019;189:1077-1090.
7. Tschaharganeh DF, Chen X, Latzko P, et al. Yes-associated protein up-regulates Jagged-1 and activates the Notch pathway in human hepatocellular carcinoma. Gastroenterology 2013;144:1530-1542 e12.

Author names in bold designate shared co-first authorship.